PFC/RR-83-21 DOE/ET-51013-92

MFTFB+T MAGNETOSTATIC AND CIRCUIT FAULT INDUCED FORCES

R. D. Pillsbury, Jr., R. J. Thome
W. R. Mann, and W. G. Langton

Massachusetts Institute of Technology
Plasma Fusion Center
Cambridge, MA 02139

August 1983

Foreword

This work was performed for the Fusion Engineering Design Center, Oak Ridge, Tennessee in support of their activity for the Mirror Fusion Test Facility at the Lawrence Livermore National Laboratory. The effort was carried out by the Plasma Fusion Center Magnet Technology Division under contract no. DOE-AC02-78ET-51013.

TABLE OF CONTENTS

0.0 INTRODUCTION

Magnet systems consisting of multiple, inductively coupled coils can experience substantial changes in their usual operating load patterns in the event of a fault condition such as a short circuit followed by a rapid system discharge. The methods for determining the load changes are straightforward, but time consuming and the number of cases requiring consideration grows rapidly as the number of coils and circuits in a system increases.

As magnet systems become larger and more complex, the electromagnetic load redistribution or other effects such as excessive temperature rise can become so severe that a thorough fault condition examination is essential. The Magnet Technology Division at the Plasma Fusion Center has been developing codes to improve the efficiency and turn around time for model construction and fault condition analysis. In this report the codes were applied to a system of 24 coils in nine circuits which constitute MFTFB+T, a joule mirror fusion system under consideration by LLNL. The process begins by system field/force model construction using sufficient detail to analyze parameters selected as indicative of the severity of a fault condition (e.g. - total load in a particular direction on a coil or load per unit length at a point in a coil), but not so detailed that turn around time is unattractive. If a severe condition is found it is assumed that the design group will investigate the condition with a more detailed model.

An estimation of "severity" of a fault condition requires a well defined set of "usual' operating conditions for comparison. We define the latter as the extreme maximum or minimum values of the critical parameters for any combination of the circuits in a fully "on" or "off" condition. In itself, this magnetostatic analysis is nontrivial in a complex system. For example, for the nine circuits in MFTFB+T, there are 512 (2 to the ninth power) usual operating conditions. It should be emphasized that these represent feasible conditions since it is conceivable that any combination of circuits could be fully charged during shakedown tests or system operation. This is indicative of the need for an efficient procedure and codes for fault analysis since the number of credible faults is often many times the number of usual operating conditions in a multiple coil/multiple circuit system.

In this report, the fault conditions which have been selected arise from assuming that all circuits are charged to their operating level, a short circuit occurs across one coil and a discharge of the entire system follows. Each case requires a transient circuit analysis required by em load determination as a function of time because, in general, the extreme loads do not necessarily occur at the time a discharge current in a circuit passes through its maximum value.

In general, the four C-shaped magnets at each machine end (WM2, WM1, WT2, and WT1) experience the worst case loading under static current conditions. The central cell solenoids (WS6, WS5, WS4, and WS3) experience their peak loads during discharge transients with a neighboring coil short-circuited. The coils at the machine center (WS2, WS1, WCC1, WTDFS2, etc.) have peak axial loads that occur primarily in the static condition. However, the peak radial loads occur during the discharge transients.

The current scenarios chosen for the analyses were by no means exhaustive from a fault condition standpoint. An entire class of faults which requires consideration involves system behavior during discharge execution with a section of one of the superconducting coils in the resistive state. Even though the coils are designed to be stable under usual conditions, that is, complete LHe coolant immersion, a resistive region is possible in the event of a fault in the form of a low helium level. The temperature rise in a resistive region which is not immersed is strongly dependent on the coupled discharge character of the circuits and the level of operating current and dump voltage selected.

Substantial progress has been made in the ability to turn around certain classes of fault conditions as evidenced by the cases treated in this report. As indicated above, however, other classes of severe conditions exist and development of codes for rapid turnaround of these cases should continue.

1.0 SUMMARY

This report presents the results of work performed to date on the estimation of the Lorentz forces acting on the various coils in the MFTFB+T mirror machine. The analyses include: (1) static loading under normal operating conditions; (2) transient loading during a normal discharge; and (3) transient loading for one coil short circuits with all coils discharging. For the purposes of this memo, normal operation is defined as any possible combination of circuits fully charged to their operating current level or at zero current. This definition would then include any possible scenario for the entire system or partial system at full operating current.

Figure 1.1 shows both an isometric and side view of the coils in the machine. Twenty four coils are shown and consist of two large central solenoids, two high field choke coils, and twelve identical solenoids in the central cell. Each of the machine ends has four coils: two transition coils and a yin-yang pair. Only the coil centerlines are shown. Superimposed are the coordinate system, the coil numbering system and coil nomenclature adopted for this effort. The coils are numbered consecutively from the coil with the largest positive axial (z) coordinate (coil 1) to the largest negative coordinate (coil 24). Table 1.1 lists the coil number, name, their circuit number, and full operating current. The circuit numbering is arbitrary, but collects the 24 coils into nine circuits corresponding to the expected power supply configuration for this machine. Note that each of the four yin-yang coils are in an independent circuit whereas other similar coils are in series in the same circuit. Results may change considerably if different current levels or circuit configurations are postulated.

The models of the coils and circuits are described in section 2.0. The results from the static analyses are given in section 3.0. The transient analyses are presented in section 4.0. The remainder of this section summarizes the results.

Table 1.2 summarizes the peak values of the net axial force which can act on each coil out of the possible normal operating conditions. Both the largest positive and largest negative loads are given along with the current scenario that produces those forces. The current scenarios are given as a nine digit number. Each digit represents the current multiplier in each circuit. For example, the current scenario 110011001 implies that circuits 1,2,5,6, and 9 are at full current, while circuits 3,4,7, and 8 are at zero current. The forces given represent the total axial load acting on the coil.

It can be seen that, except for the two end coils, the worst case loadings do not occur when all coils are at full operating current. Similarly, none of the cases of the single circuit on - all others off generates maximum or minimum forces. In general, the worst case loading occurs when as many coils as possible to one side of the coil under

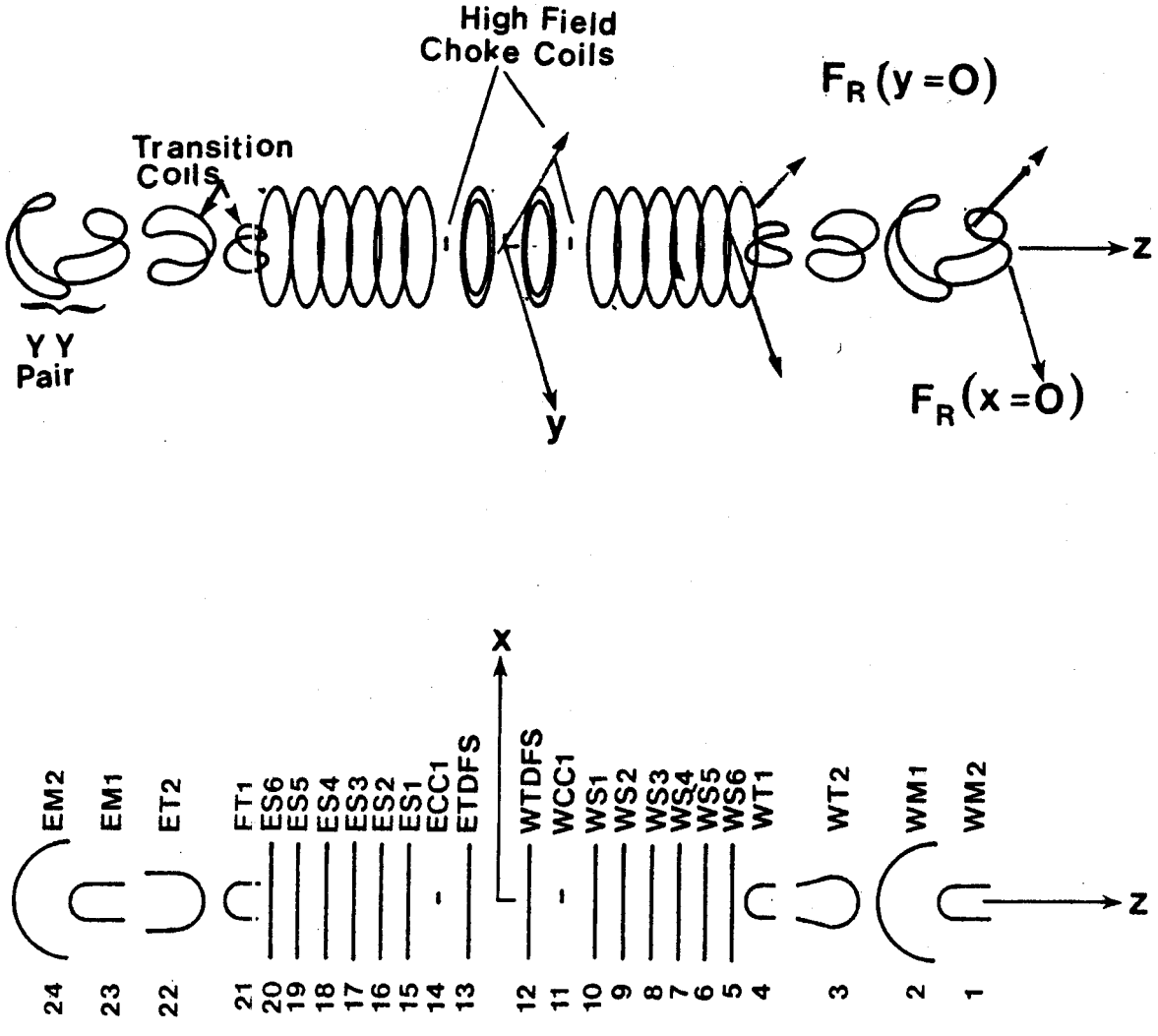

Figure 1.1 MFTF+T Coil Centerlines, Numbers and Nomenclature

6375

Table 1.1 Coil/Circuit Numbering and Nomenclature

coil #	coil name	Circuit #	Operating Current (A)
1	WM2	1	4403
2	WM1	2	3872
3	WT2	3	5206
4	WT1	4	2328
5	WS6	5	1823
6	WS5	5	1823
7	WS4	5	1823
8	WS3	5	1823
9	WS2	5	1823
10	WS1	5	1823
11	WCC1	6	107190
12	WTDFS2	7	8000
13	ETDFS2	7	8000
14	ECC1	6	107190
15	ES1	5	1823
16	ES2	5	1823
17	ES3	5	1823
18	ES4	5	1823
19	ES5	5	1823
20	ES6	5	1823
21	ET1	4	2328
22	ET2	3	5206
23	EM1	8	3872
24	EM2	9	4403

Table 1.2 Peak Axial Loads Under Normal Operating Conditions

coil #	coil name	Maximum Fz (MN)	Current Scenario*	Minimum Fz (MN)	Current Scenario*
1	WM2	0	-	-5.27	111111111
2	WM1	4.75	110000000	-5.02	011111111
3	WT2	4.96	111000000	-1.51	001111111
4	WT1	1.04	111100000	-0.48	000111111
5	WS6	0	-	-4.44	000011111
6	WS5	0	-	-2.17	000011111
7	WS4	0	-	-1.63	000011111
8	WS3	0.43	111110000	-1.84	000011111
9	WS2	1.41	111110000	-2.80	000011111
10	WS1	3.91	111110000	-4.82	000011111
11	WCC1	0.21	111111000	-1.68	000001111
12	WTDF52	0	-	-102.	000000111
13	ETDF52	102.	110000100	0	-
14	ECC1	1.68	110001100	-0.21	001111011
15	ES1	4.82	110011100	-3.91	001110011
16	ES2	2.80	110011100	-1.41	001110011
17	ES3	1.84	110011100	-0.43	001110011
18	ES4	1.63	110011100	0	-
19	ES5	2.17	110011100	0	-
20	ES6	4.44	110011100	0	-
21	ET1	0.48	110111100	-1.04	001100011
22	ET2	1.51	111111100	-4.96	001000011
23	EM1	5.02	111111110	-4.75	000000011
24	EM2	5.27	111111111	0	-

* each digit represents a circuit on (1) or off (0)
e.g. 110011100 means circuits 1,2,5,6,7 are on and circuits 3,4,8,9 are off

consideration have zero current and as many as possible on the other side have full current. Due to the connection symmetry of most of the circuits the worst case load does not correspond to all coils on one side on and all coils on the other off.

Forces that are listed as 0 imply there is no scenario that gives a force of that sign or direction on that coil. For example, WS6 (coil #5) has a zero maximum (positive) force. This means that there is no possible combination of circuits completely on or off that produces a net force on WS6 that is away from the machine center. However, there are several combinations that produce a net force on WS6 toward the machine center. The worst case load is -4.44 MN and occurs when circuits 1,2,3 and 4 are off and circuits 5-9 are on (i.e. a current scenario of 000011111).

Figure 1.2 shows the same information in bar chart form. The worst case maximum (positive) and minimum (negative) net axial force on each coil is shown. For scaling purposes the forces on the large solenoids have been clipped and the peak value written adjacent to the bars. There is anti-symmetry about the machine center, as is expected.

Table 1.3 summarizes the peak radial loading per unit length acting on each coil for normal operating conditions. In a solenoid, the forces per unit length are indeed radial. For C-shaped coils, these forces are local running loads (N/m) which contribute to the lobe-opening forces. For the purposes of this memo these forces are denoted as radial for all coils. There are two values presented. The first is in the X=0 plane; the second in the Y=0 plane. The two radial force directions are illustrated in Figure 1.1 for a typical C-shaped magnet and for a typical solenoid. Note that the force in the X=0 plane is y-directed and the force in the y=0 plane is x-directed. In a purely solenoidal system, these two forces would be equal. The lack of equality is a function of the non-solenoidal fields produced by the C-shaped magnets in the system. The radial forces are positive for all cases and are usually extreme for all circuits on. However, some of the coils (e.g. WT2) experience the worst case radial loading when an adjacent coil is off and unable to hold the axial flux from the system away from the winding in question.

Figure 1.3 shows the information from this table in bar chart form. The solid lines represent the radial forces (per unit length) in the X=0 plane; and the dashed lines the Y=0 plane. Only the C-shaped coils at the machine ends experience a significant loading difference in the two planes. The end solenoids do experience a slight difference in force, but the difference is too small to see at this scale and the solid lines hide the dashed ones. A more detailed discussion and presentation of some of the individual current scenarios for usual operating conditions can be found in section 3.0. The cases considered in detail were all coils on, and individual circuits off with all others on.

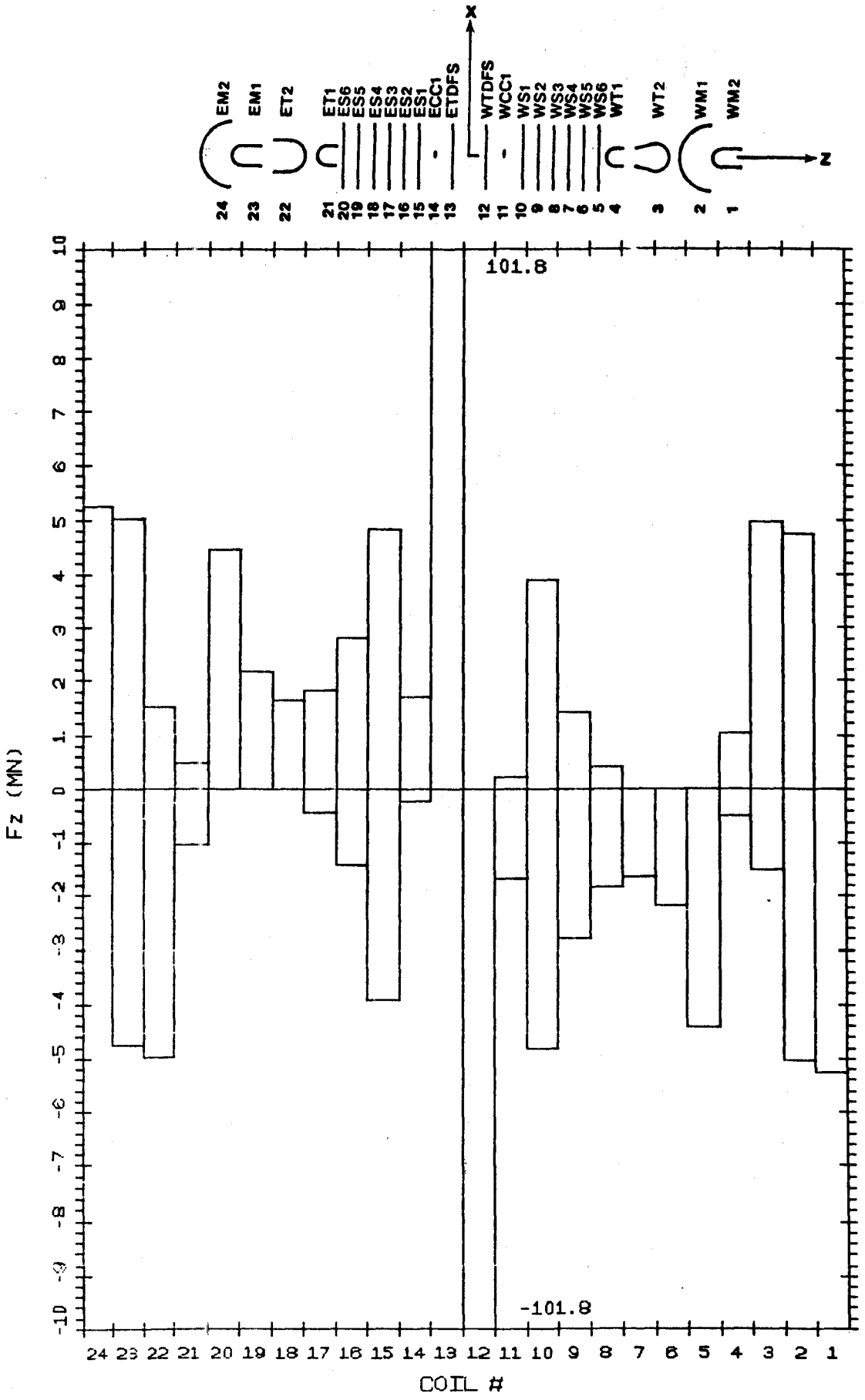

Figure 1.2 Peak Axial Loads - Static

Table 1.3 Peak Radial Loads per Unit Length Under Normal Operating Conditions

coil #	coil name	X=0 Plane Fr (MN/m)	Current Scenario*	Y=0 Plane Fr (MN/m)	Current Scenario*
1	WM2	4.95	111111111	5.41	111111111
2	WM1	6.03	111111111	3.99	111111111
3	WT2	0.80	101111111	1.34	111111111
4	WT1	0.87	111111111	0.66	111111111
5	WS6	0.67	111011111	0.65	110111111
6	WS5	0.75	111011111	0.75	111111111
7	WS4	0.82	111111111	0.83	111111111
8	WS3	0.90	111111111	0.90	111111111
9	WS2	1.01	111111111	1.01	111111111
10	WS1	1.16	111110111	1.16	111110111
11	WCCL	34.0	111111111	34.0	111111111
12	WTDPS2	28.1	111110111	28.1	111110111
13	ETDPS2	28.1	111110111	28.1	111110111
14	ECCL	34.0	111111111	34.0	111111111
15	ES1	1.16	111110111	1.16	111110111
16	ES2	1.01	111111111	1.01	111111111
17	ES3	0.90	111111111	0.90	111111111
18	ES4	0.83	111111111	0.82	111111111
19	ES5	0.75	111111111	0.75	111011111
20	ES6	0.65	110111111	0.67	111011111
21	ET1	0.66	111111111	0.87	111111111
22	ET2	1.34	111111111	0.80	111111101
23	EM1	3.99	111111111	6.03	111111111
24	EM2	5.41	111111111	4.95	111111111

---

* each digit represents a circuit on (1) or off (0)
e.g. 110011100 means circuits 1,2,5,6,7 are on and circuits 3,4,8,9 are off

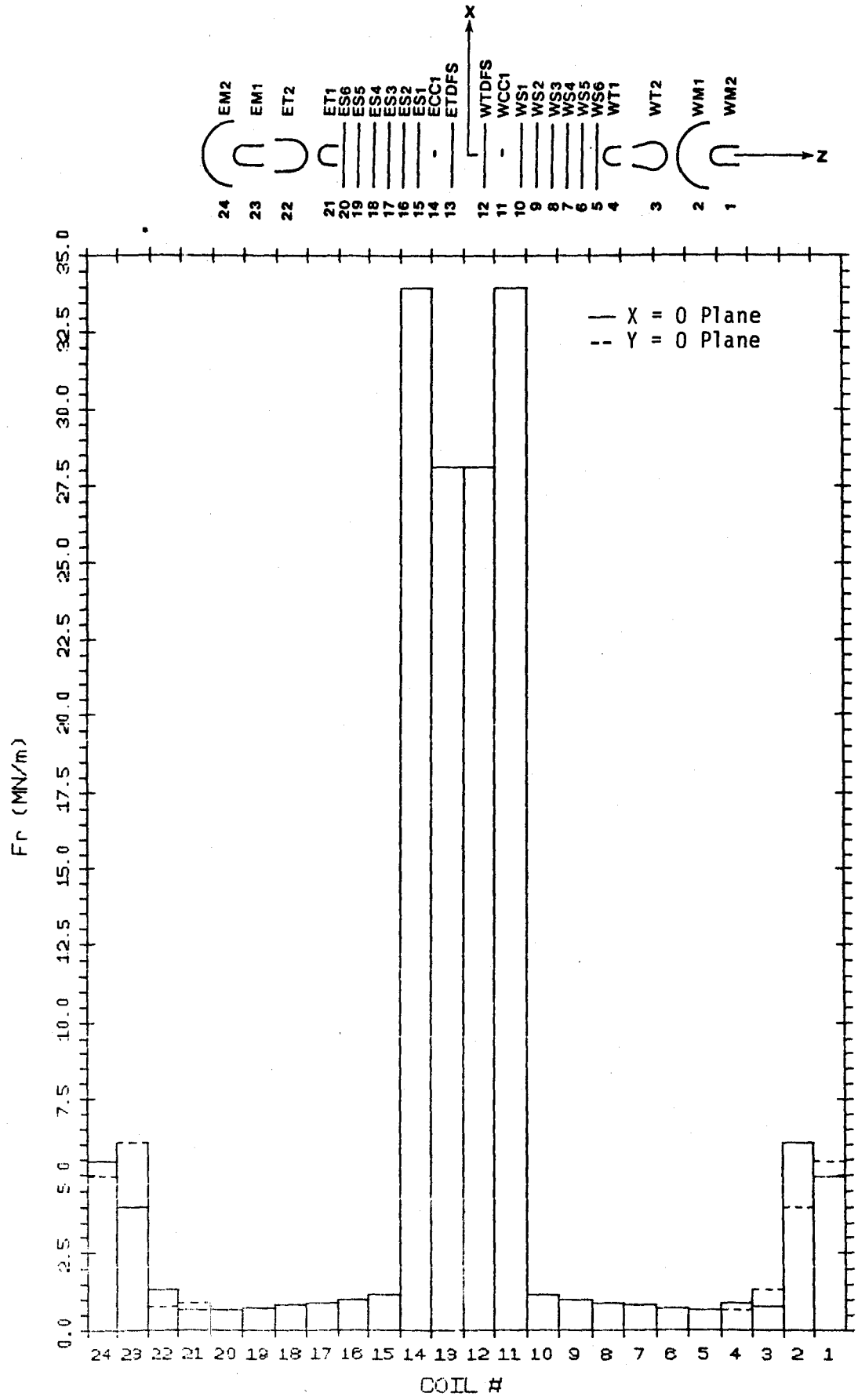

Figure 1.3 Peak Radial Loads Per Unit Length - Static

The next set of analyses investigated the coil loading experienced during discharge transients. The lumped circuit parameter model used is discussed in section 2.0. The scenarios considered were: (1) all coils on and then discharged simultaneously, and (2) all coils on then a single coil short-circuited with all others discharging. The extreme loads on different coils can occur at different times during the transient, and, therefore, cannot be used to represent a subsystem loading - e.g. peak axial loads on coils 1 and 2 (WM2 and WM1) cannot be summed to get a worst case loading on the set. Such an assumption would be conservative, but possibly too much so.

Table 1.4 presents the worst case axial forces acting on each coil for the normal discharge case. Some coils actually experience a load reversal during discharge, because all coils do not discharge at identical rates. Figure 1.4 shows the same information in bar chart form. Table 1.5 and Figure 1.5 present the worst case radial forces per unit length in the X=0 plane (solid lines) and Y=0 plane (dashed lines) for the normal discharge case.

Similarly, Tables 1.6 and 1.7 and Figures 1.6 and 1.7 present the worst case loads on each coil for all the single coil short-circuit transients. Each coil from 1 to 12 (WM2 to WTFDS2) in turn was assumed to have a short across the entire coil with a short resistance of 1 micro-Ohm. The other coils discharge through their dump resistors. The case numbers correspond to the coil number that contains the short during the worst transient for the coil. Case 0 is the normal discharge of all coils. The notation 0+ implies a small load (order of kN). WT2 experiences a small load reversal in the radial force per unit length in the X=0 plane. Since only half the coils were shorted individually because of the system symmetry, the worst case forces on the coils are tabulated for coils 1-12 only. The loads on all the coils are presented in the figures.

A more detailed discussion of the transient analyses is given in Section 4.0. Also presented are the loadings for the individual current scenarios.

Finally, Tables 1.8 and 1.9 list the worst case loadings for each coil from all the usual and fault current scenarios investigated. If the load is from a static scenario, the scenario is given as the nine digit number describing which circuits are charged and which are not. If the load arises during a coil short-circuit transient, the coil being shorted is given. Only the first 12 coils are listed. The peak forces on the other coils will have the expected symmetry or anti-symmetry. These worst case loads are shown in Figures 1.8 and 1.9. All coils are shown.

Table 1.4 Peak Axial Loads Under Normal Discharge Conditions

coil #	coil name	Maximum Fz (MN)	Minimum Fz (MN)
1	WM2	0	-5.27
2	WM1	0	-0.28
3	WT2	3.44	0
4	WT1	0.56	0
5	WS6	0	-3.89
6	WS5	0	-1.84
7	WS4	0	-1.46
8	WS3	0	-1.74
9	WS2	0.15	-2.75
10	WS1	0+	-4.78
11	WCC1	0	-1.47
12	WTDFS2	0	-90.3
13	ETDFS2	90.3	0
14	ECC1	1.47	0
15	ES1	4.78	0+
16	ES2	2.75	-0.15
17	ES3	1.74	0
18	ES4	1.46	0
19	ES5	1.84	0
20	ES6	3.89	0
21	ET1	0	-0.56
22	ET2	0	-3.44
23	EM1	0.28	0
24	EM2	5.27	0

0+ denotes a small force on the order of kN.

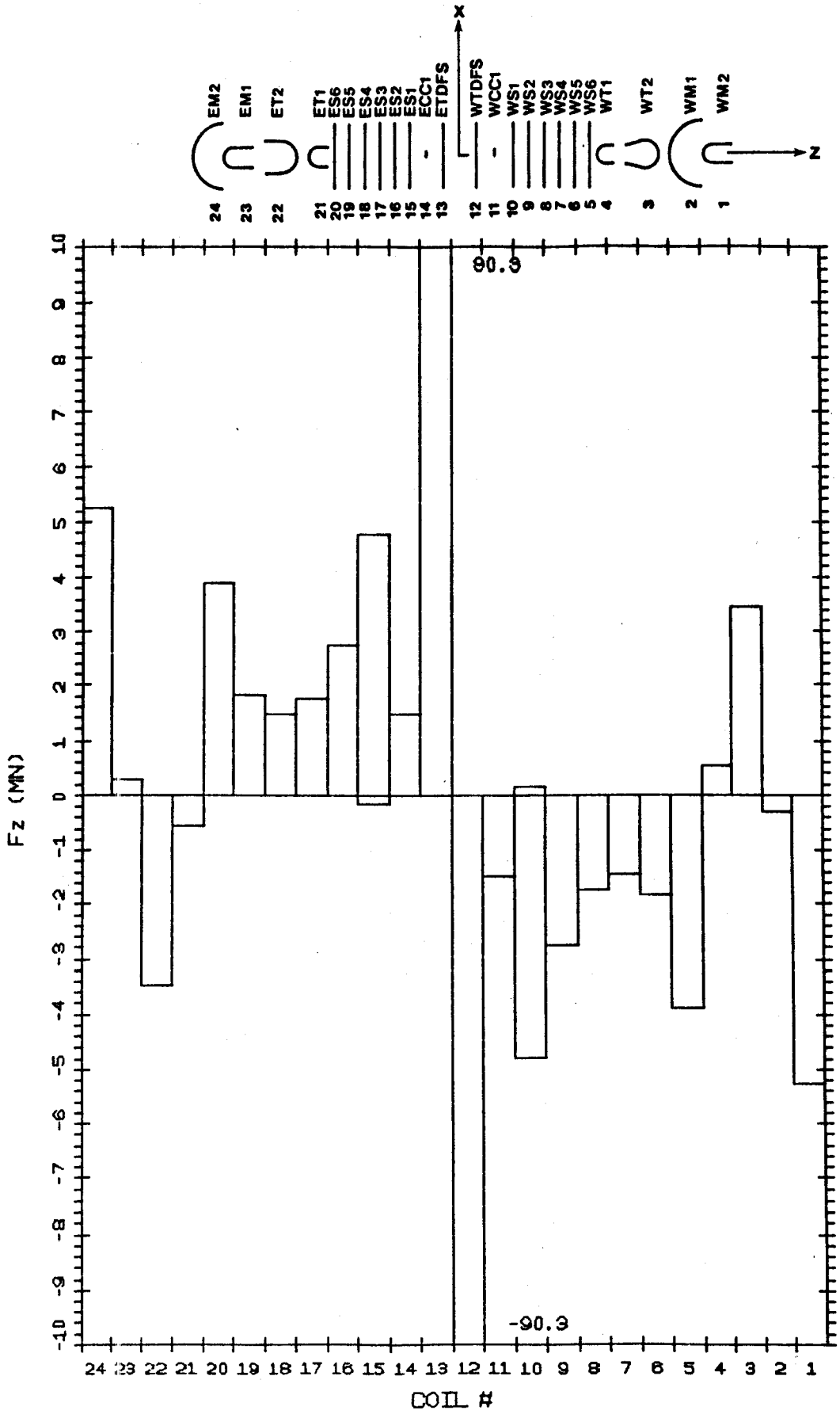

Figure 1.4 Peak Axial Forces - Normal Discharge

Table 1.5 Peak Radial Loads per Unit Length Under Normal Discharge Conditions

coil #	coil name	X=0 Plane Fr (MN/m)	Y=0 Plane Fr (MN/m)
1	WM2	4.95	5.41
2	WM1	6.03	3.99
3	WT2	0.47	1.34
4	WT1	0.87	0.66
5	WS6	0.64	0.65
6	WS5	0.75	0.75
7	WS4	0.82	0.83
8	WS3	0.90	0.90
9	WS2	1.01	1.01
10	WS1	1.18	1.18
11	WCC1	34.0	34.0
12	WTDFS2	28.1	28.1
13	ETDFS2	28.1	28.1
14	ECC1	34.0	34.0
15	ES1	1.18	1.18
16	ES2	1.01	1.01
17	ES3	0.90	0.90
18	ES4	0.83	0.82
19	ES5	0.75	0.75
20	ES6	0.65	0.64
21	ET1	0.66	0.87
22	ET2	1.34	0.47
23	EM1	3.99	6.03
24	EM2	5.41	4.95

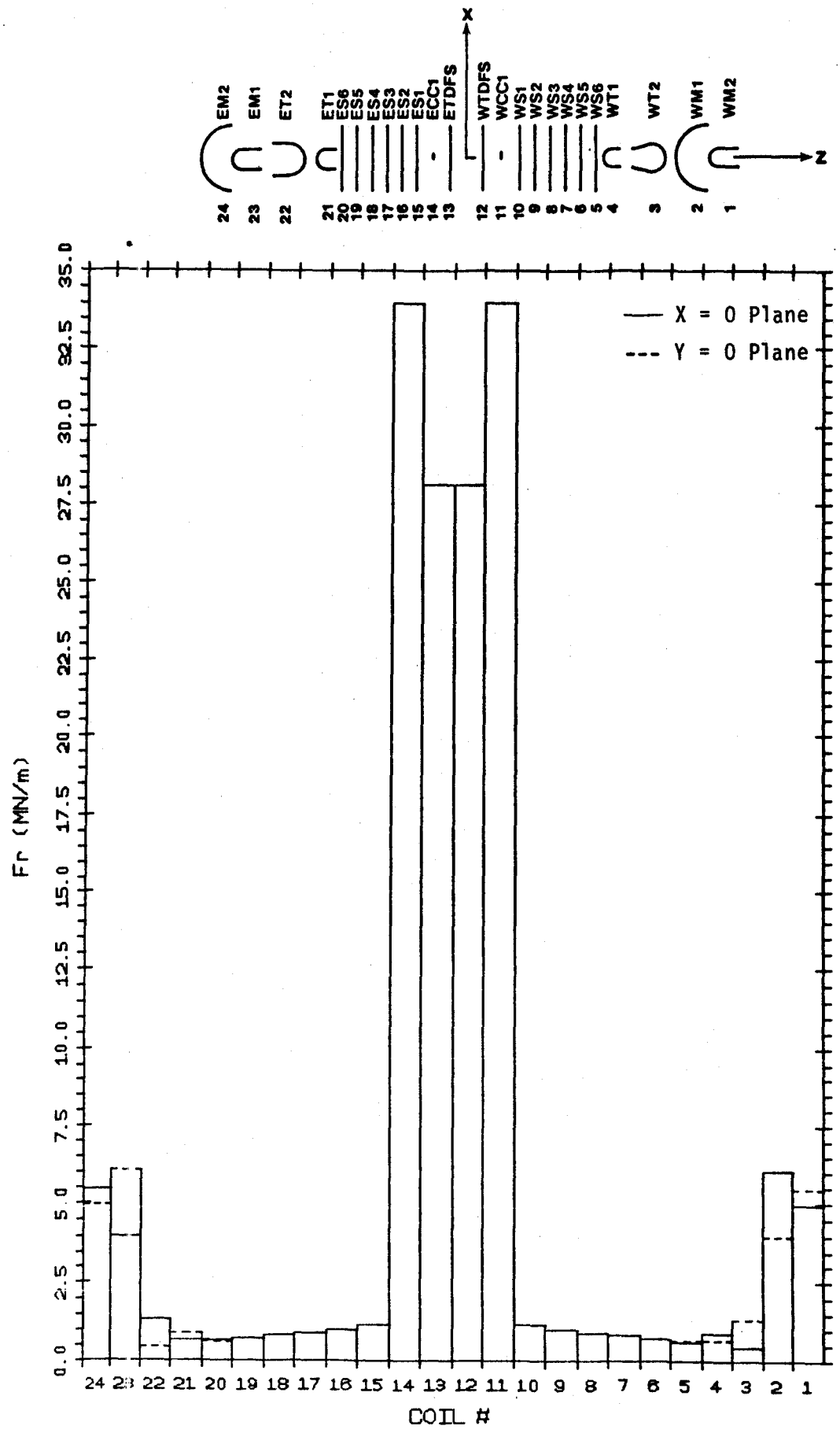

Figure 1.5 Peak Radial Forces Per Unit Length - Normal Discharge

Table 1.6 Peak Axial Loads On Coils Due to Single Coil Short-Circuits

Coil #	Coil Name	Maximum Fz(MN)	Case #	Minimum Fz(MN)	Case #
1	WM2	0	-	-5.27	12
2	WM1	1.09	1	-1.39	3
3	WT2	3.60	2	-1.12	4
4	WT1	0.56	0	-0.04	4
5	WS6	0+	4	-3.99	5
6	WS5	0.56	5	-2.29	6
7	WS4	0.75	6	-1.86	8
8	WS3	0.89	7	-2.10	8
9	WS2	1.12	8	-3.06	9
10	WS1	1.85	9	-4.83	10
11	WCC1	0	-	-1.47	12
12	WTDSF2	0.90	10	-90.3	12

Table 1.7 Peak Radial Loads Per Unit Length On Coils Due to Single Coil Short-Circuits

Coil #	Coil Name	X=0 Plane Maximum Fr(MN/m)	Case #	Y=0 Plane Minimum Fr(MN/m)	Case #
1	WM2	4.95	0	5.41	0
2	WM1	6.03	0	4.13	2
3	WT2	0.51/-.03^	3/2	1.34	0
4	WT1	0.87	0	0.66	0
5	WS6	1.15	5	1.15	5
6	WS5	1.53	6	1.53	6
7	WS4	1.78	7	1.78	7
8	WS3	2.05	8	2.05	8
9	WS2	2.46	9	2.46	9
10	WS1	3.23	10	3.23	10
11	WCC1	49.0	11	49.0	11
12	WTDSF2	30.4	12	30.4	12

0+ denotes a small force on the order of kN.

^ a slight force reversal

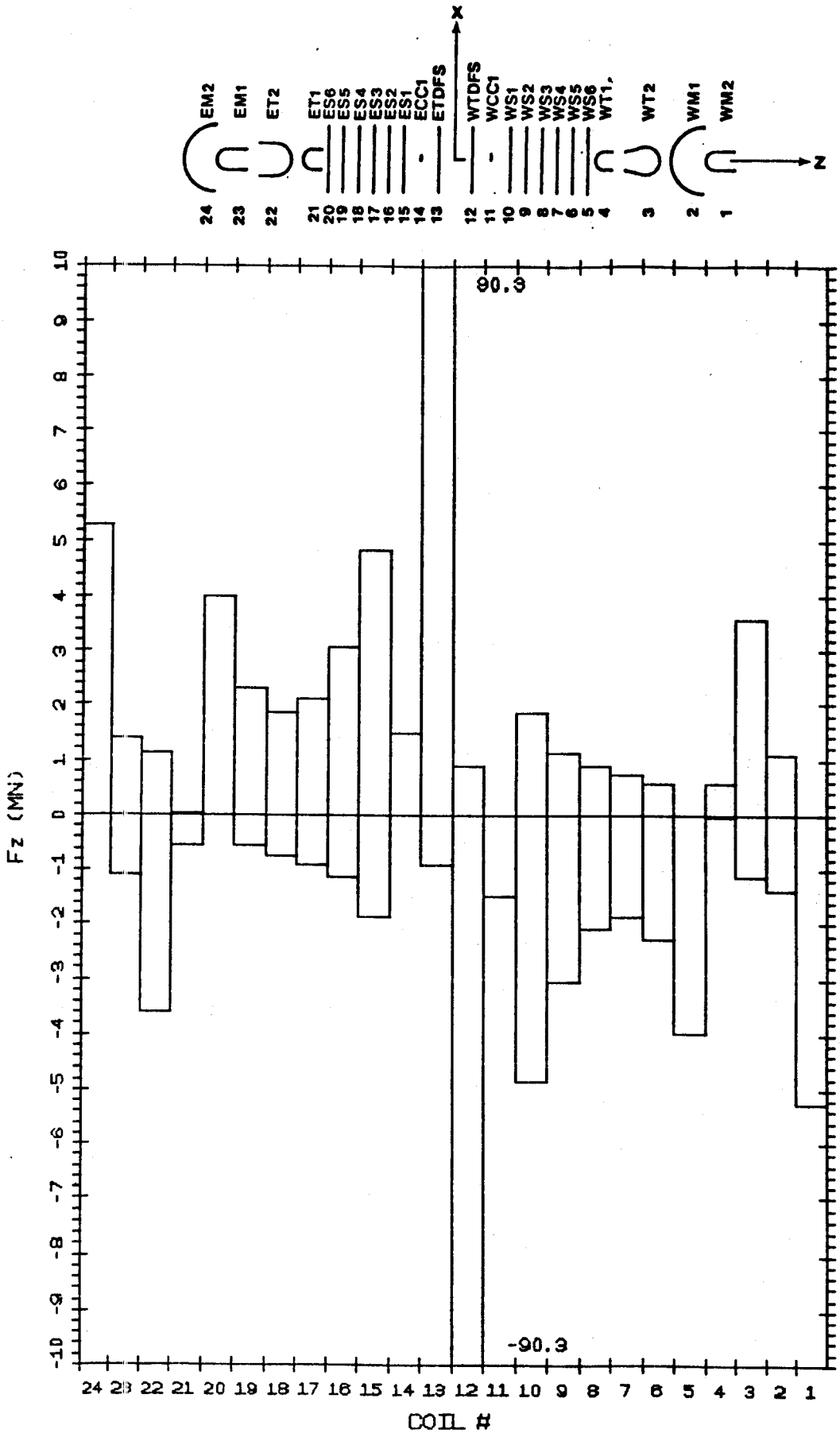

Figure 1.6 Peak Axial Forces Due To A Single Coil Short Circuit

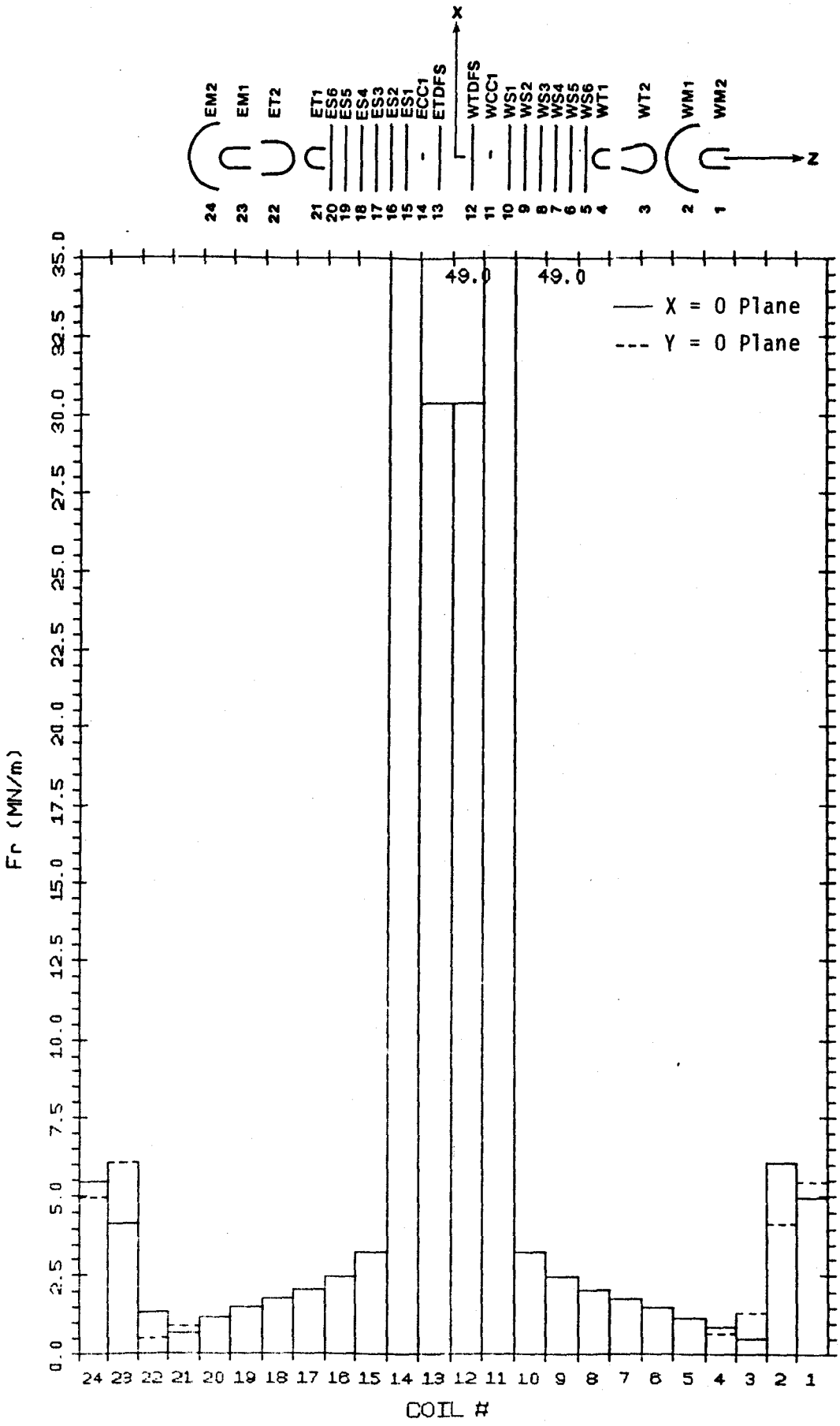

Figure 1.7 Peak Radial Forces Per Unit Length Due To A Single Coil Short

Table 1.8 Peak Axial Loads Under All Conditions

coil #	coil name	Maximum Fz (MN)	Current Scenario*	Minimum Fz (MN)	Current Scenario*
1	WM2	0	-	-5.27	111111111
2	WM1	4.75	110000000	-5.02	011111111
3	WT2	4.96	111000000	-1.51	001111111
4	WT1	1.04	111100000	-0.48	000111111
5	WS6	0+	short 4	-4.44	000011111
6	WS5	0.56	short 5	-2.29	short 6
7	WS4	0.75	short 6	-1.86	short 8
8	WS3	0.89	short 7	-2.10	short 8
9	WS2	1.41	111110000	-2.80	000011111
10	WS1	3.91	111110000	-4.83	short 10
11	WCC1	0.21	111111000	-1.68	000001111
12	WTDFS2	0.90	short 10	-102.	000000111

Table 1.9 Peak Radial Loads Per Unit Length
All Conditions

coil #	coil name	X=0 Plane Fr (MN/m)	Current Scenario*	Y=0 Plane Fr (MN/m)	Current Scenario*
1	WM2	4.95	111111111	5.41	111111111
2	WM1	6.03	111111111	4.13	short 2
3	WT2	0.80/-.03^	101111111	1.34	111111111
4	WT1	0.87	111111111	0.66	111111111
5	WS6	1.15	short 5	1.15	short 5
6	WS5	1.53	short 6	1.53	short 6
7	WS4	1.78	short 7	1.78	short 7
8	WS3	2.05	short 8	2.05	short 8
9	WS2	2.46	short 9	2.46	short 9
10	WS1	3.23	short 10	3.23	short 10
11	WCC1	49.0	short 11	49.0	short 11
12	WTDFS2	30.4	short 12	30.4	short 12

---

* each digit represents a circuit on (1) or off (0)
e.g. 110011100 means circuits 1,2,5,6,7 are on and circuits 3,4,8,9 are off

0+ denotes a small force of the order of kN.

^ force reversal for short 2.

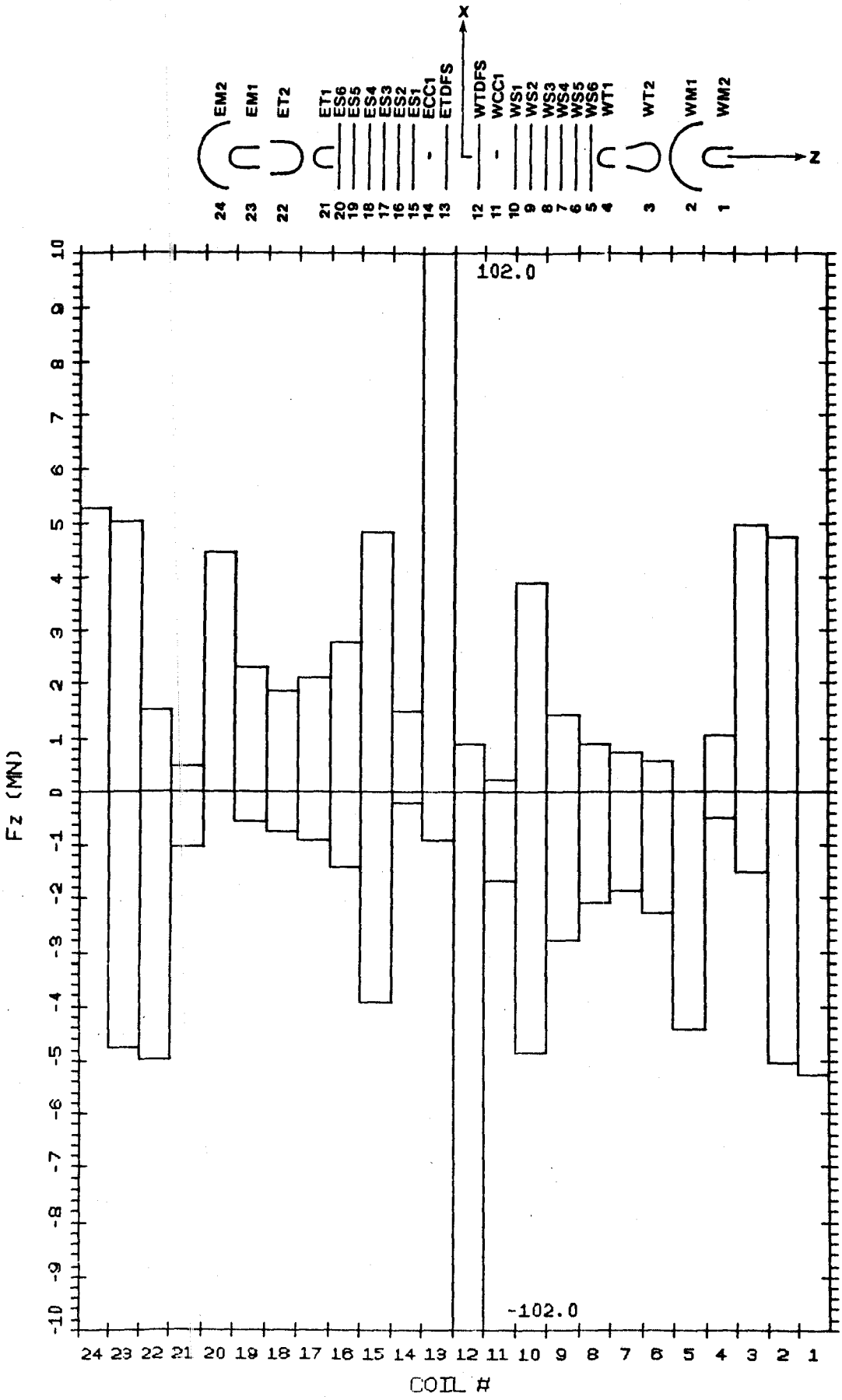

Figure 1.8 Peak Axial Loads For All Current Scenarios Considered

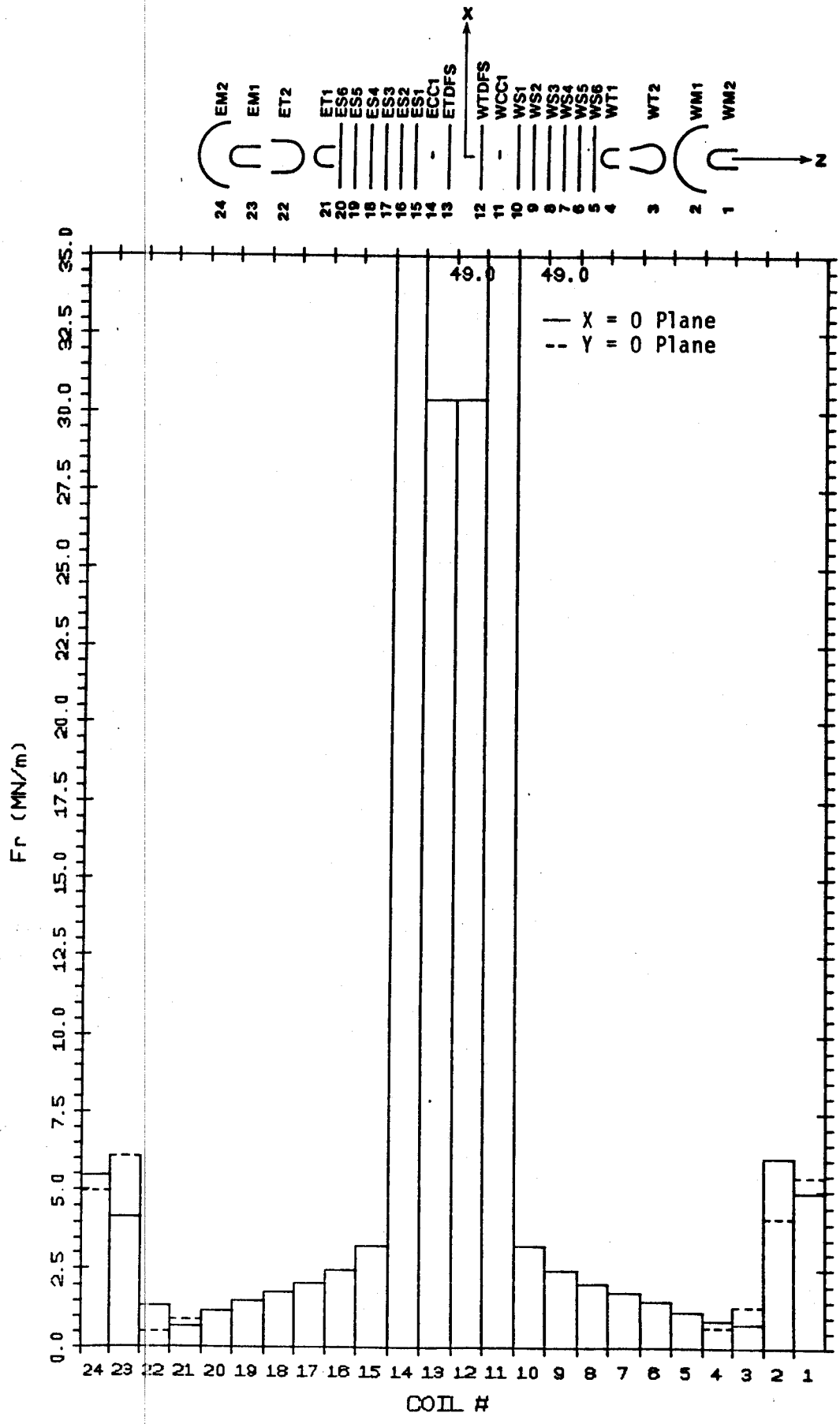

Figure 1.9 Peak Radial Loads Per Unit Length For All Current Scenarios

2.0 COIL AND CIRCUIT MODELS

The individual coils in the mirror machine were modeled with lumped current filaments made up of piecewise straight segments or sticks. The number of filaments used to represent the coil cross-section varied from coil to coil. Filaments were used in the solenoids for convenience. Checks on the accuracy of both inductance and force were made using uniform current density solenoid models.

Figure 2.1 shows the typical coil geometries for a C-shaped and solenoid magnet. Also indicated are the necessary inputs to generate a stick model of the coil. Table 2.1 lists the inputs and other critical parameters for each coil in the machine. In addition to the geometry, the table also lists the overall current density, the ampere-turns, the full operating current, the number of turns, the size of the dump resistor, and the coil self-inductance.

The model used for both the inductance and force calculations is shown in Figure 2.2. The coils WM2, WM1, EM2, and EM1 were modeled with 6 filaments (2 by 3). The other four C-shaped magnets were modeled with 4 filaments (2 by 2). The central cell solenoids were modeled with 2 filaments (radially). The choke coils each had 4 filaments (2 by 2). Each layer of the large solenoids was modeled with 2 filaments (axially). Each filament was broken up into 40 sticks for both solenoids and C-shaped magnets.

The effect of the number of filaments on the calculation is shown in Figure 2.3. The axial field profile is shown for both the model described above as well as for a single filament model for each coil. Note that the peak field under the choke coils decreased from 14.7 to 12.7 T. The primary effect of a finer model is to determine more accurately the peak fields under the choke and C-shaped coils. Since the model was to be used for calculating inductances and fields at the coils, the finer model was used.

The fine model was used to construct three force influence coefficient matrices. Each element of these 24 by 24 matrices represented the force on a coil (or force per unit length at a point) due to another coil. The terms were per unit current in all coils. Therefore, given a current scenario, the necessary multiplication yields the axial force. That is:

$$F(k)=I(k)\sum_{j=1}^{24} f(k,j)*I(j) \quad ,$$

where I(k) is the current in the kth coil. f(k,j) is the force on coil k per unit current in coil k due to a unit current in coil j. Similar expressions hold for the radial forces per unit length.

Model of a C-Shaped Magnet

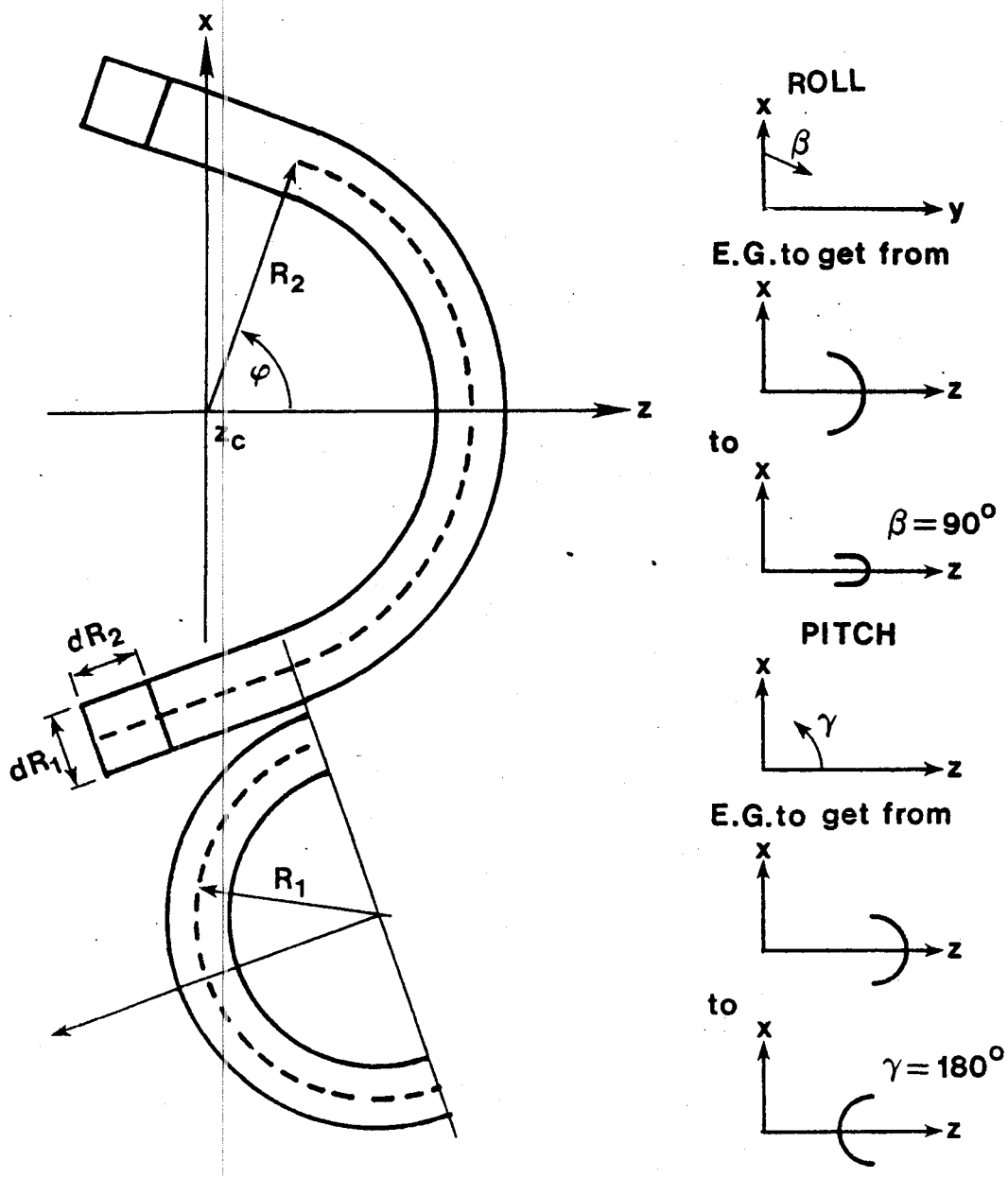

INPUTS C-Shaped:

$R_1, R_2, dR_1, dR_2, \left\{ \begin{matrix} \lambda j \\ NI \end{matrix} \right\}$

φ, γ β

↑ ↑

PITCH ROLL

Figure 2.1.a C-Shaped Magnet Model

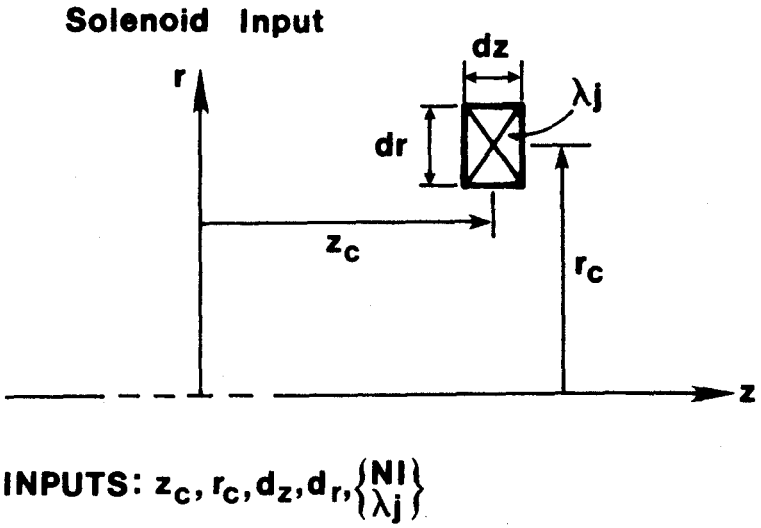

Figure 2.1.b Solenoid Magnet Model

TABLE 2.1 MFTFB+T COIL PARAMETERS

COIL NAME	COIL #	Z_o (m)	R_1 (m)	R_2 (m)	dR_1 (m)	dR_2 (m)	ϕ (°)	γ (°)	β (°)	λj^2 (A/cm²)	NI (MA-T)	I (A)	N	R_D (m)	L (H)
WM2, EM2	1, 24	± 20.15	0.75	2.50	0.3277	0.8235	75	0,180	90,0	2271	6.13	4403	1392	.085	11.1
WM1, EM1	2, 23	± 19.85	0.75	2.50	0.3277	0.8235	75	180,180	0,90	1997	5.39	3872	1392	.085	11.1
WT2, ET2	3, 22	± 15.20	1.35	1.20	0.337	0.340	110	0,0	0,90	2726	3.12	5206	600	.020	2.7
WT1, ET1	4, 21	± 11.86	0.70	0.875	0.204 ΔR	0.449 ΔZ	100	0,130	90,0	1220	1.12	2328	480	.044	.86
WS6, ES6	5, 20	± 10.625	2.50	-	0.336	0.163	-	-	-	1997	1.09	1823	600	.029	3.6
WS5, ES5	6, 19	± 9.375	2.50	-	0.336	0.163	-	-	-	1997	1.09	1823	600	.029	3.6
WS4, ES4	7, 18	± 8.125	2.50	-	0.336	0.163	-	-	-	1997	1.09	1823	600	.029	3.6
WS3, ES3	8, 17	± 6.875	2.50	-	0.336	0.163	-	-	-	1997	1.09	1823	600	.029	3.6
WS2, ES2	9, 16	± 5.625	2.50	-	0.336	0.163	-	-	-	1997	1.09	1823	600	.029	3.6
WS1, ES1	10, 15	± 4.375	2.50	-	0.336	0.163	-	-	-	1997	1.09	1823	600	.029	3.6
WCC1, ECC1	11, 14	± 2.778	0.272	-	0.30	0.480	-	-	-	3573	5.15	107190	48	4.7×10^{-4}	5.56×10^{-4}
WTDFS2, ETDFS2	12, 13	± 1.3625	2.092	-	0.184	0.80	-	-	-	1075	1.58		198		
		± 1.3625	2.276	-	0.184	0.80	-	-	-	1326	1.95	8000	244	.125	16.4
		± 1.3625	2.460	-	0.184	0.80	-	-	-	1889	2.78		347		
		± 1.3625	2.741	-	0.378	0.80	-			2135	6.46		807		

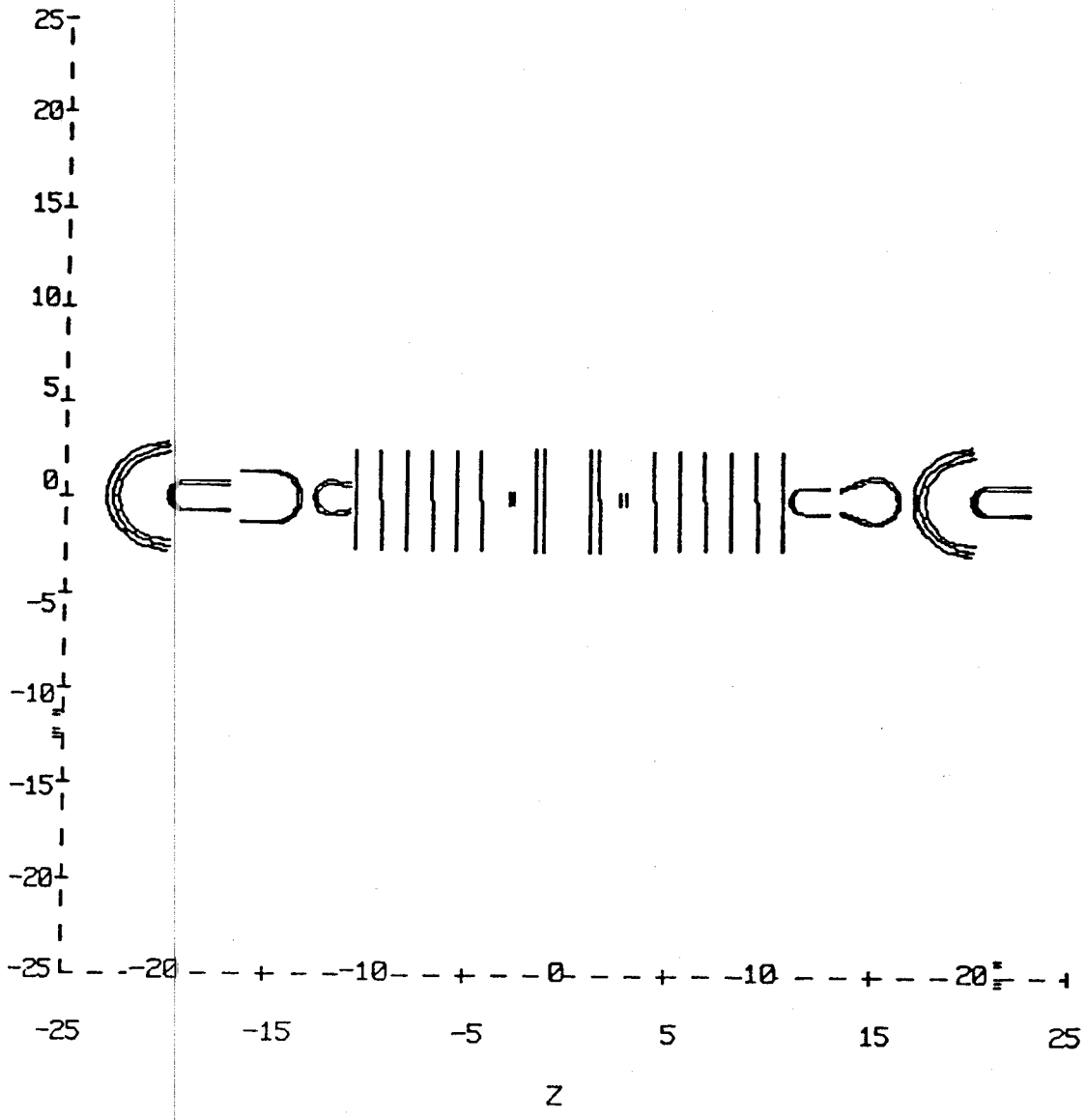

Figure 2.2 Side View of Multiple Filament Model of MFTFB+T

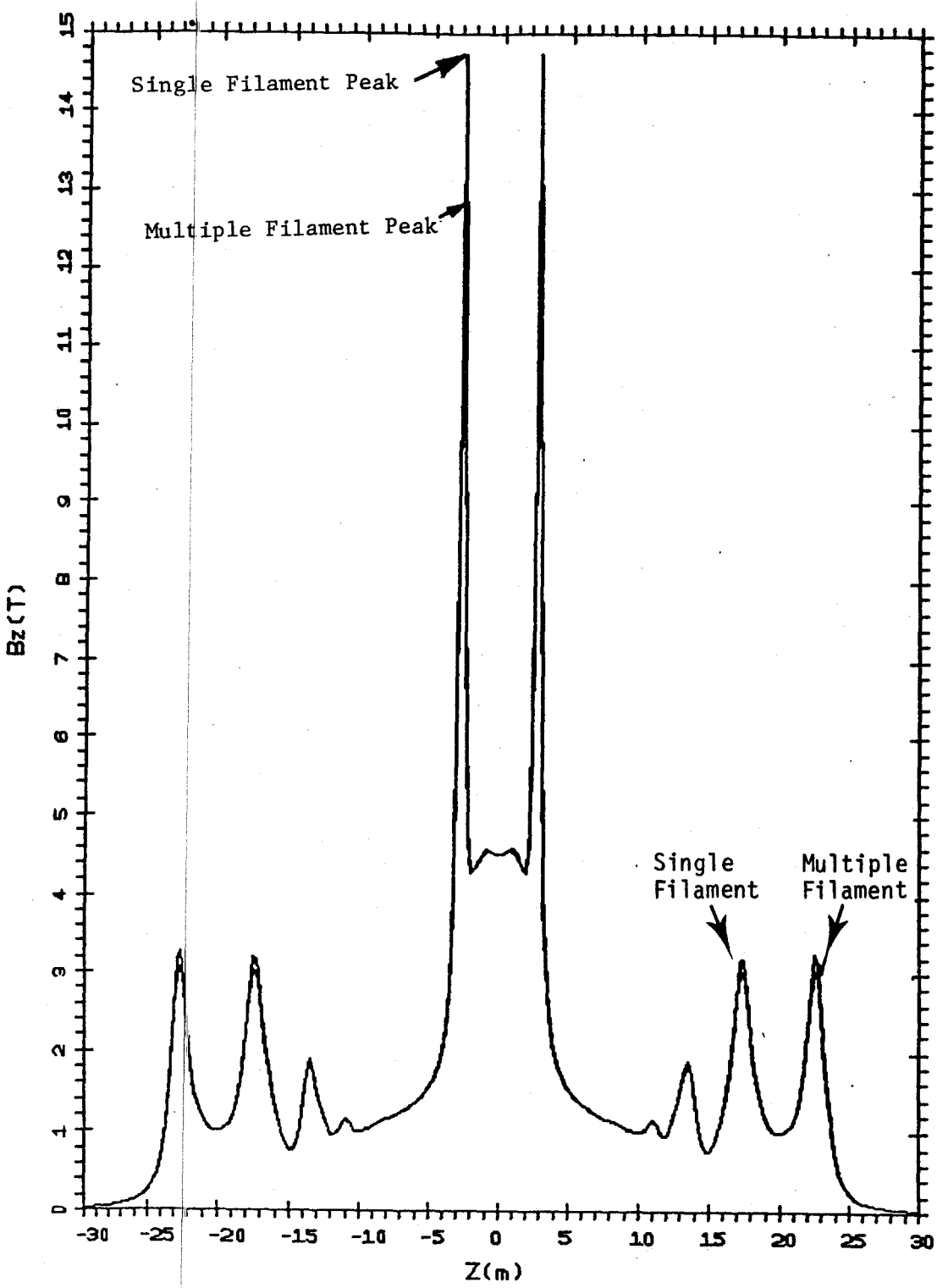

Figure 2.3 Axial Field Profile for Two Models

The axial force calculations are on a coil basis. That is, the J x B body force densities are integrated over the coil volume to obtain a total force. The radial forces, on the other hand, are a local force calculated on a per unit running length basis. The integrated radial force is, of course, zero. The radial forces per unit length were calculated at two points in each coil. These points are in the X=0 and Y=0 planes and correspond to local y-directed and x-directed forces, respectively. In a purely solenoidal system, these forces (per unit length) would be equal because of the axial symmetry. The presence of the C-shaped coils perturbs the solenoidal nature of the field and produces nonuniform loadings on the C-shaped coils and on the closest solenoids.

The static load analyses discussed in section 3.0 used these matrices along with a static current scenario vector to determine the forces on the coils.

An inductance matrix was calculated using the fine model discussed above. This matrix was used in the transient load calculations along with the lumped circuit model discussed below. The transient currents were calculated using an eigenvalue/eigenvector expansion for each transient current case. These expansions were used to determine the current versus time behavior of each coil. These current versus time behavior then multiplies the force influence matrices to get the force versus time. The maximum and minimum forces for each scenario were calculated throughout the transient to determine the extreme loads.

The circuit model for the machine is shown in Figure 2.4. As can be seen there are nine independent circuits. The four coils that form the two yin-yang pairs at either end of the machine are on individual circuits. The two transition (C-shaped) coils at either end are connected across the machine to the mirror image coil at the other end. The ten solenoids are on one circuit. The two choke coils are on a single circuit as are the two large solenoids. Also shown are the circuit parameters assumed for the transient analyses. The only transients considered for this effort were full coil shorts with all other coils discharging through their individual dump resistors. Under this assumption the circuits become 24 independent L-R circuits coupled only through the mutuals inductances from coil to coil.

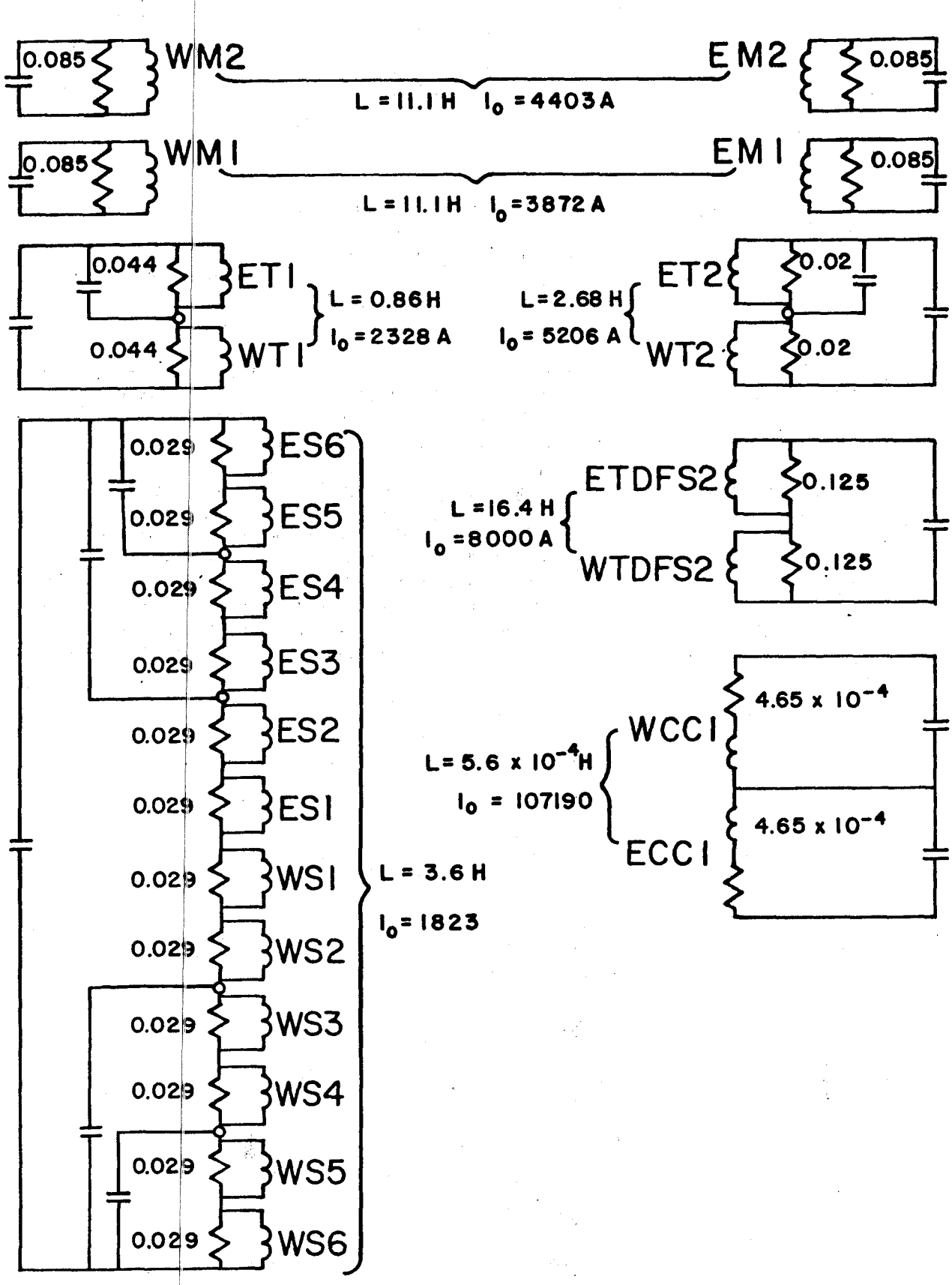

Figure 2.4 MFTFB+T Circuits and Circuit Parameters

3.0 MAGNETOSTATIC LOAD ANALYSES

The first set of analyses performed investigated the worst case loading on the coils under various static normal operating conditions. A normal operating scenario is defined as any combination of one to nine circuits at full current and the remaining circuits at zero current. The data obtained from this analysis are summarized in Tables 1.2 and 1.3 and Figures 1.2 and 1.3.

This section presents the loading for a few of the individual current scenarios. The scenarios given are: (1) all circuits at full operating current; and (2) certain circuits at full current with all others at zero current. These are not necessarily the worst case scenarios.

In the following set of figures, the axial force on each coil is presented in one figure. For scaling purposes, the bars representing the two large solenoids are clipped and the peak values written. The two radial forces per unit length are presented in one figure. The radial force in the X-0 plane is shown as a solid line and the force in the Y=0 plane as a dashed line. For coils with little or no difference in the two forces, the dashed line is hidden by the solid one. Shown at the top of each figure is a side view of the machine with the coils numbered. The coils that have zero current are denoted with an asterisk (*).

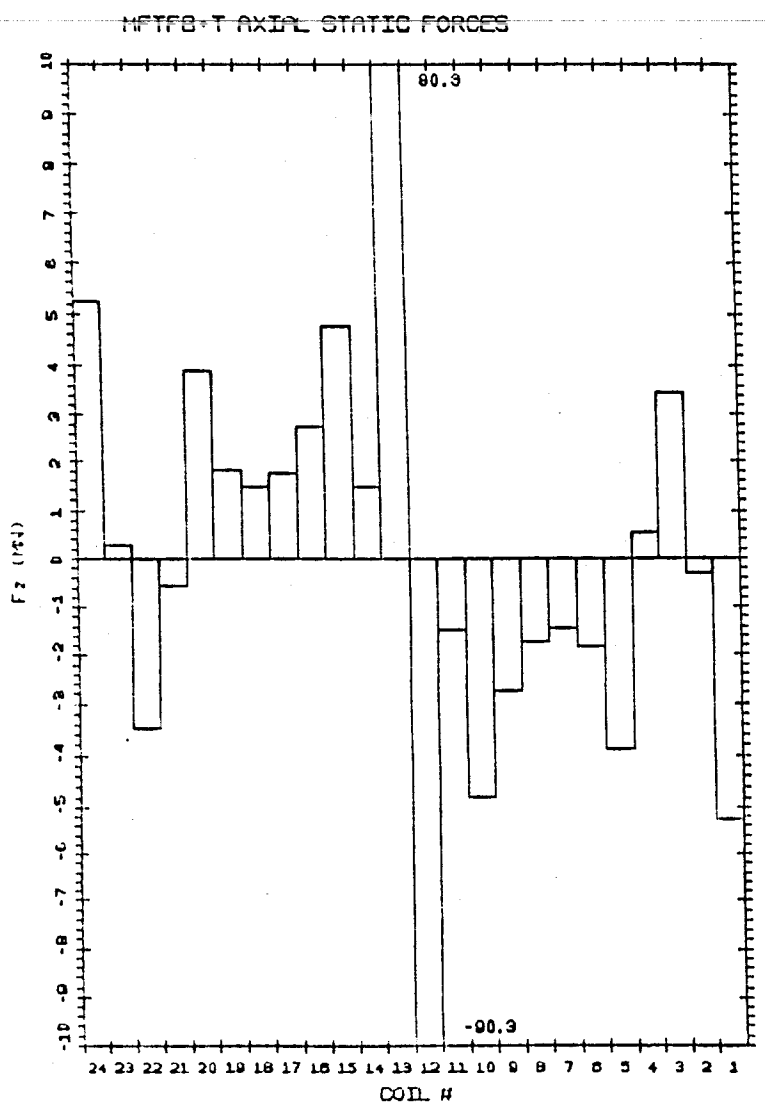

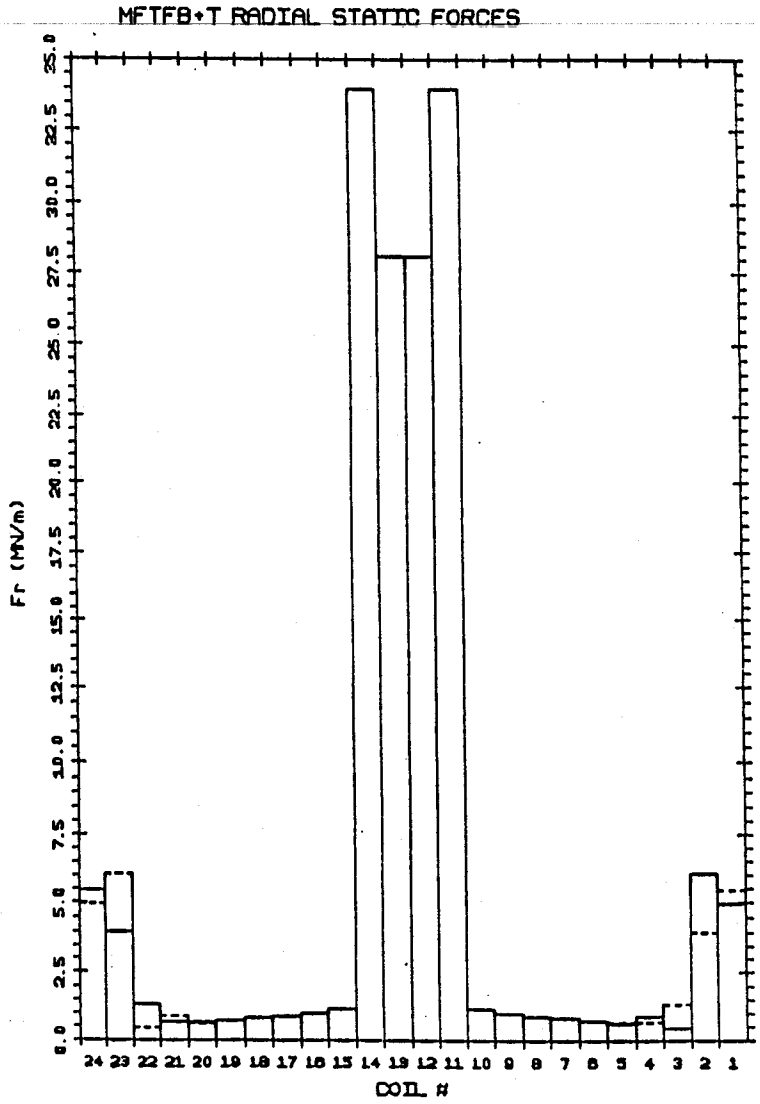

Figure 3.1 - All coils on

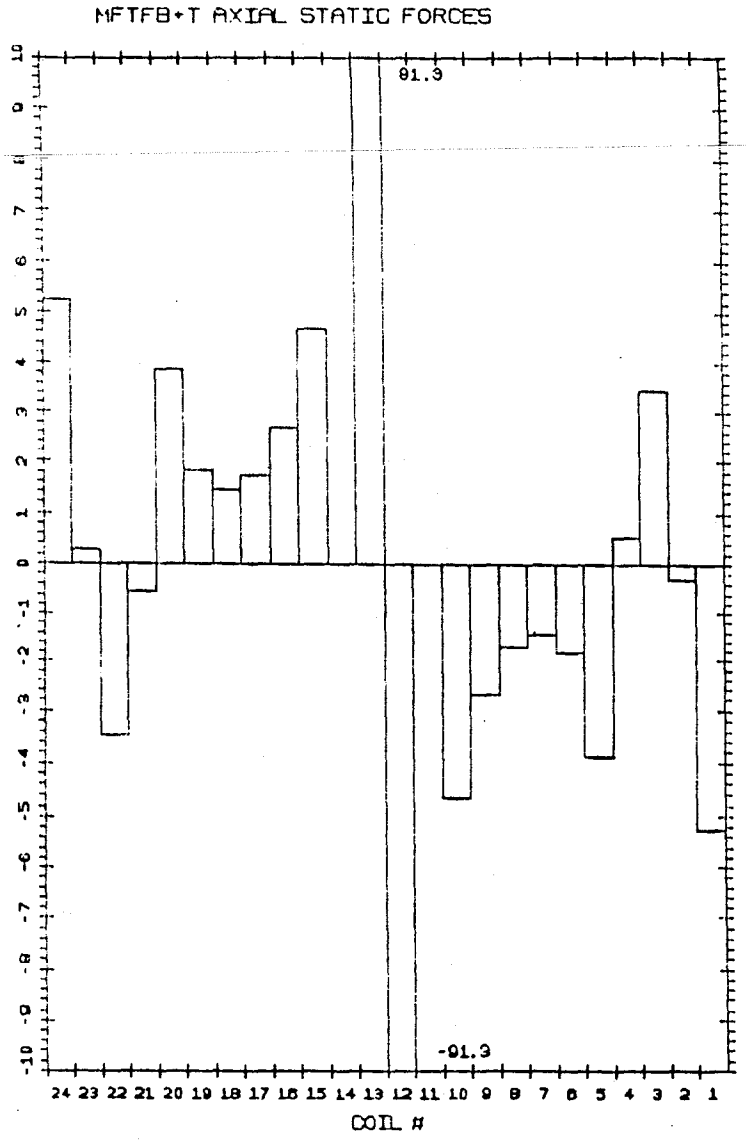

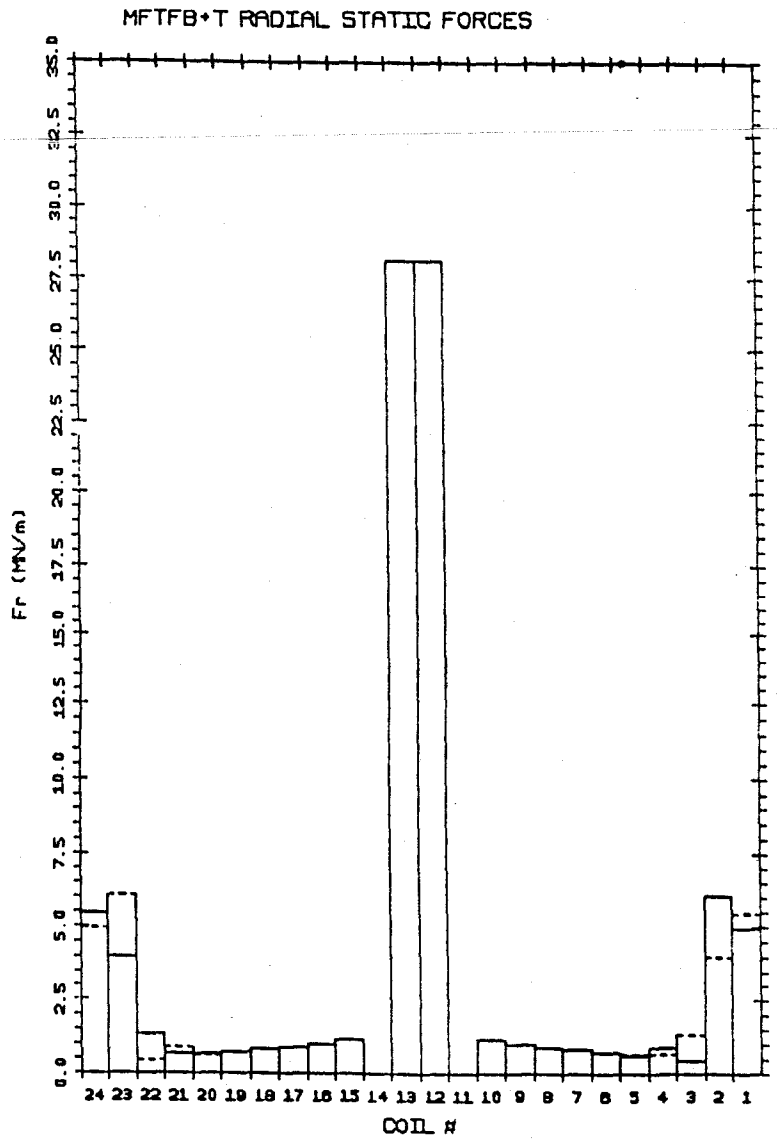

Figures 3.2 - Choke coils off

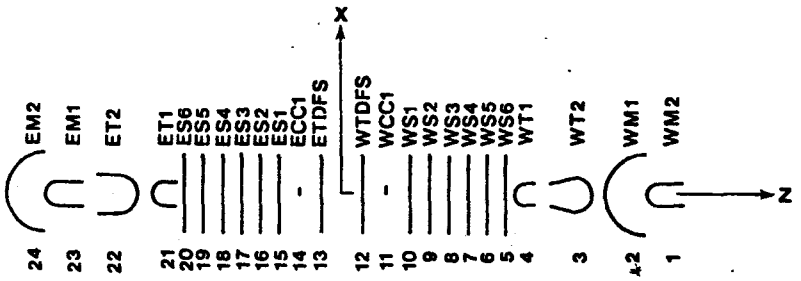

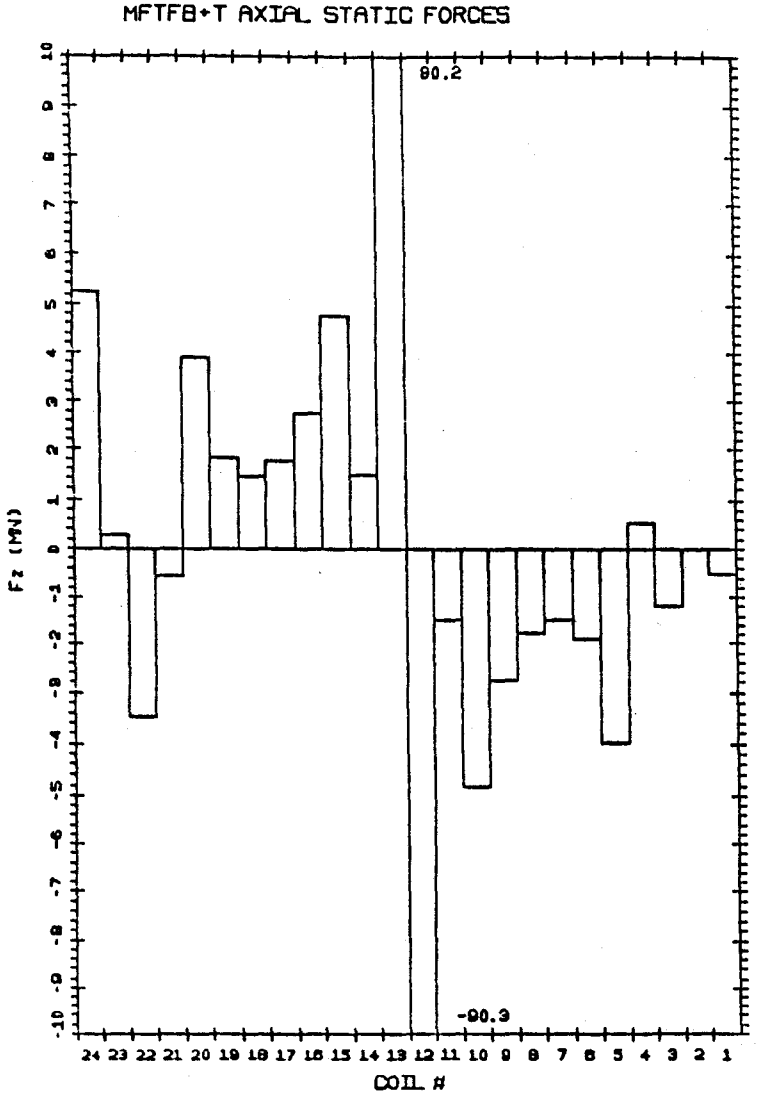

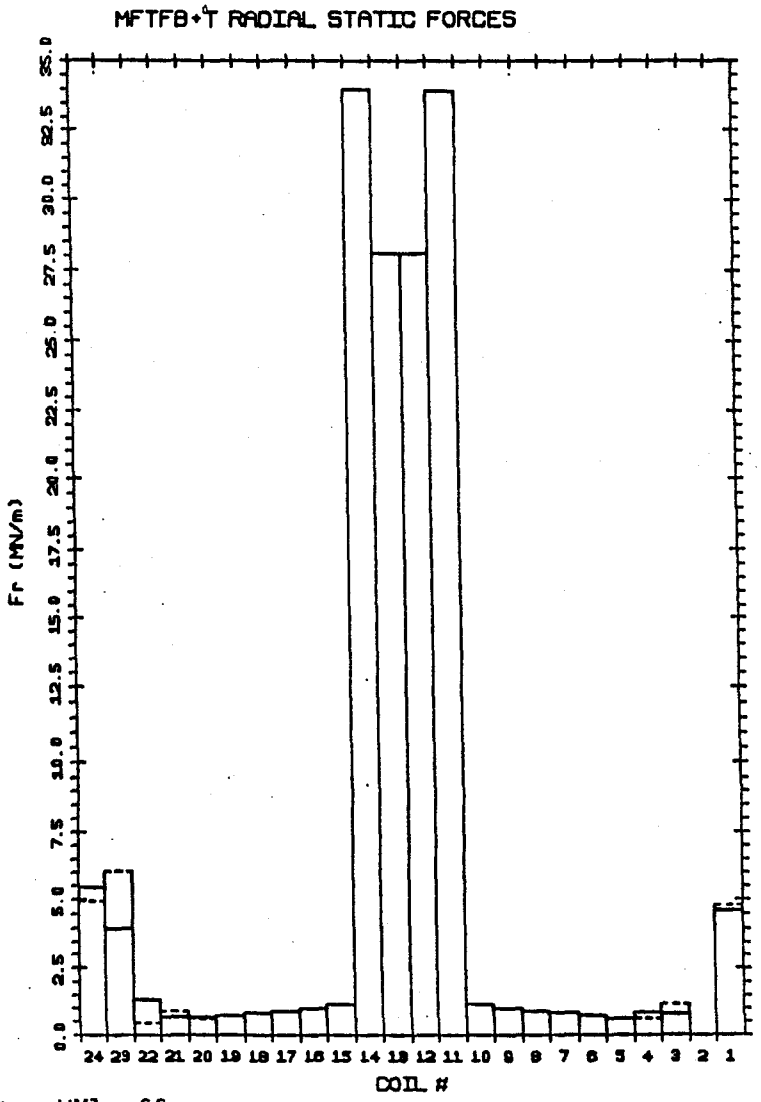

Figure 3.3 - WM1 off

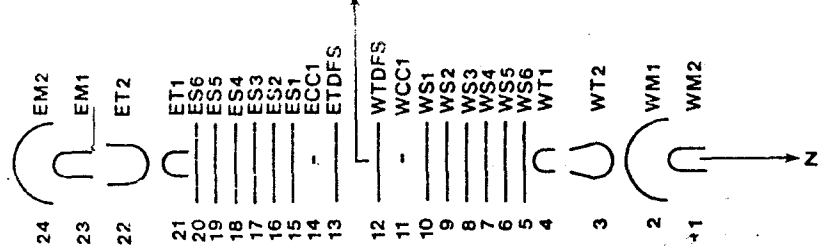

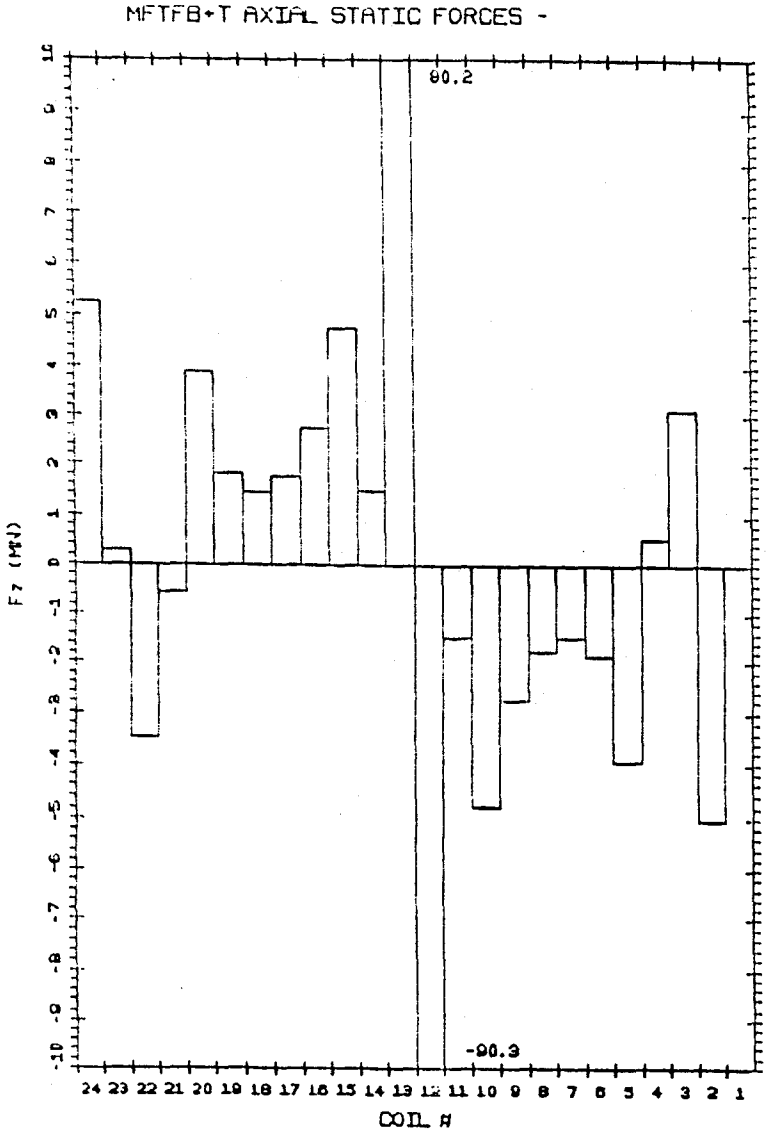

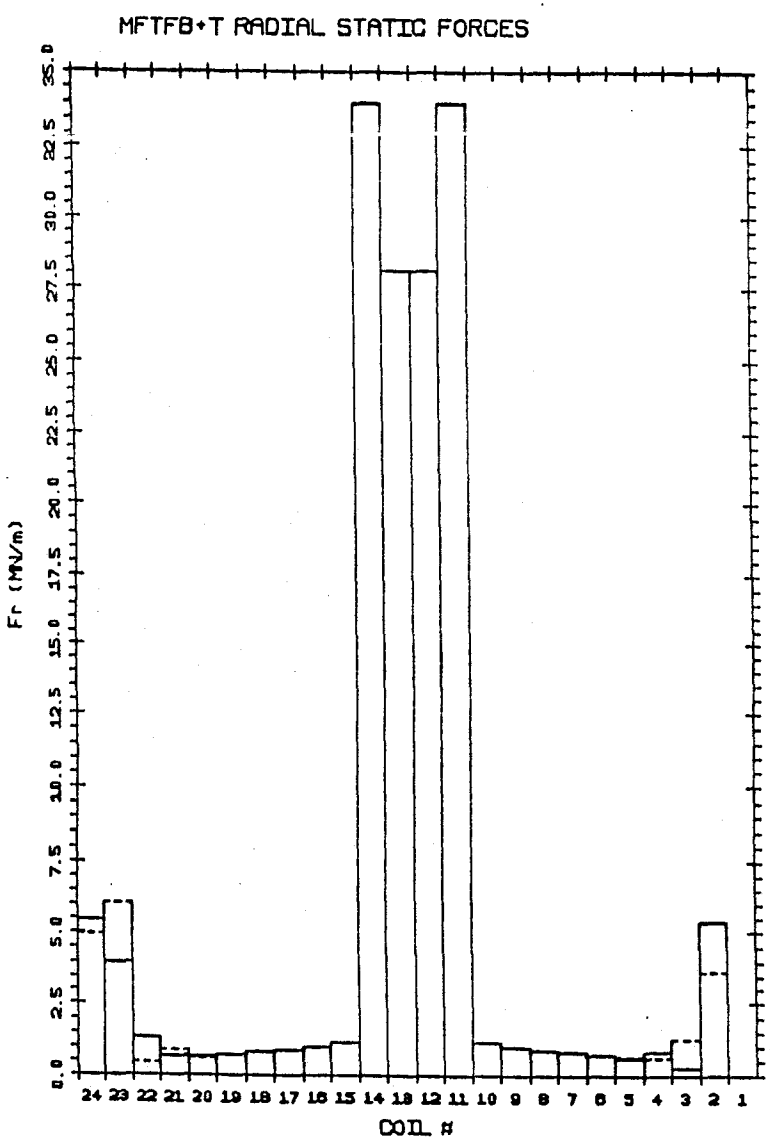

Figure 3.4 - WM2 off

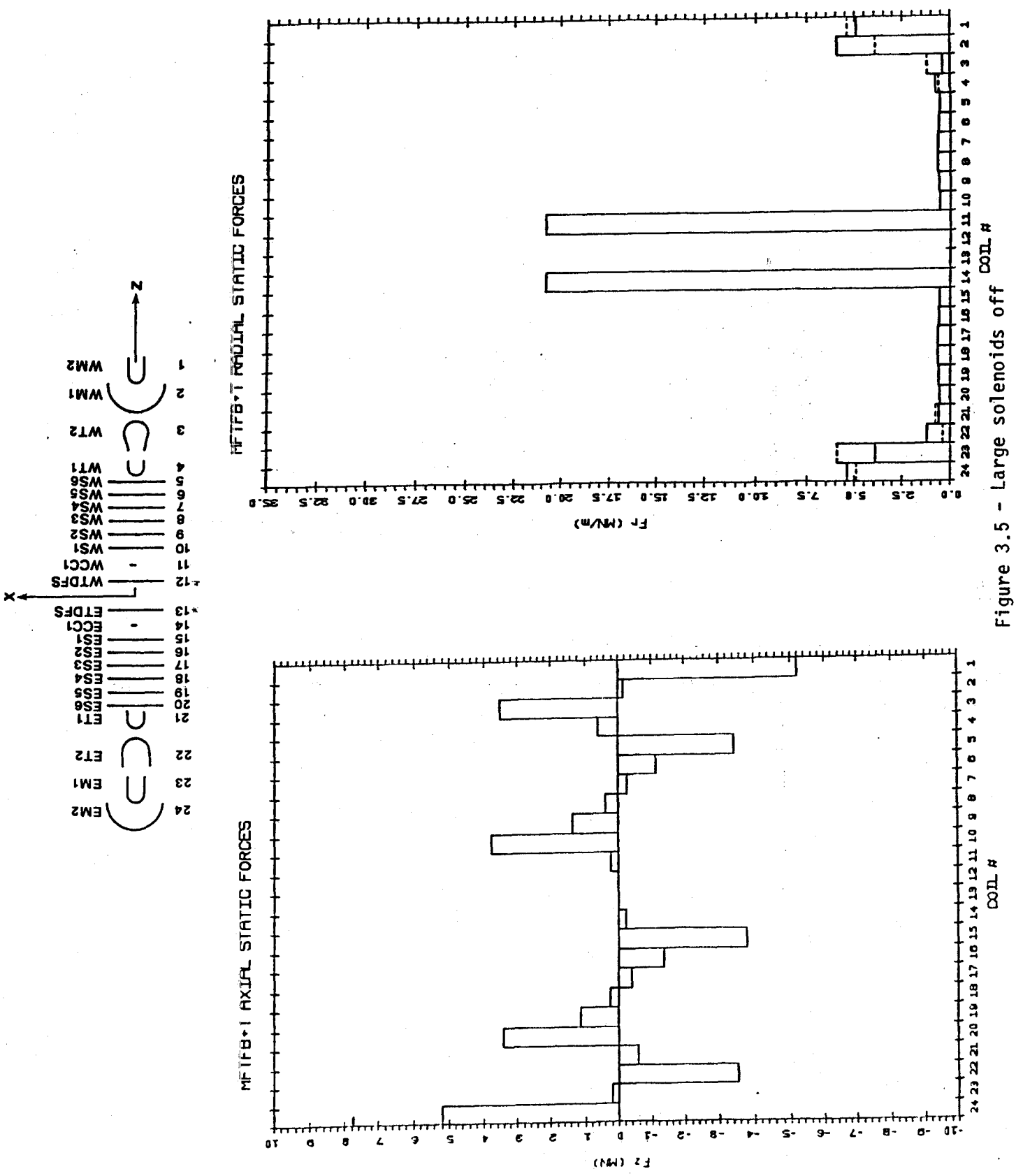

Figure 3.5 - Large solenoids off

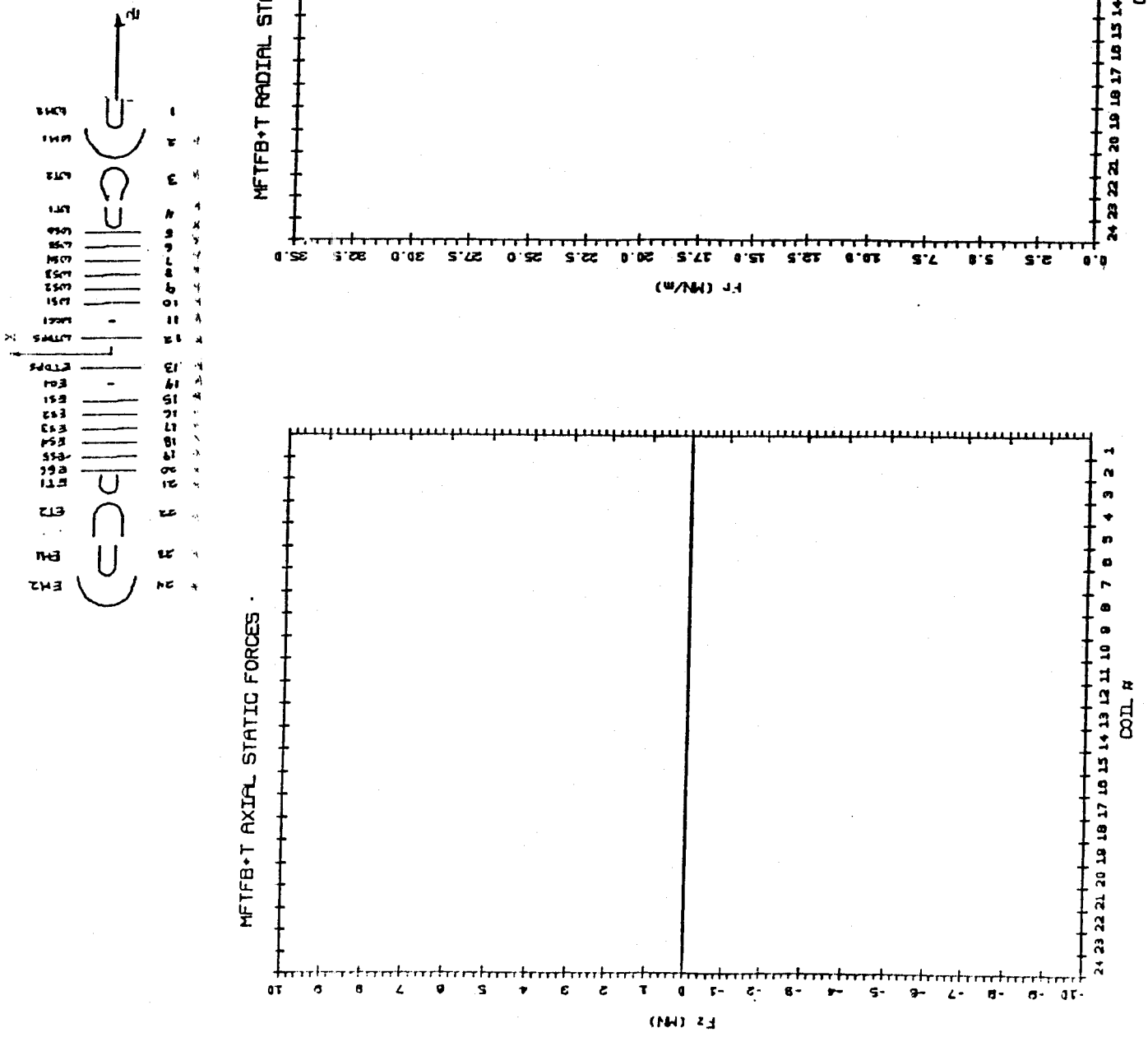

Figure 3.6 - WM2 CR

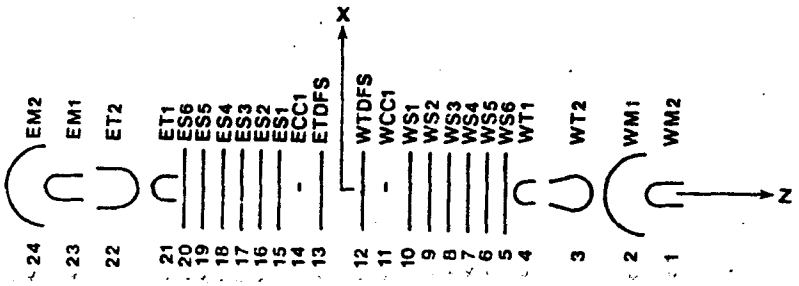

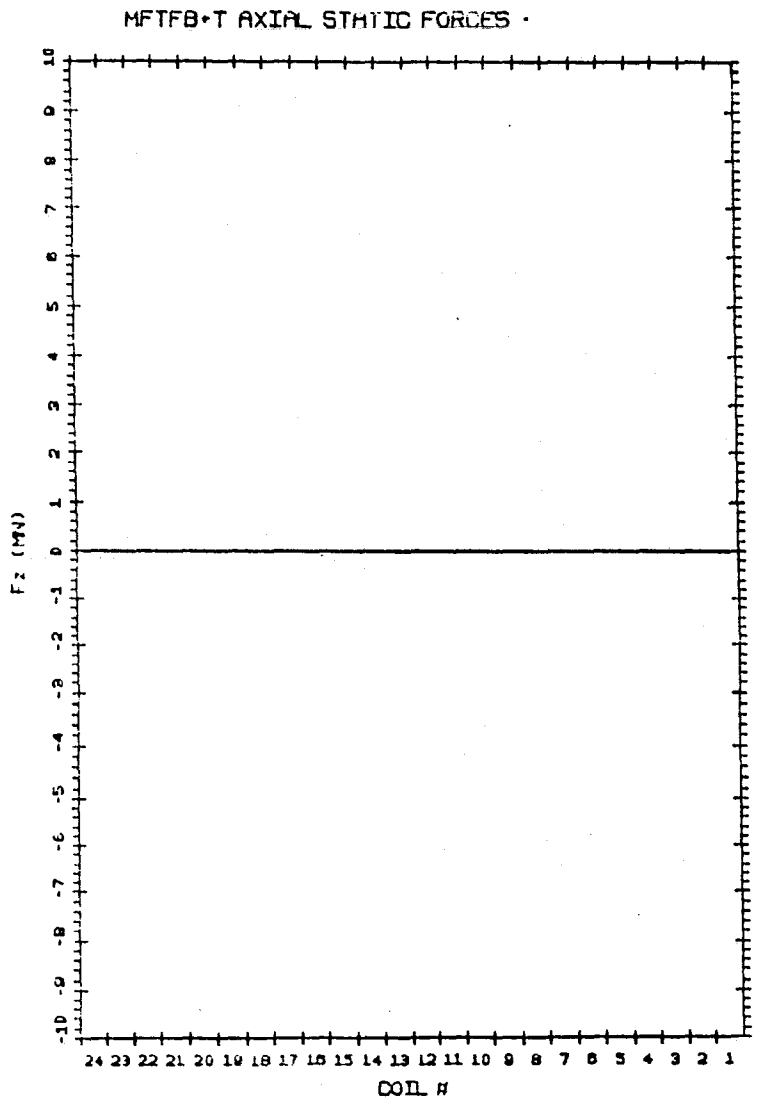

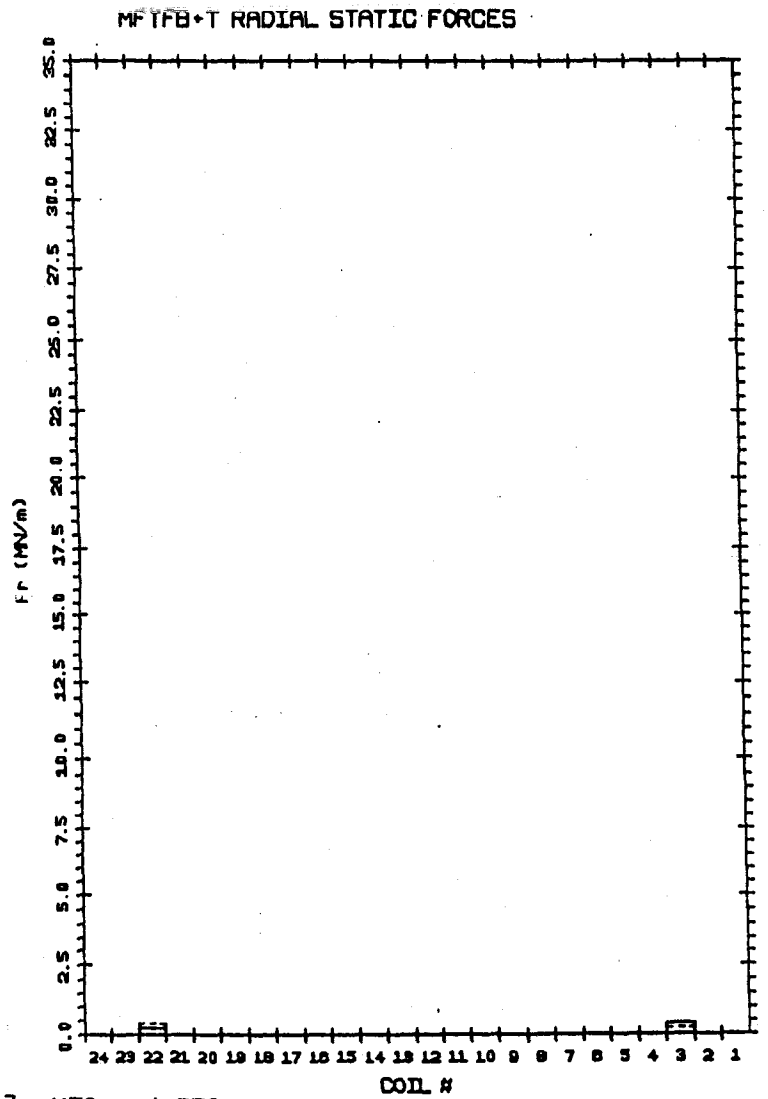

Figure 3.7- WT2 and ET2 on

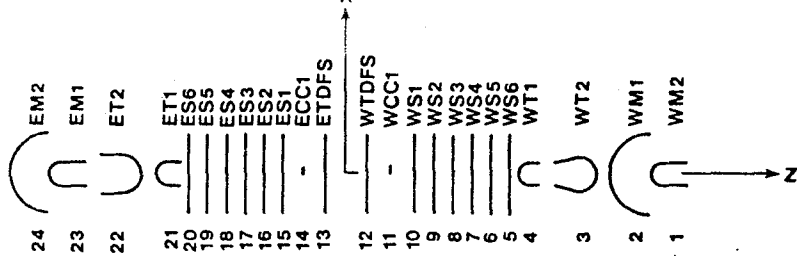

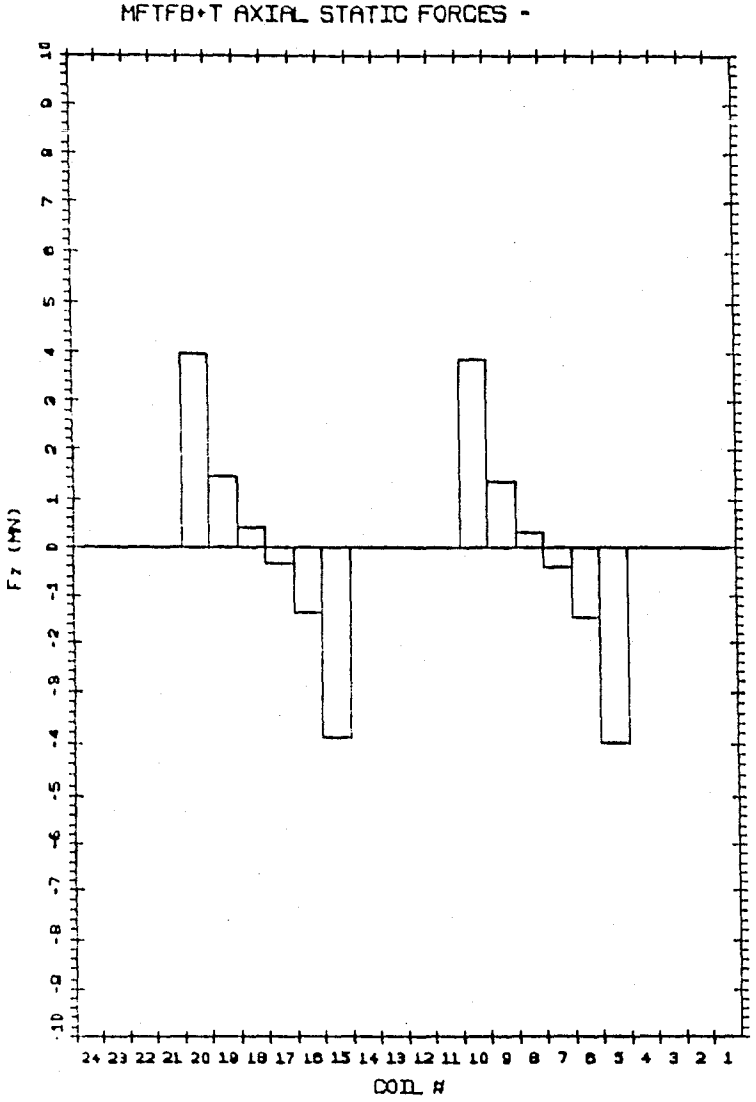

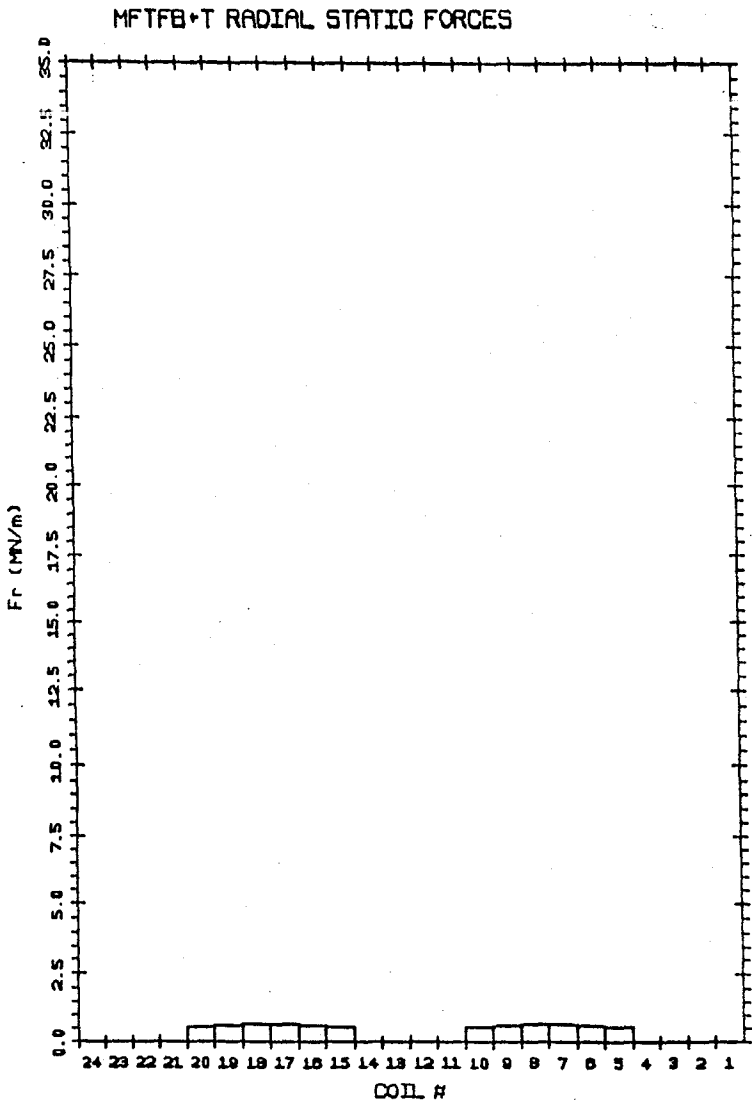

Figure 3.8 - Central solenoids on

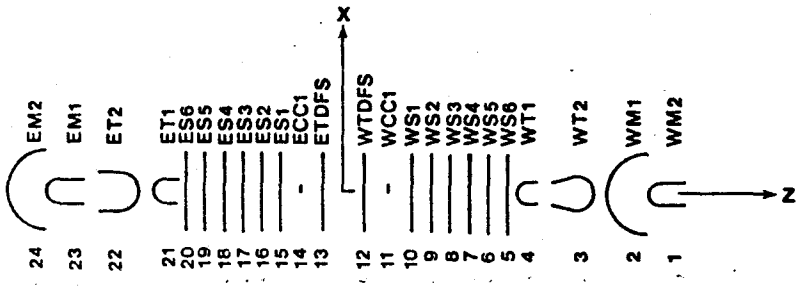

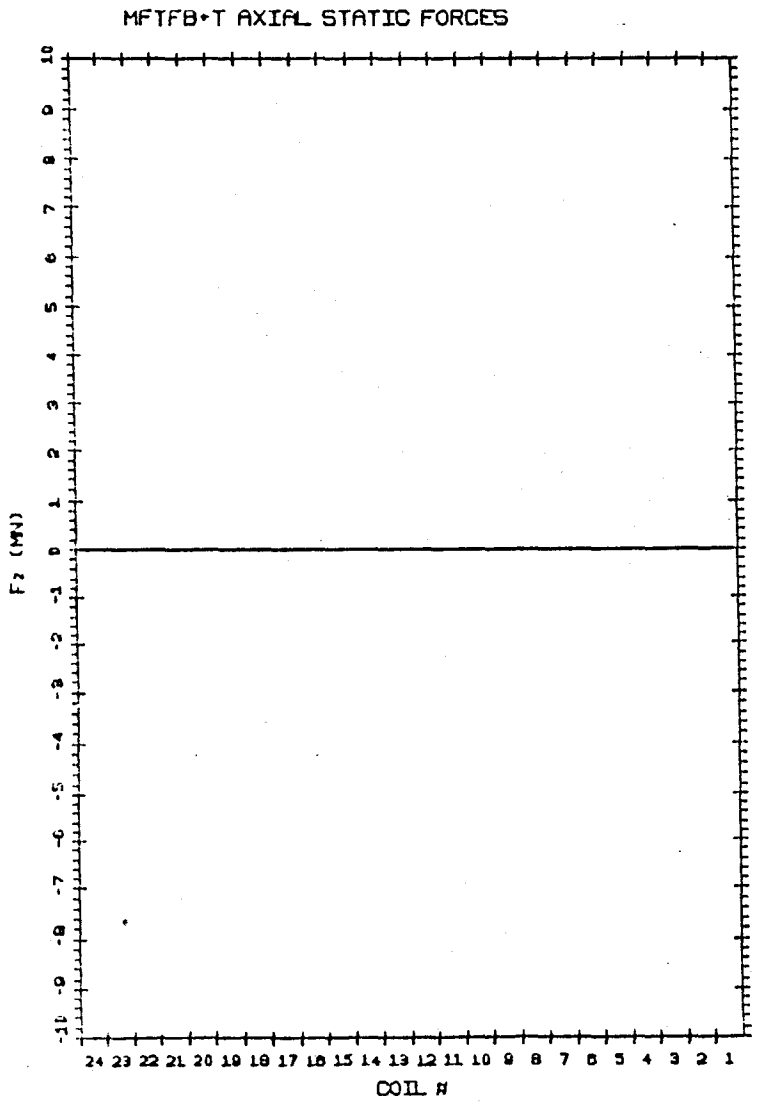

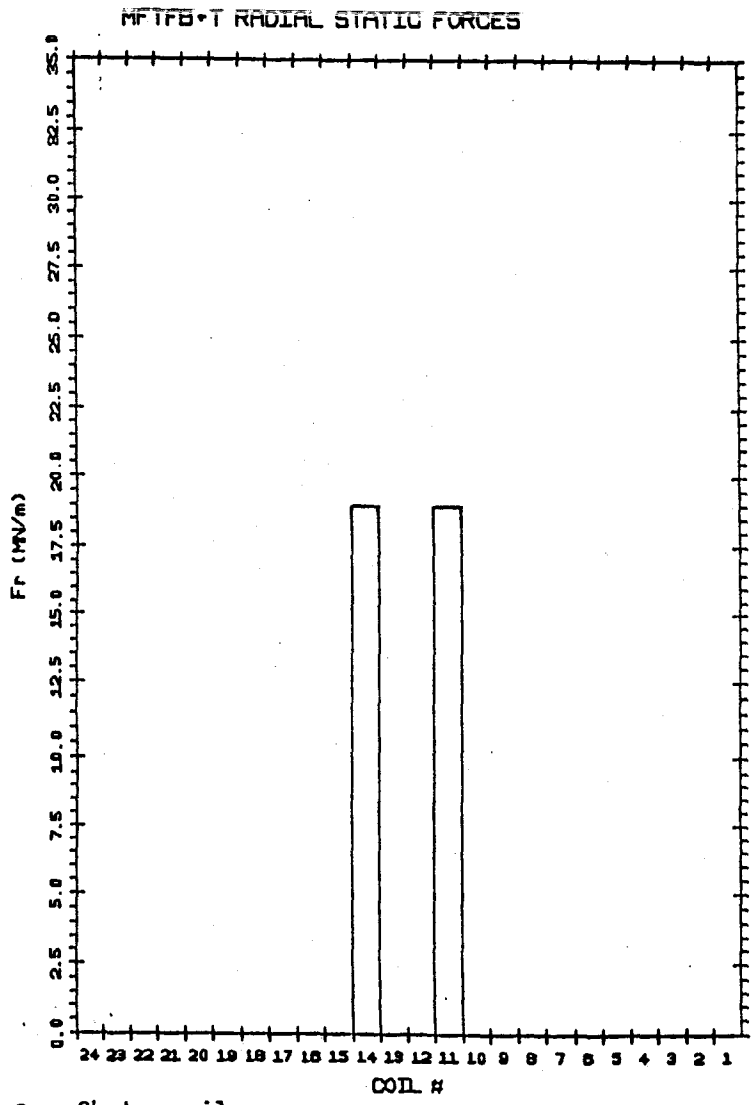

Figure 3.9 - Choke coils on

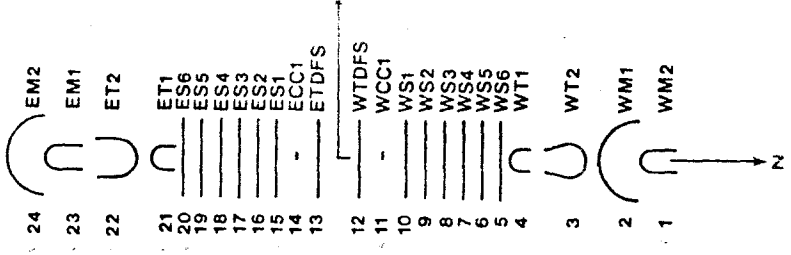

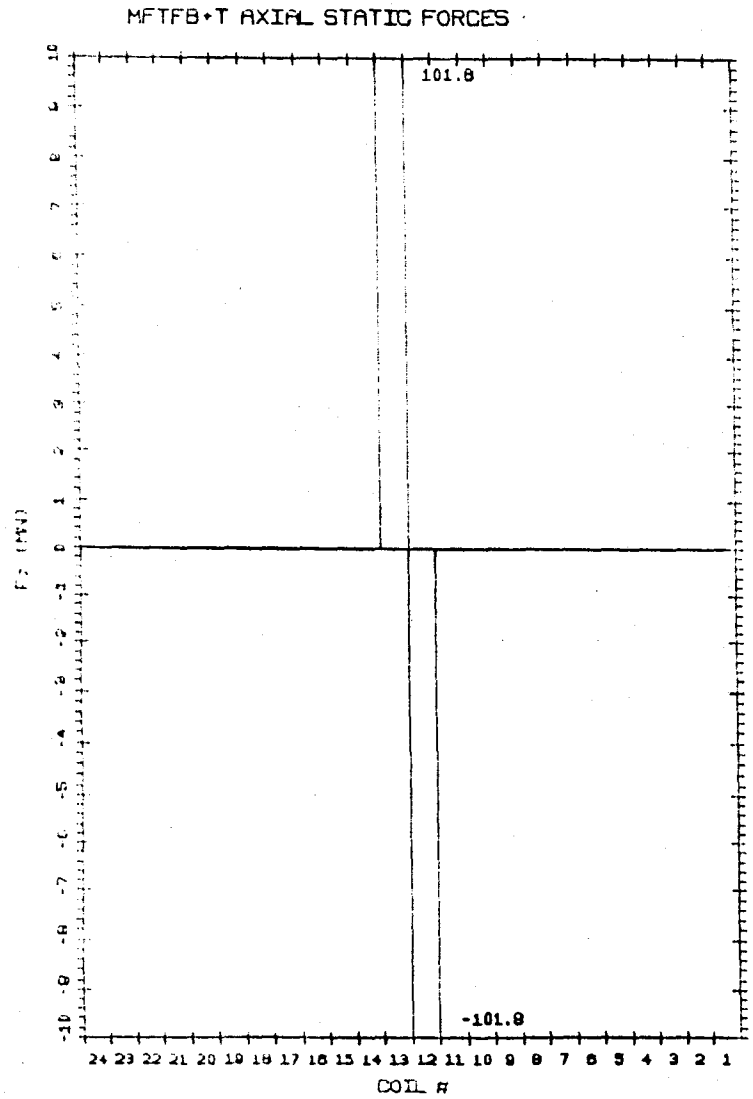

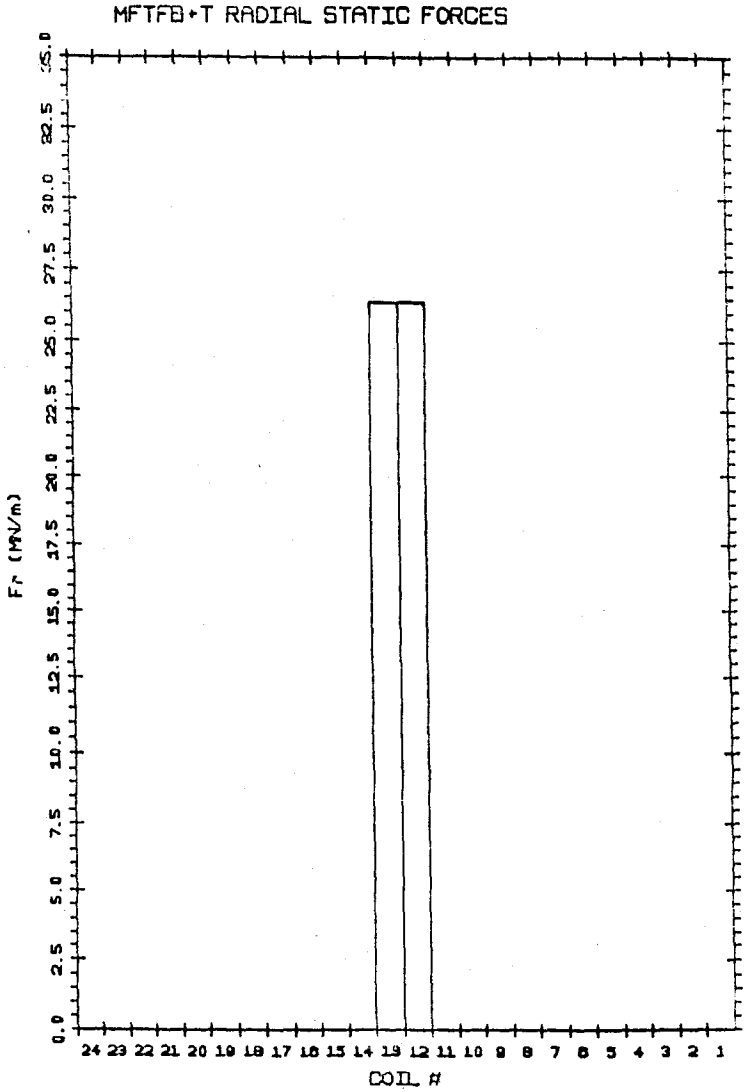

Figure 3.10 - Large solenoids on

4.0 TRANSIENT LOAD ANALYSES

The transient load analyses consisted of a sequence of runs in which all coils start from a fully charged condition; each coil from 1 to 12 (WM1 to WTDFS2) was assumed to have a short across the entire coil while the other coils are assumed to discharge through their individual dump resistors. The two choke coils are resistive and have an internal resistance rather than an external dump resistor.

Figure 2.4 shows the nine independent circuits in the machine. For a discharge scenario, the nine circuits become 24 independent L-R circuits coupled through the coil to coil mutual inductances. The matrix set of first order ordinary differential equations to be solved for the unknown current versus time is given by:

$$[L]\{\dot{I}(t)\} + [R]\{I(t)\} = \{0\}$$

where [L] is the system inductance matrix. [R] is a diagonal matrix of coil dump resistors. The initial condition for these runs was that each coil is at full operating current. For a coil short, the dump resistor value in [R] is replaced by a small number (0 is unacceptable from a numeric standpoint).

If the terms in the [L] and [R] matrices are constant, the set can be solved using an eigenvalue/eigenvector approach. The current at any time can then be found from the eigenexpansion. Figure 4.1 shows the set of currents versus time for the normal discharge case. Only the currents in 1-12 are shown since by symmetry the currents in 13-24 are identical. It can be seen that the current in coil 10 (WS1) initially increases. Because the force on a coil is a product of a row of the influence coefficient matrix and the current vector and then multiplied by the coil current, it is not obvious from the current plot when the peak forces occur. In order to find the peak forces during each scenario, the eigenexpansion was used to calculate currents at various times. The forces were calculated at each of these times and the maximum (positive) and minimum (negative) values found.

The forces versus time are shown in Figure 4.2 through 4.4 for the normal discharge case. Only the forces on coils 1-12 are shown. Figure 4.2 shows the peak axial force acting on each coil. It can be seen that certain coils actually experience a force reversal during the discharge (e.g. coil #10, WS6). Figure 4.3 shows the radial forces per unit length acting on the coils in the X=0 plane and Figure 4.4 the radial forces per unit length in the Y=0 plane (dashed lines).

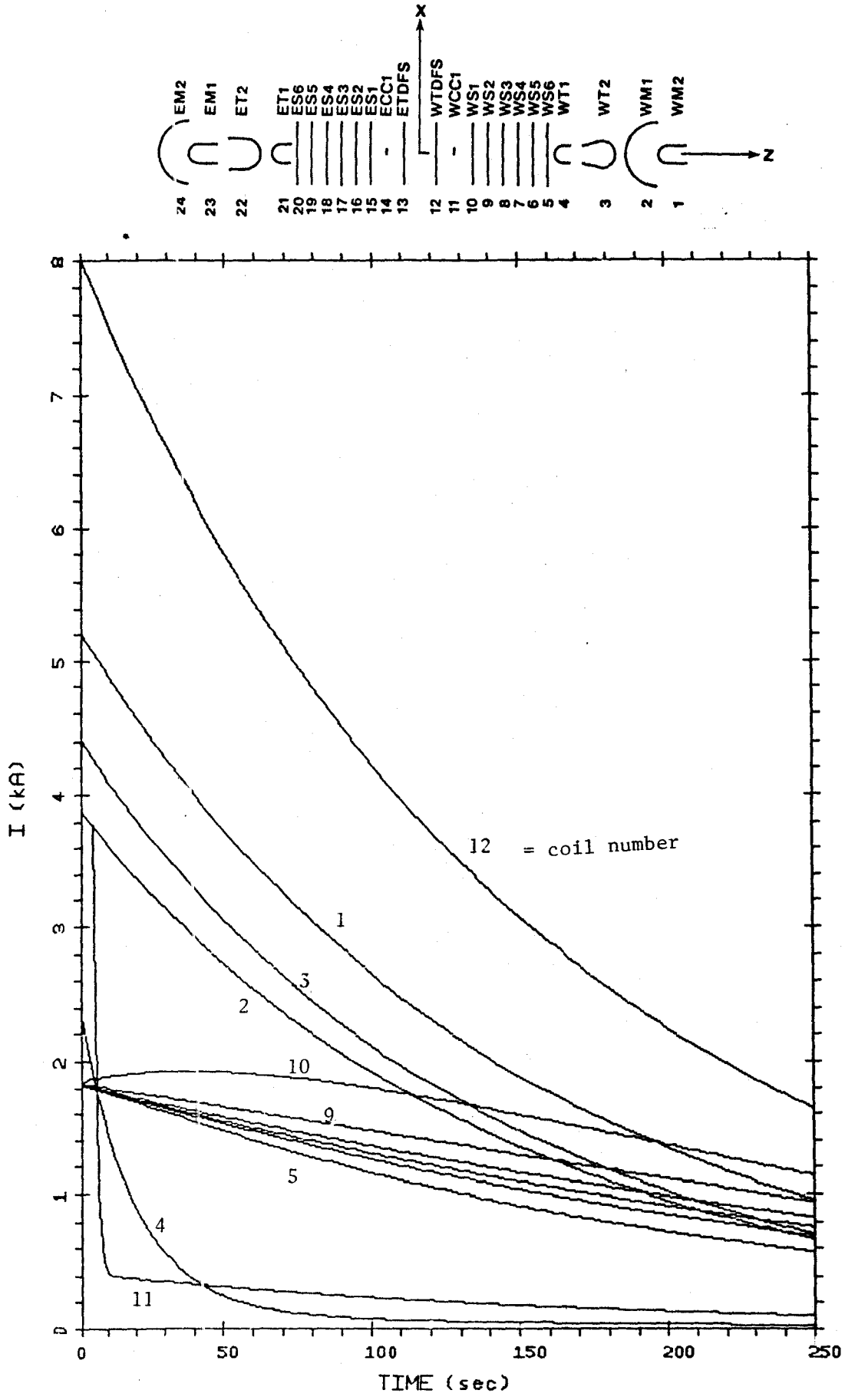

Figure 4.1 Coil Currents vs Time for Normal Discharge

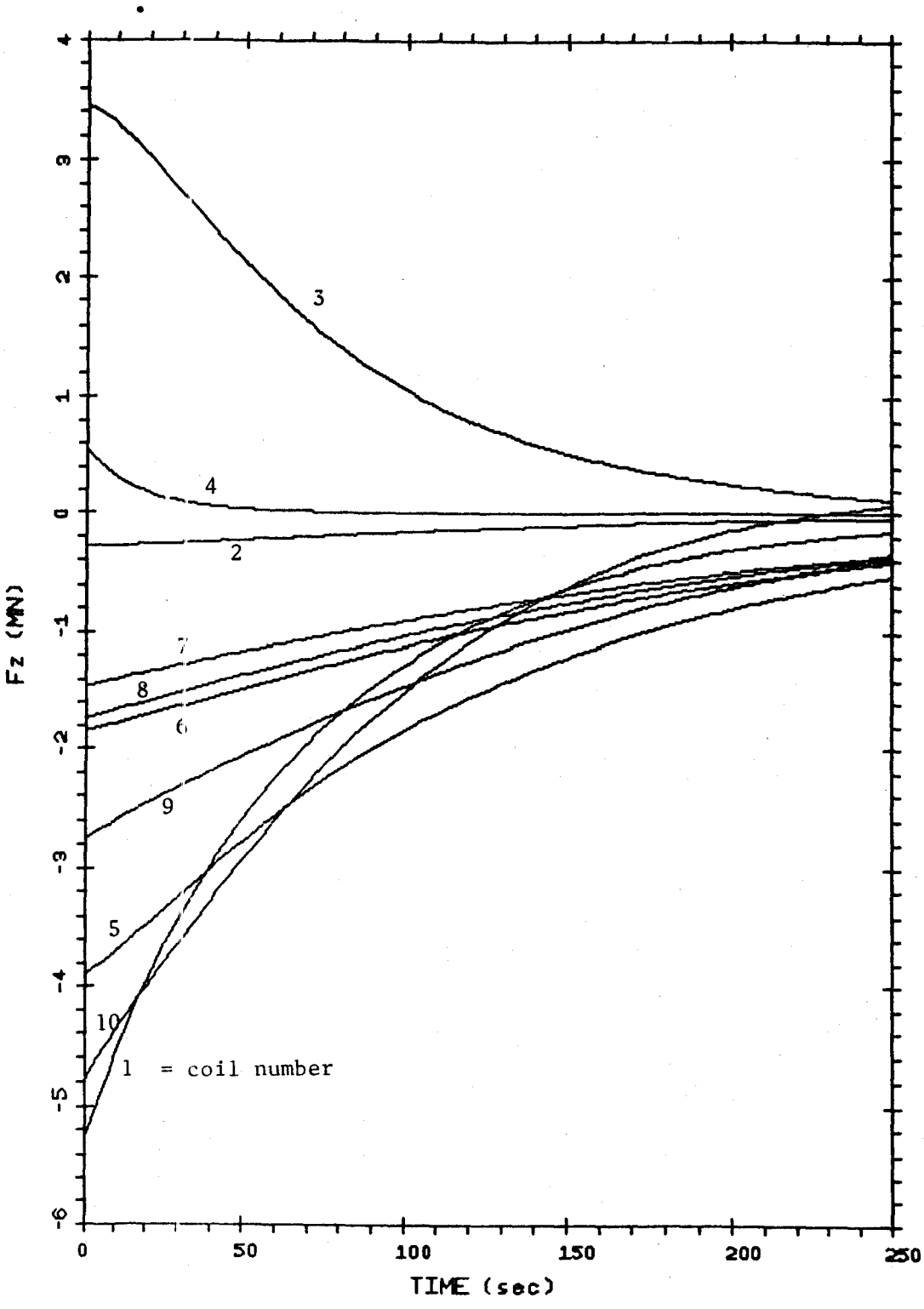

Figure 4.2 Coil Axial Forces vs Time for Normal Discharge

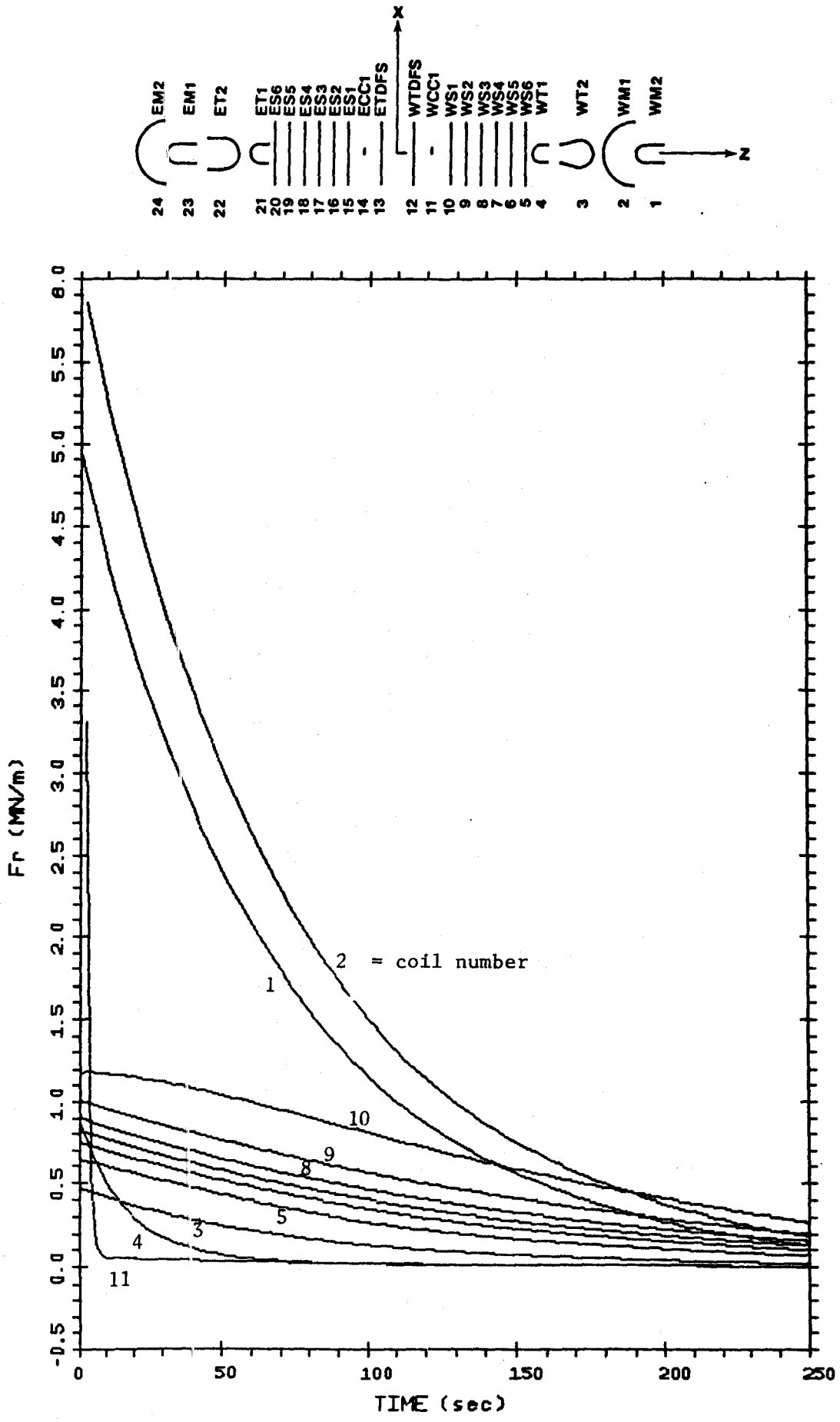

Figure 4.3 Coil Radial Force Per Unit Length (X = 0)
Normal Discharge

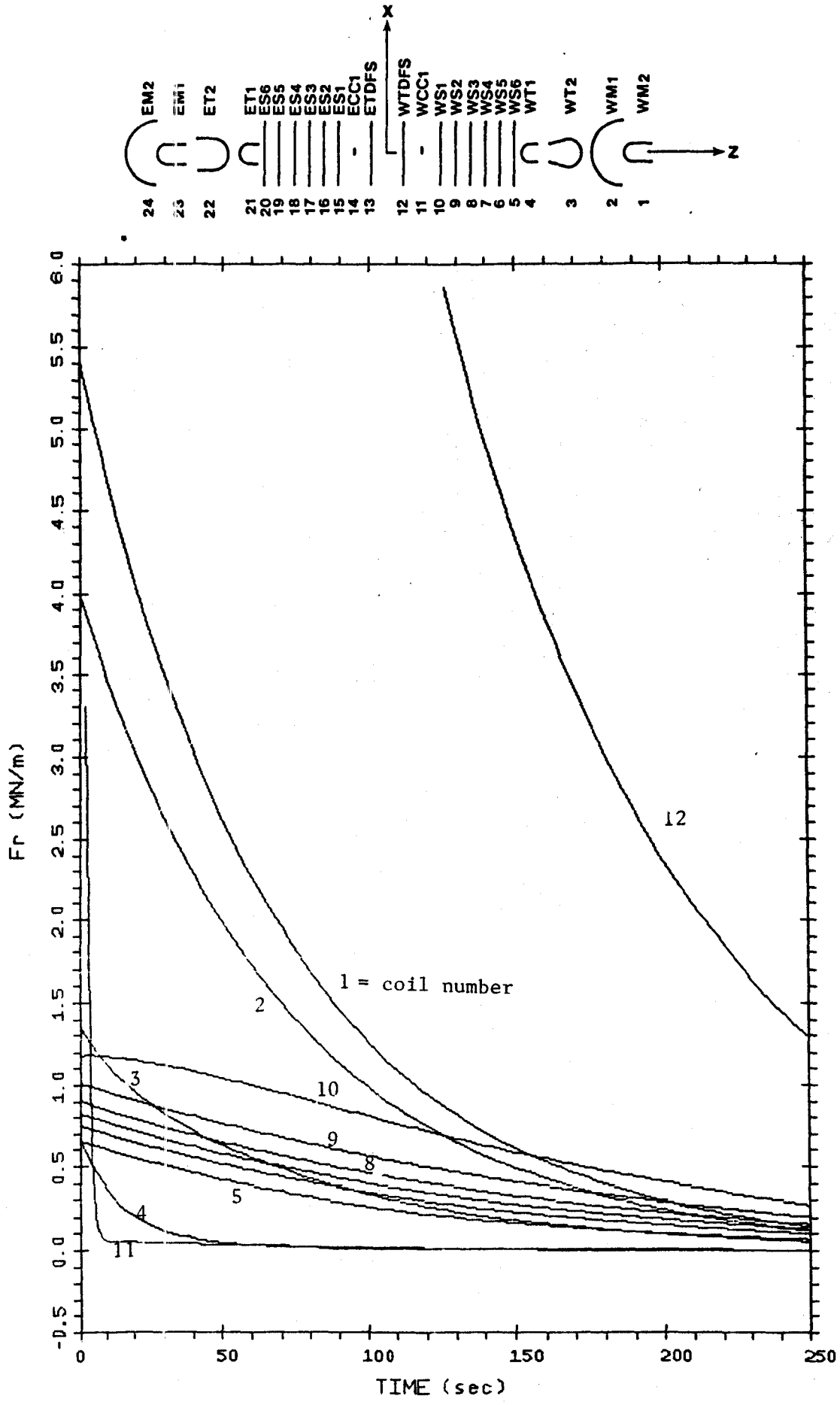

Figure 4.4 Coil Radial Force Per Unit Length (Y = 0)
Normal Discharge

One of the more interesting cases was a short circuit across coil 2 (WM1). There is a slight radial force reversal in coil #3 (WT2) in the X=0 plane. The current versus time for the coils is shown in Figure 4.5. The net axial load versus time for coils 1-12 is shown in Figure 4.6. The radial force per unit length in the X=0 plane for each of the coils is shown as a function of time in Figure 4.7. There is indeed a small reversal for this radial force in coil #3. Figure 4.8 shows the radial force per unit length in the Y=0 plane for coils 1-12.

The remaining figures in this section are the peak loads during discharge for single coil shorts. The figures have a side view of the machine with coil numbers superimposed at the top. The coil with the short is denoted by an asterisk (*). The case number in the plot title corresponds to the coil with the short. Both the worst case axial forces and radial forces per unit length are shown. The radial force per unit length is the X=0 plane is denoted by a solid line; the the force per unit length in the Y=0 plane by a dashed line. The worst case loadings across all transient runs are summarized in Tables 1.7 and 1.8 and in Figures 1.7 and 1.8.

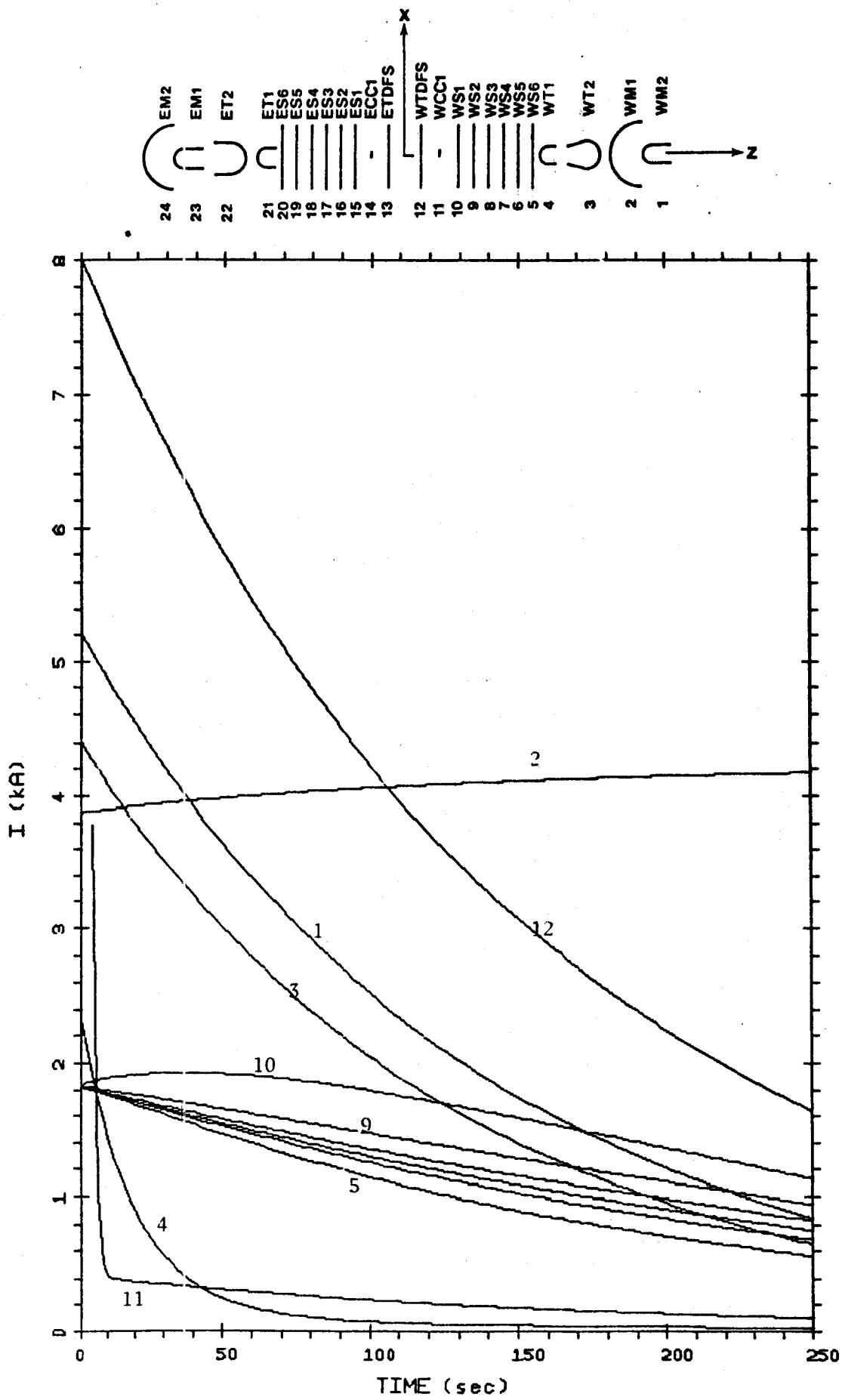

Figure 4.5 Coil Currents vs Time for Coil #2 Short-Circuited, All Others Discharging

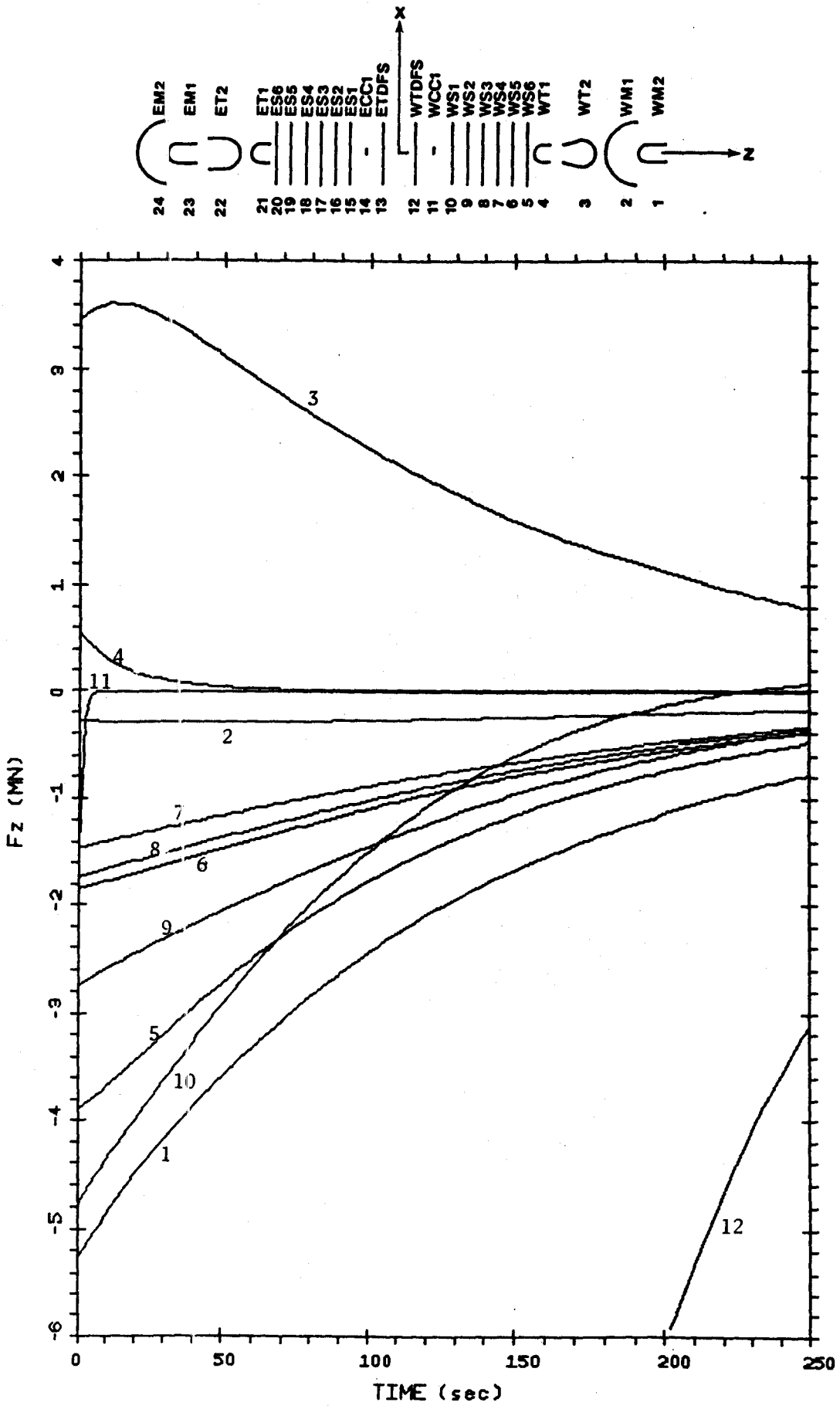

Figure 4.6 Coil Axial Forces vs Time for Coil #2 Short-Circuited; All Others Discharging

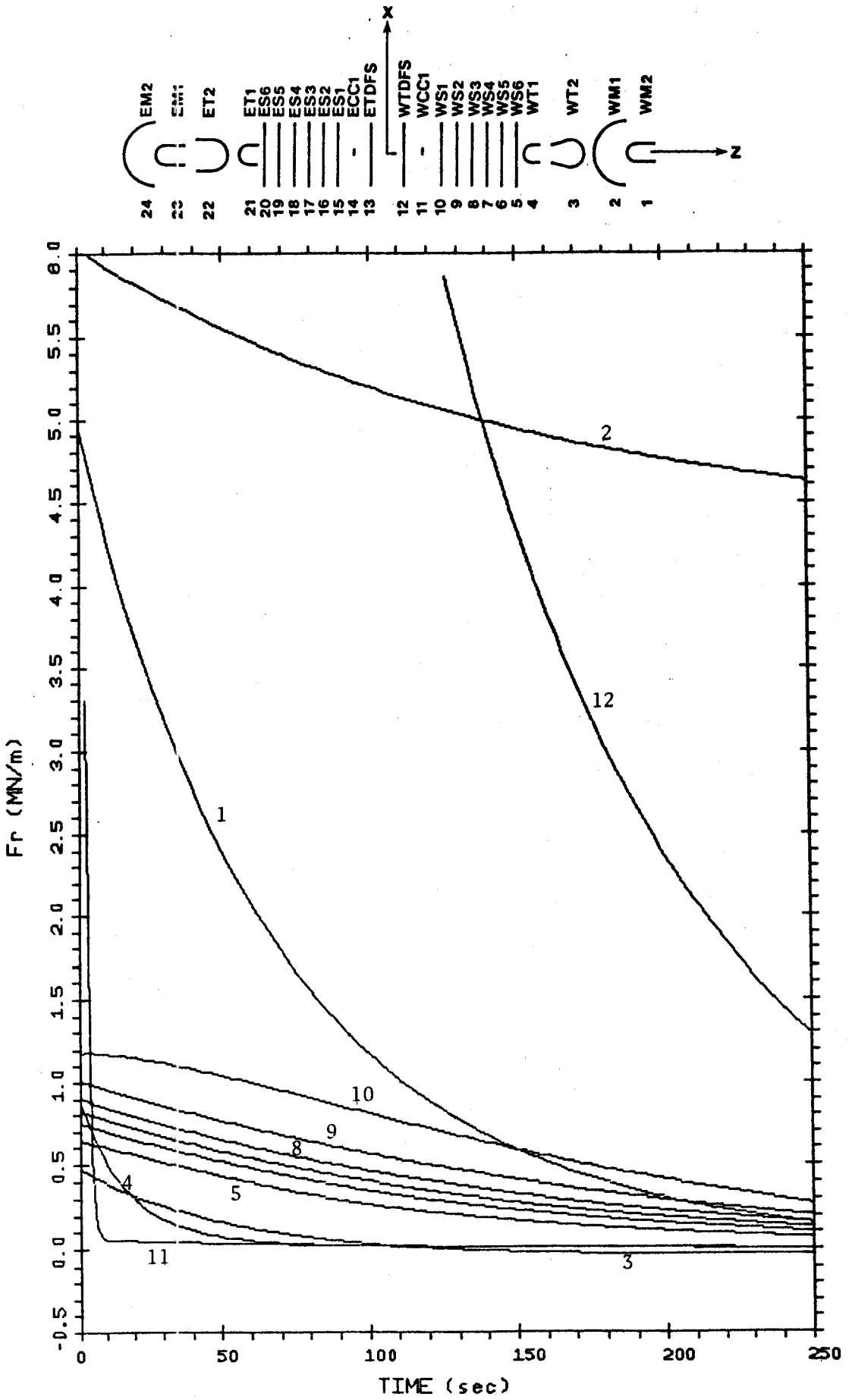

Figure 4.7 Coil Radial Forces Per Unit Length (X = 0 Plane) for Coil #2 Short-Circuited; All Others Discharging

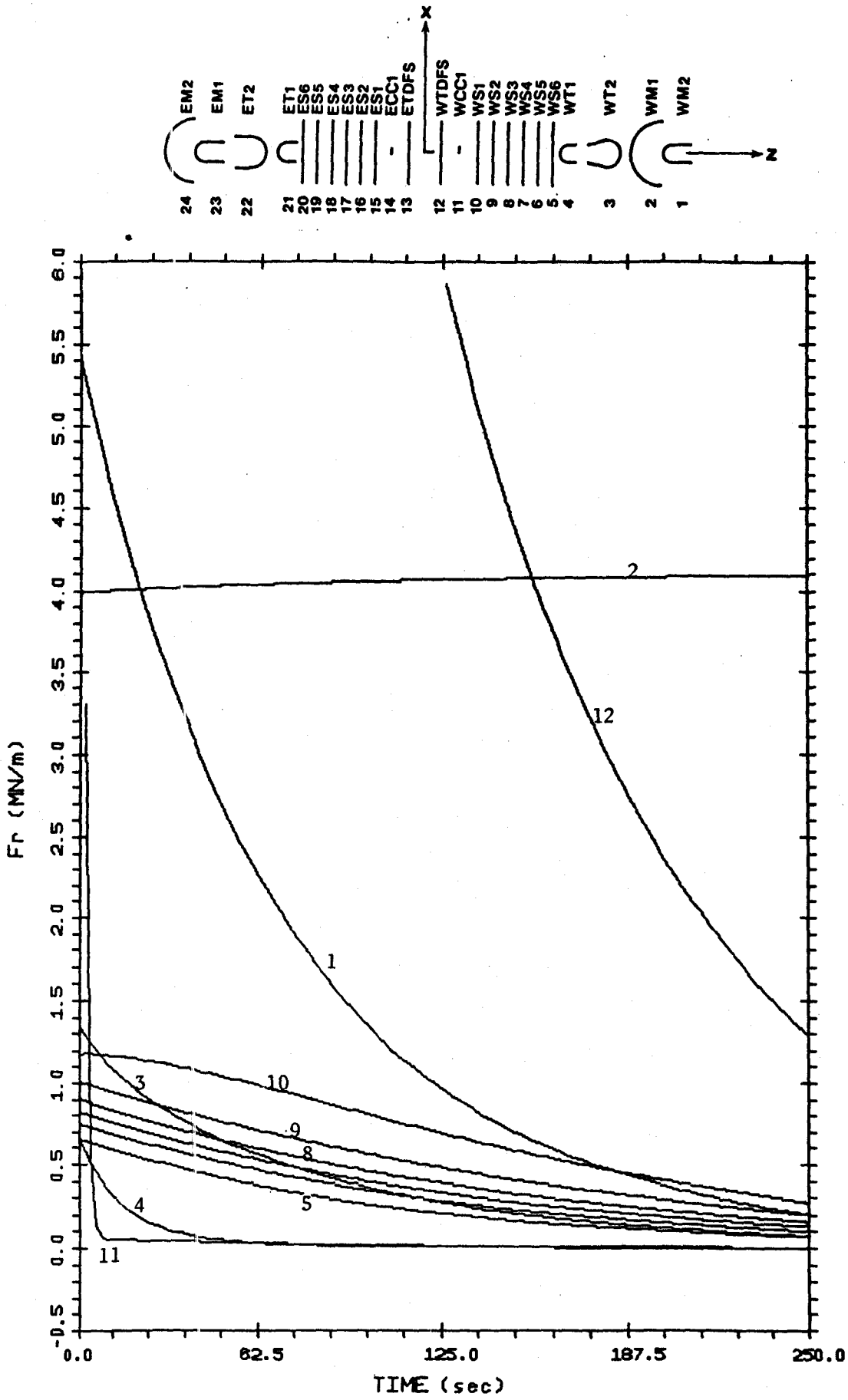

Figure 4.8 Coil Radial Forces Per Unit Length (Y = 0 Plane) for Coil #2 Short-Circuited; All Others Discharging

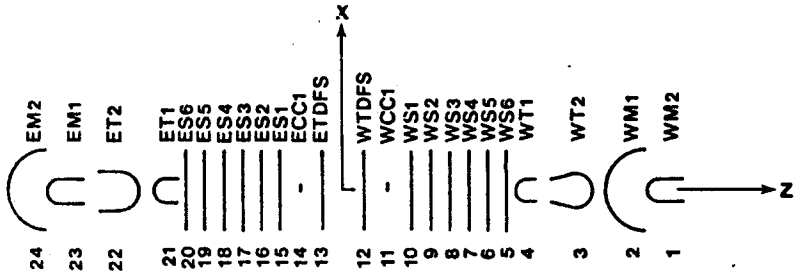

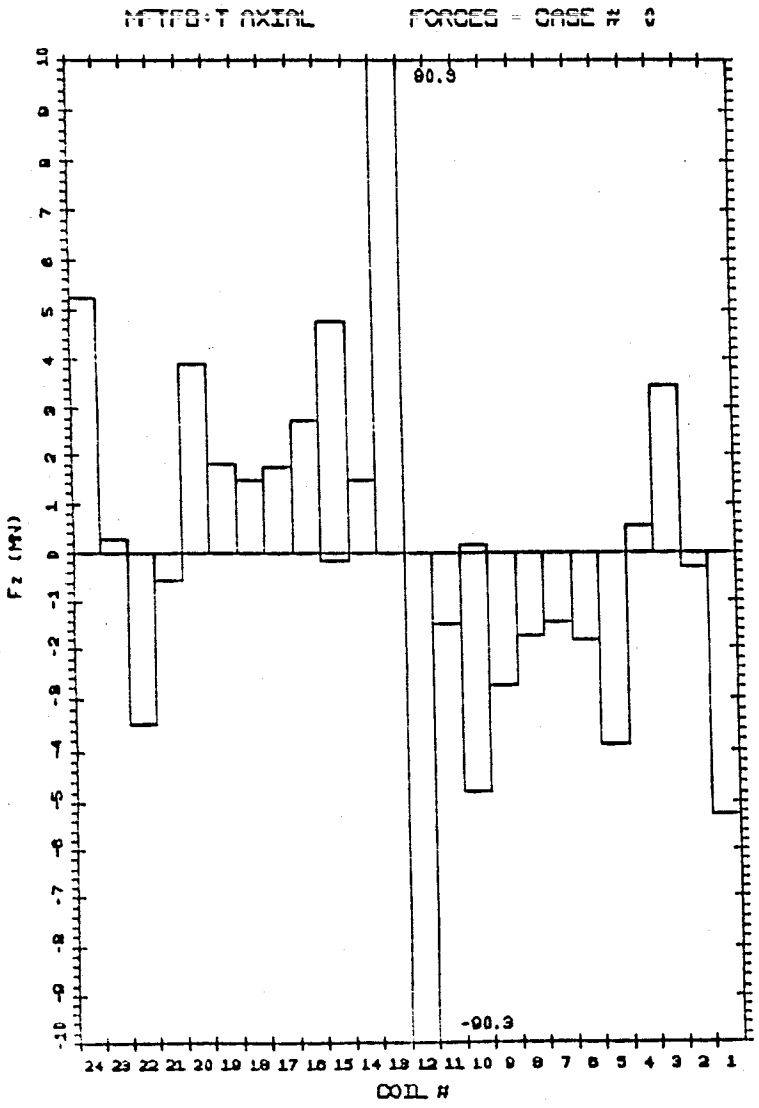

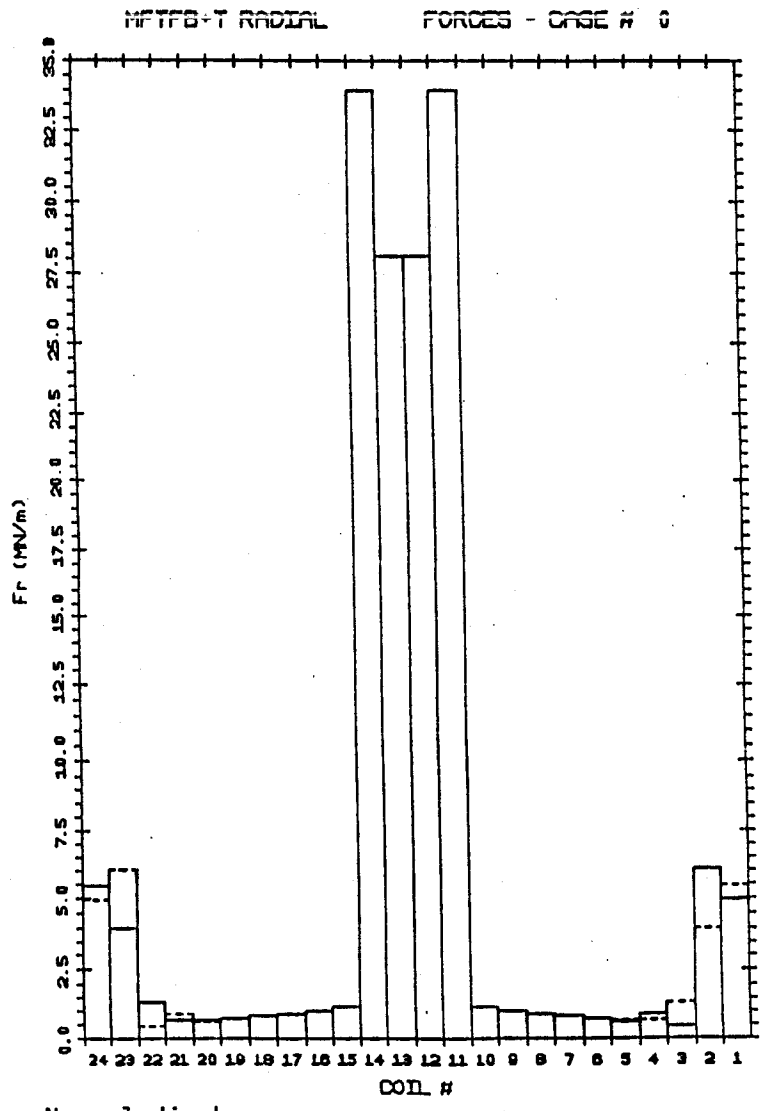

Figure 4.9 - Normal discharge

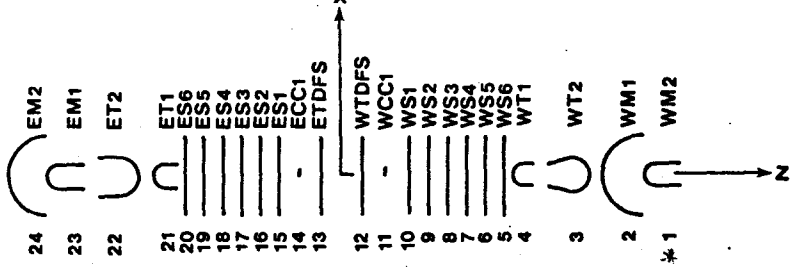

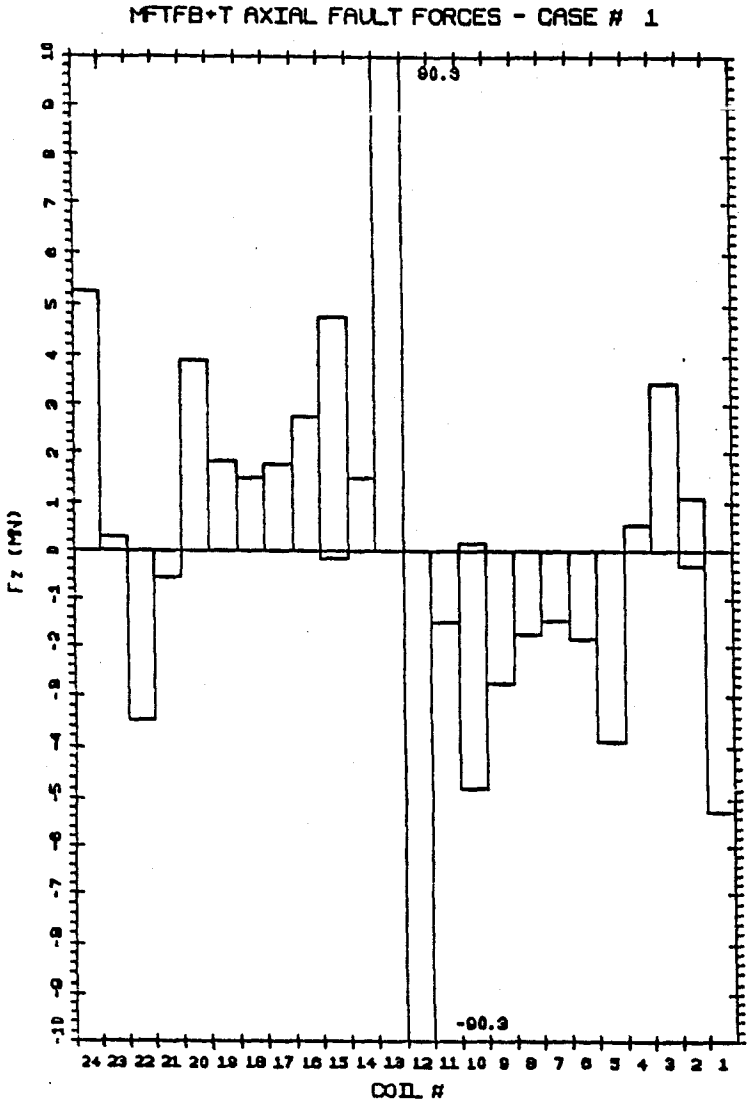

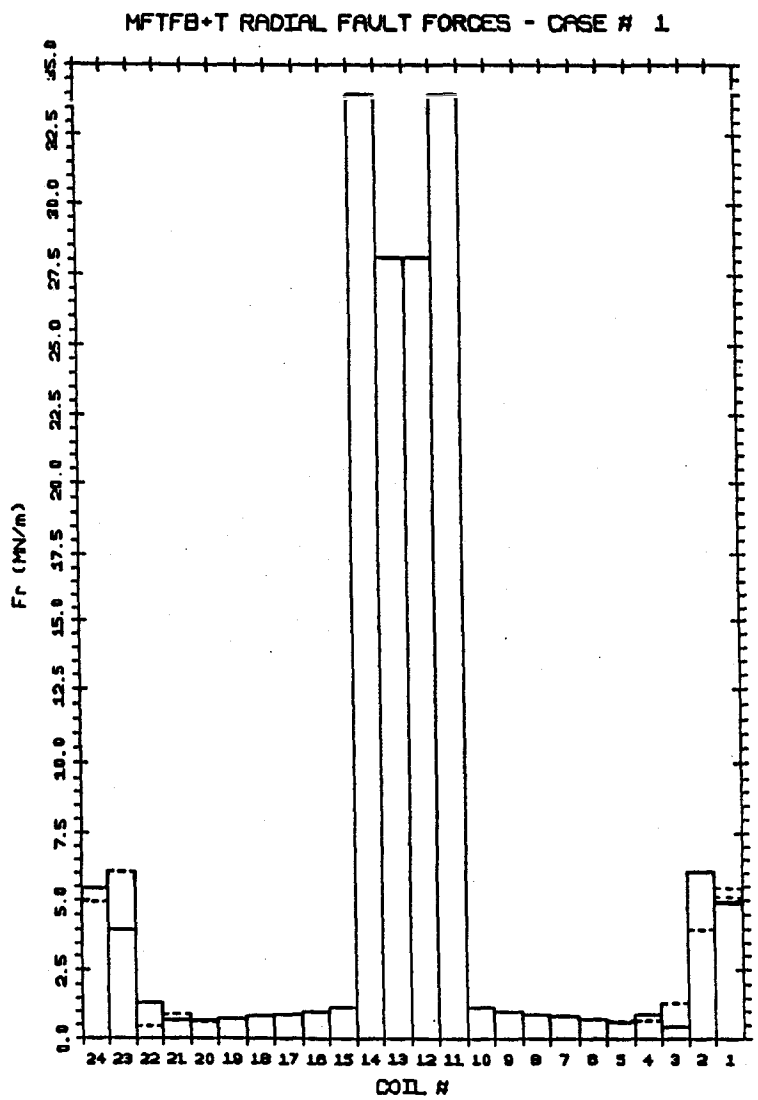

Figure 4.10 - Coil #1 shorted

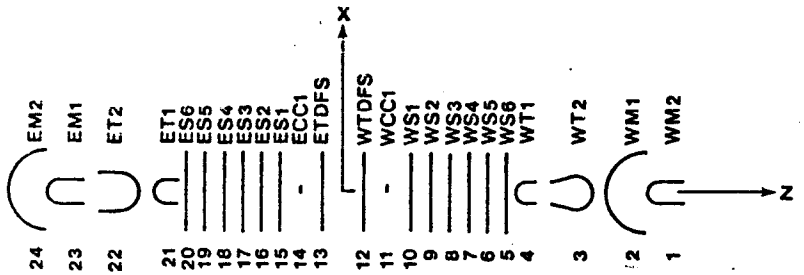

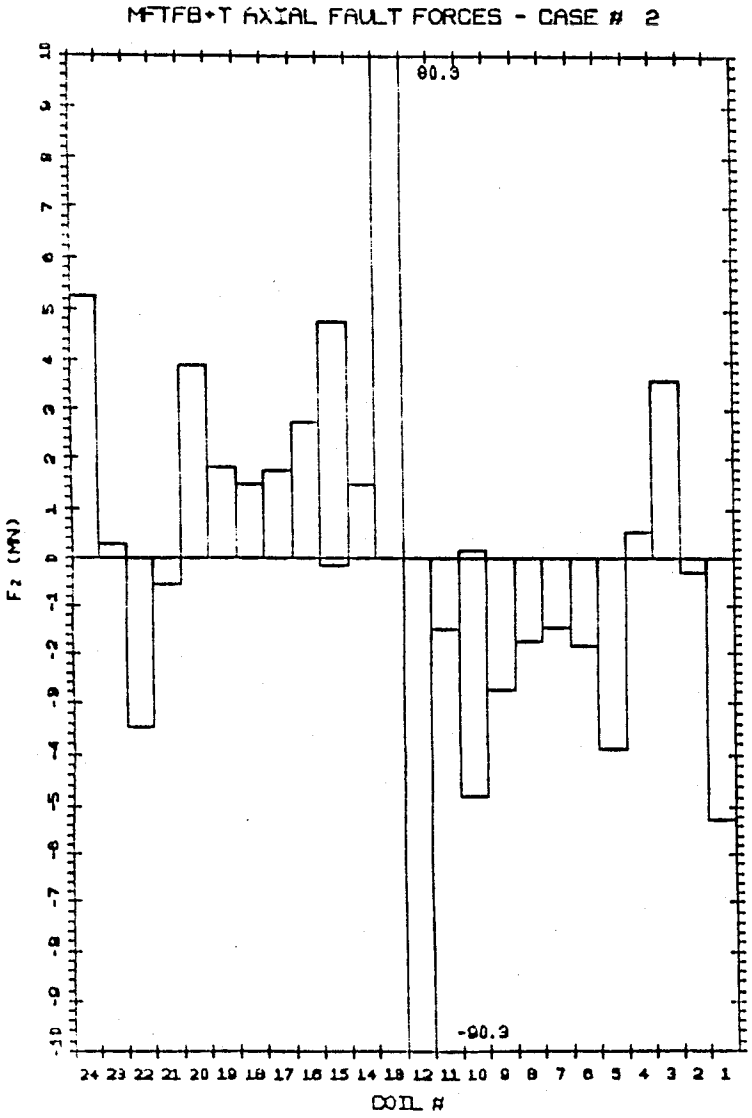

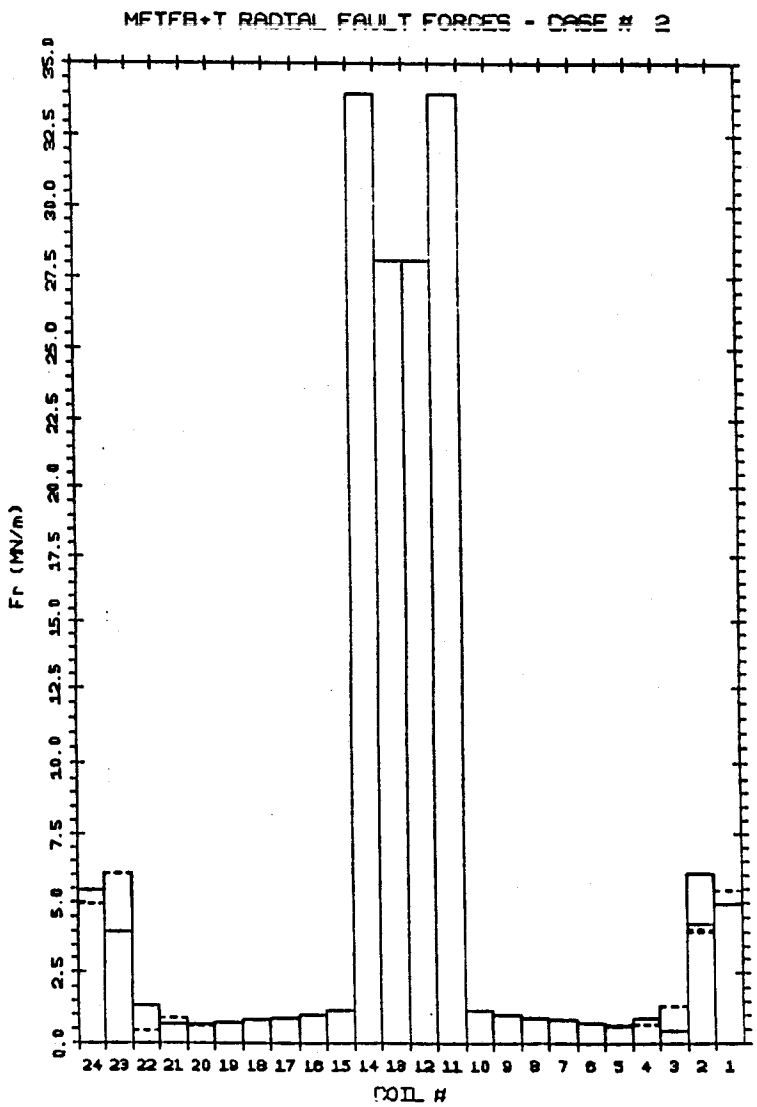

Figure 4.11 - Coil #2 shorted

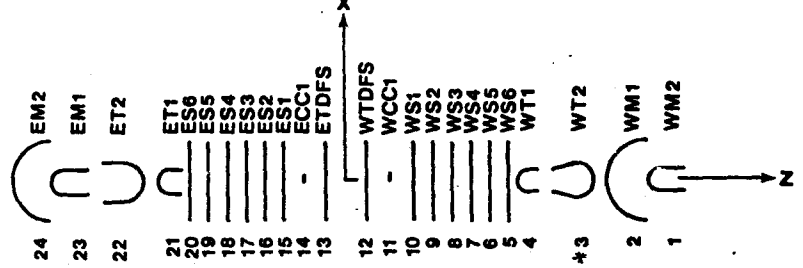

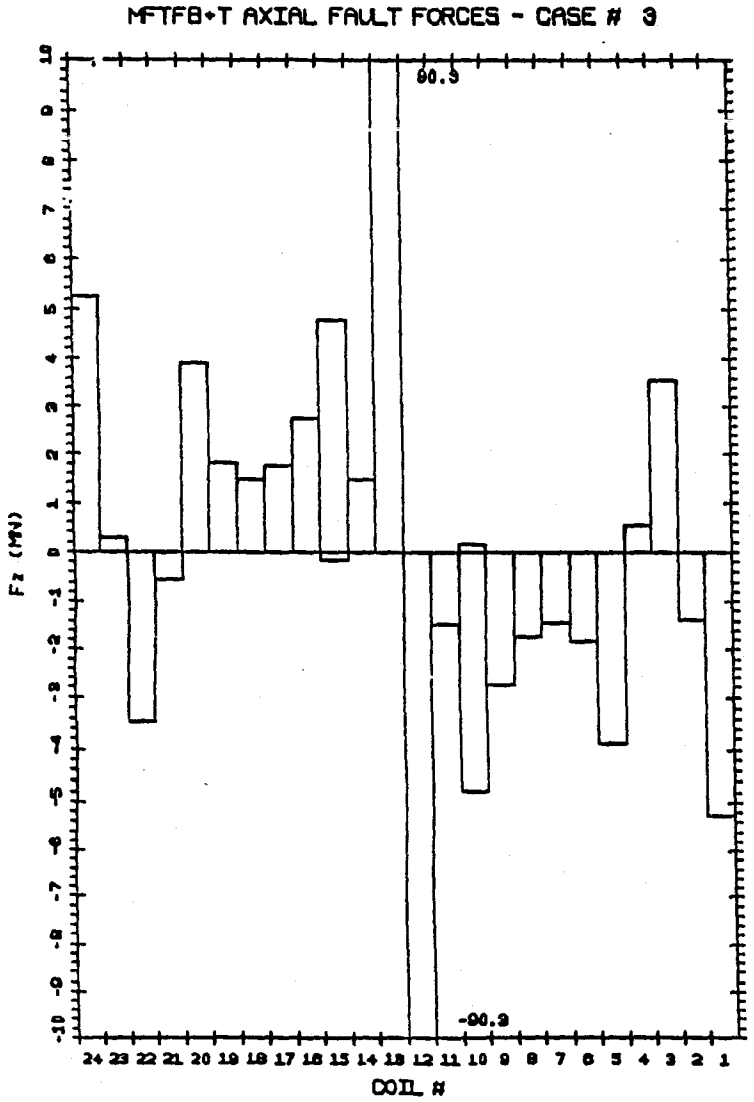

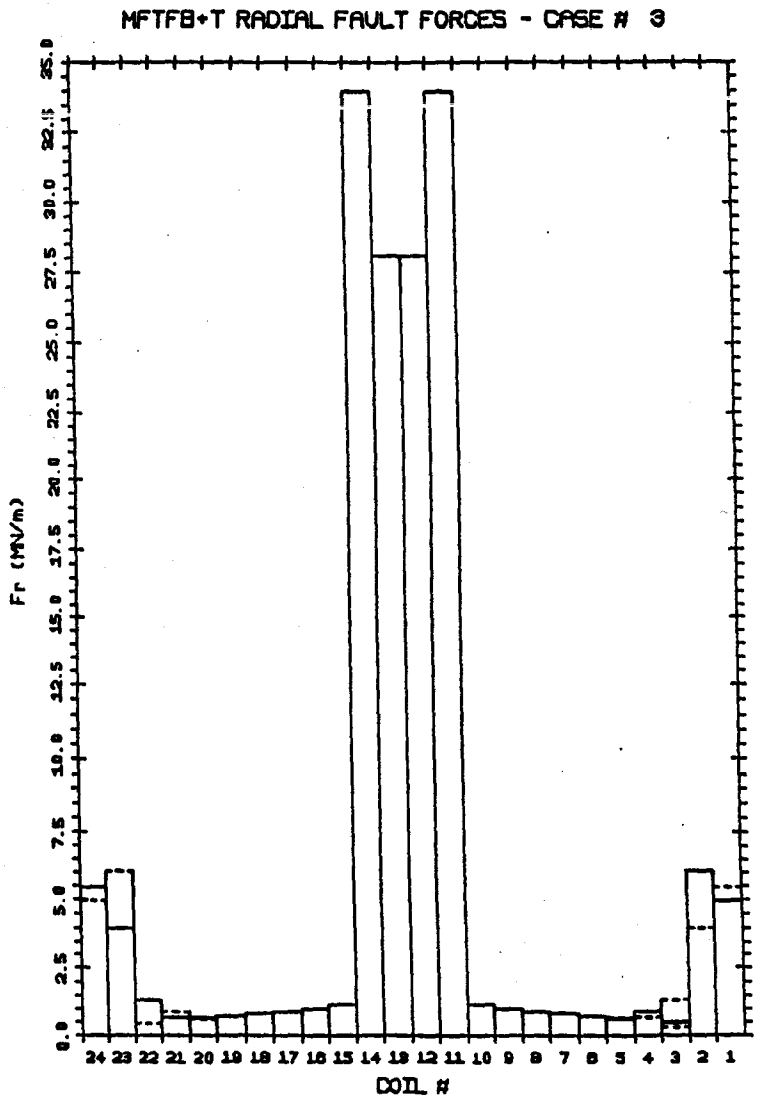

Figure 4.12 - Coil #3 shorted

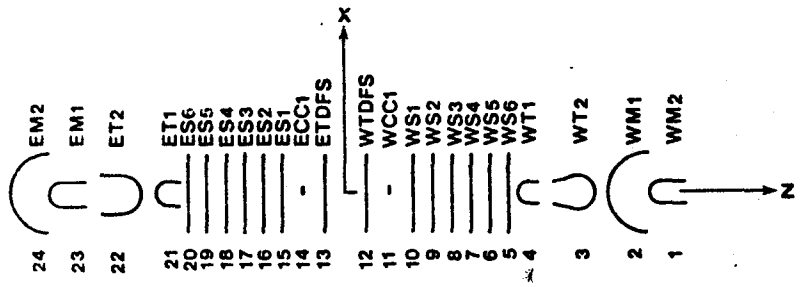

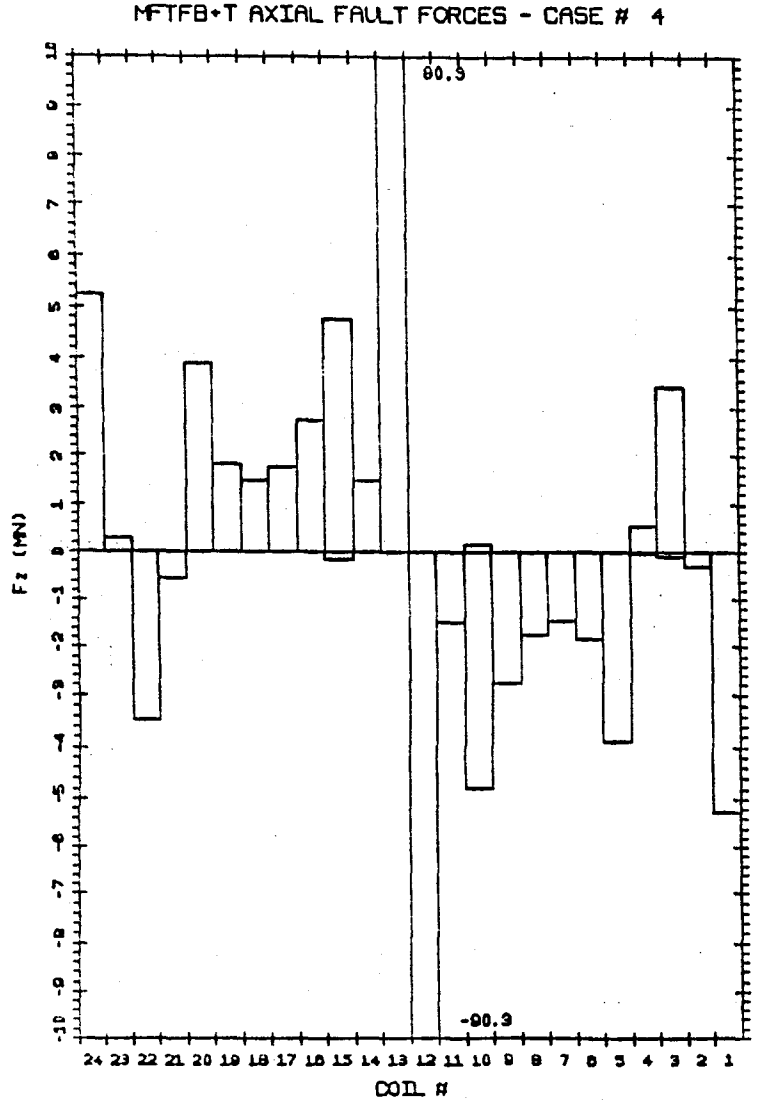

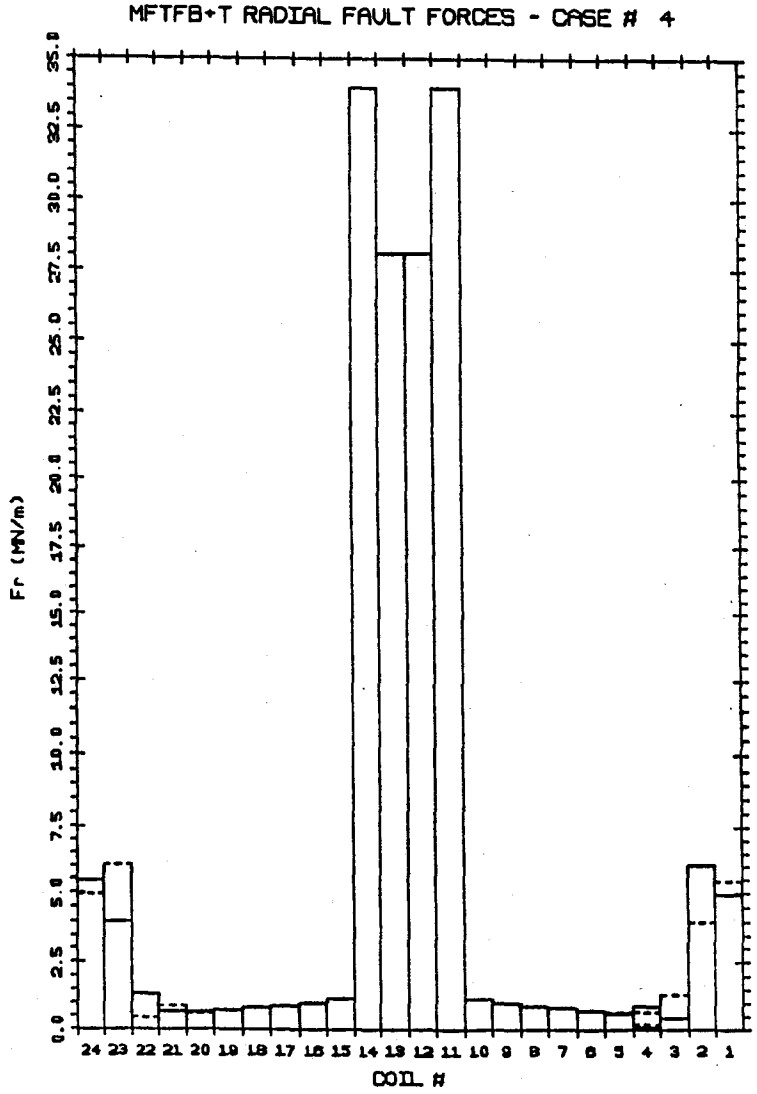

Figure 4.13- Coil #4 shorted

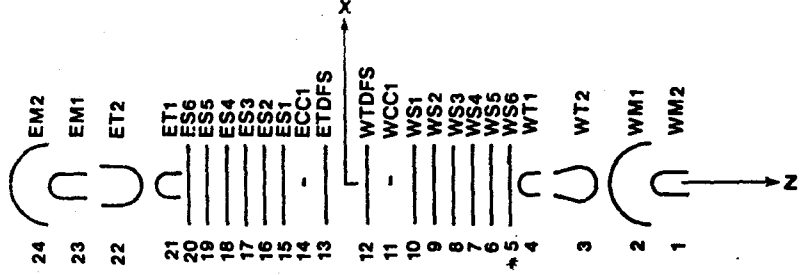

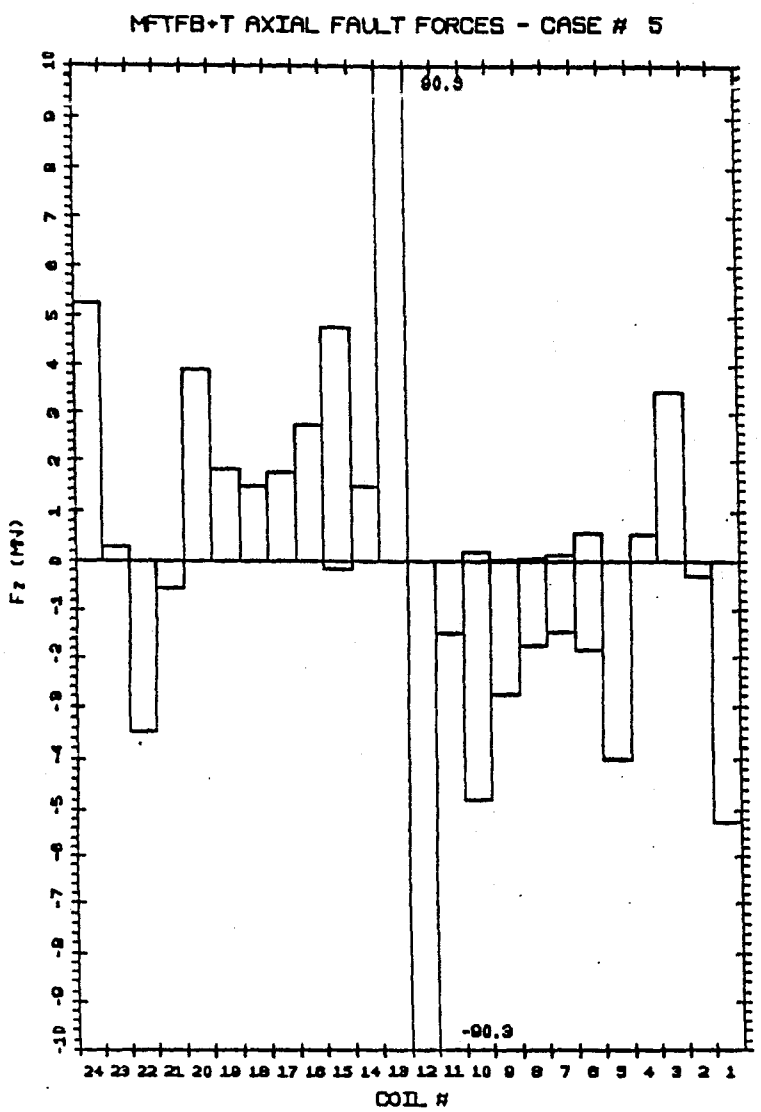

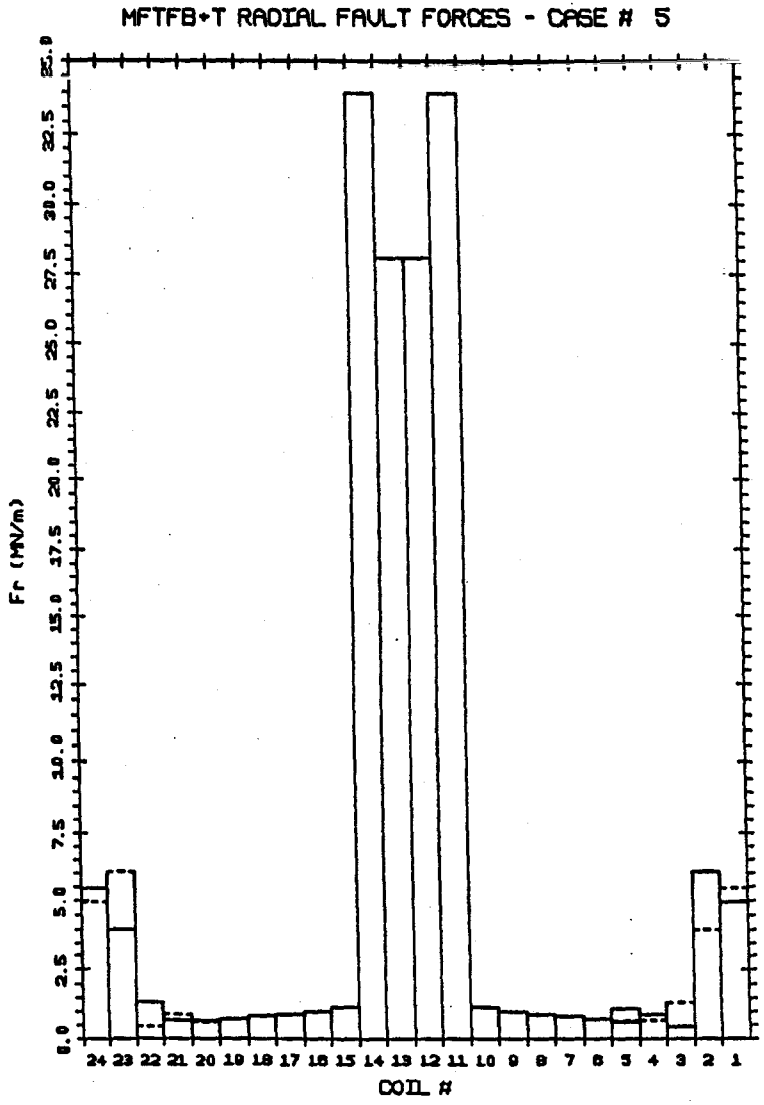

Figure 4.14 - Coil #5 shorted

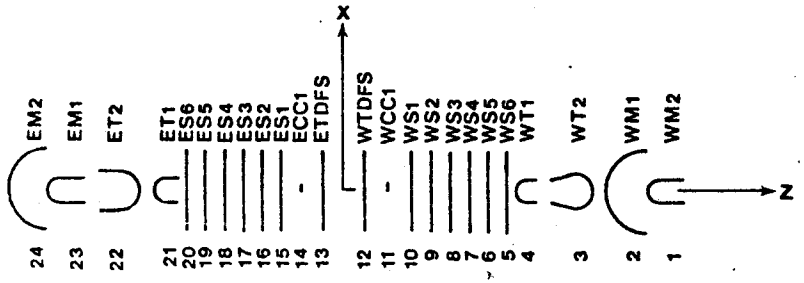

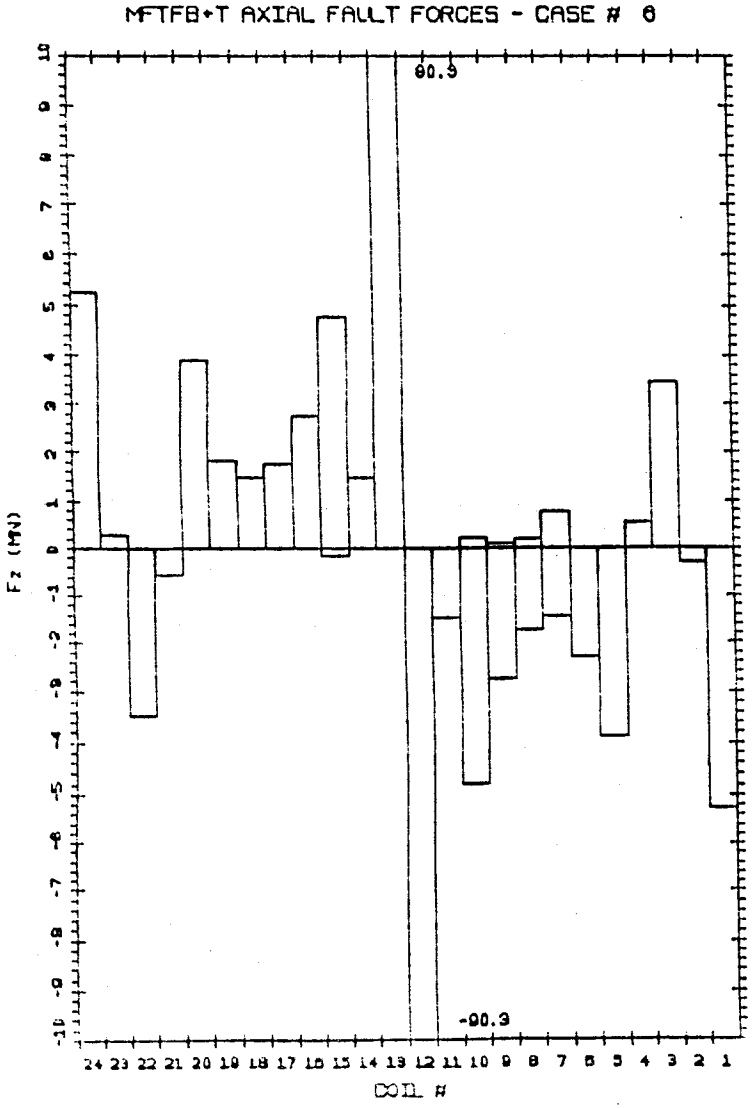

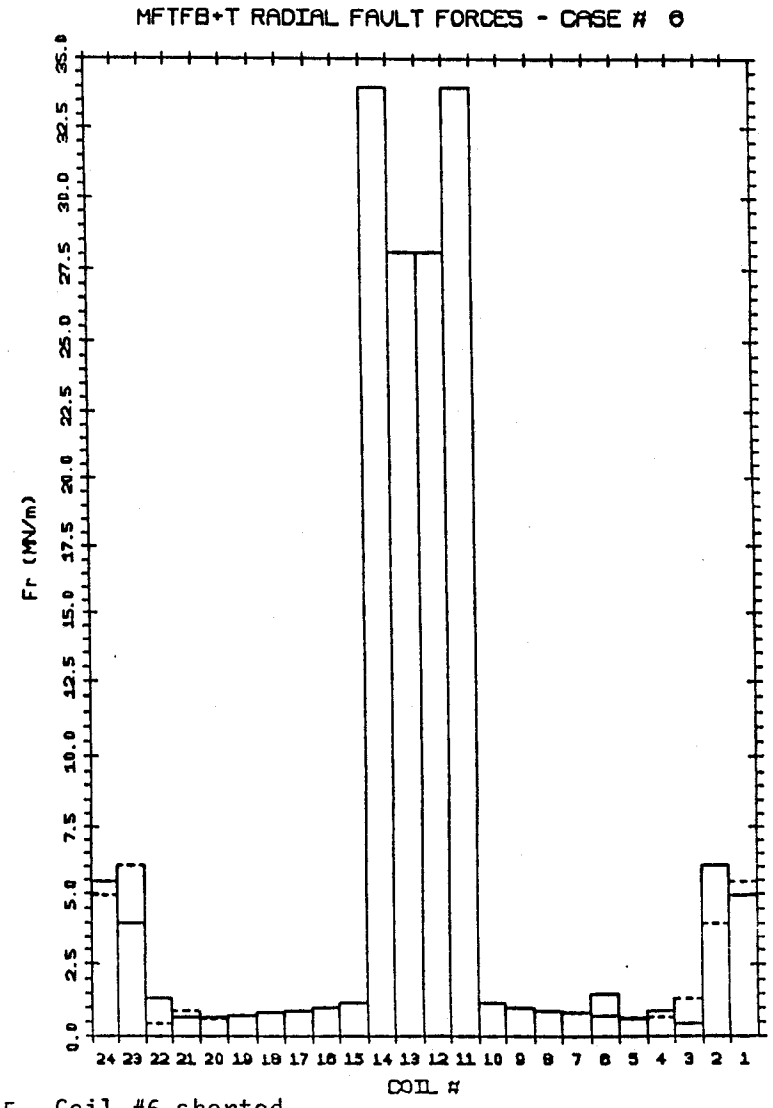

Figure 4.15- Coil #6 shorted

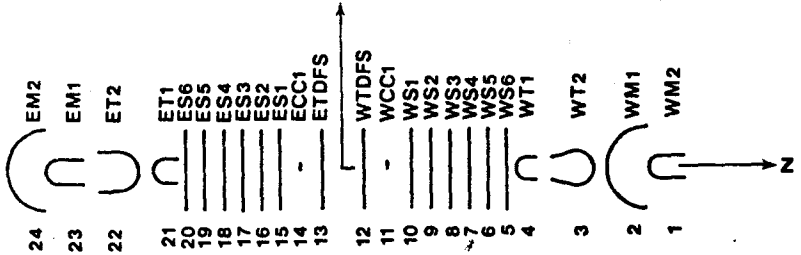

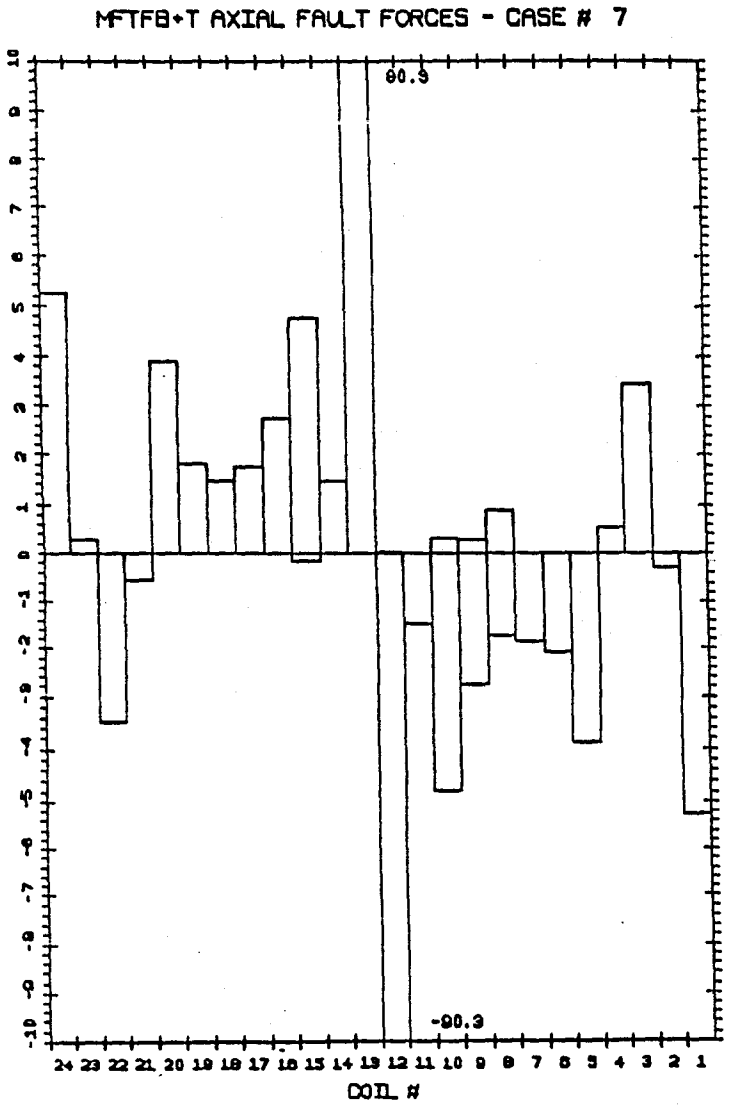

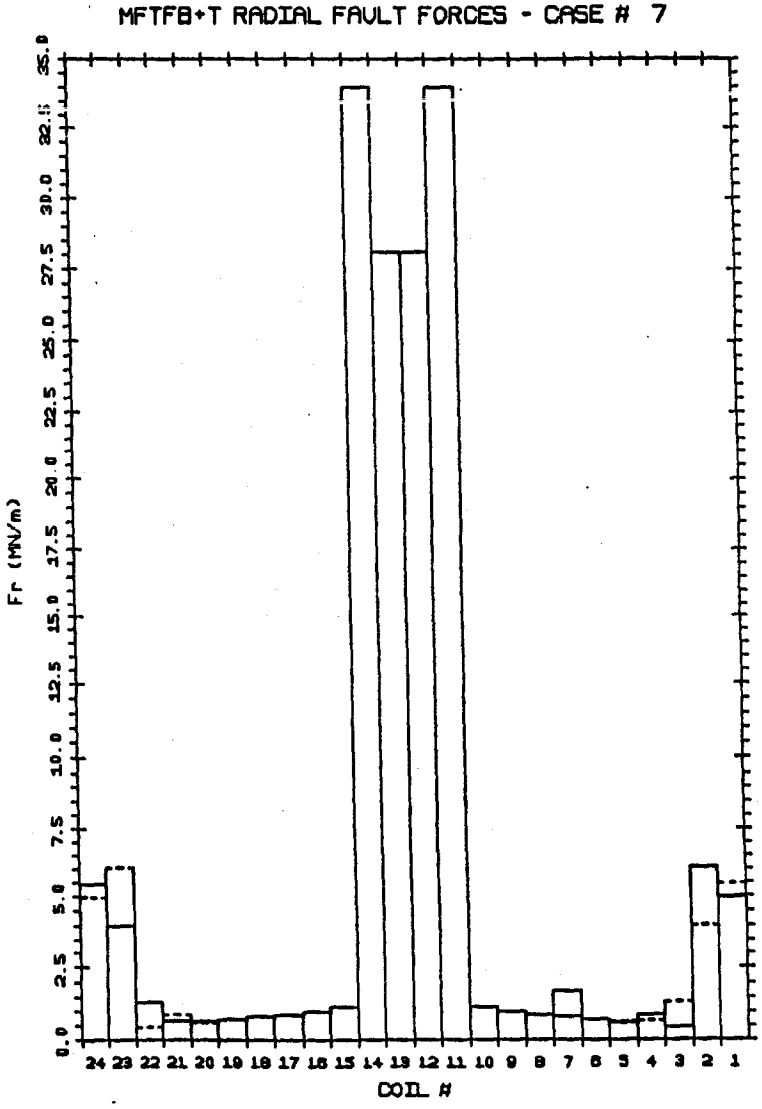

Figure 4.16 - Coil #7 shorted

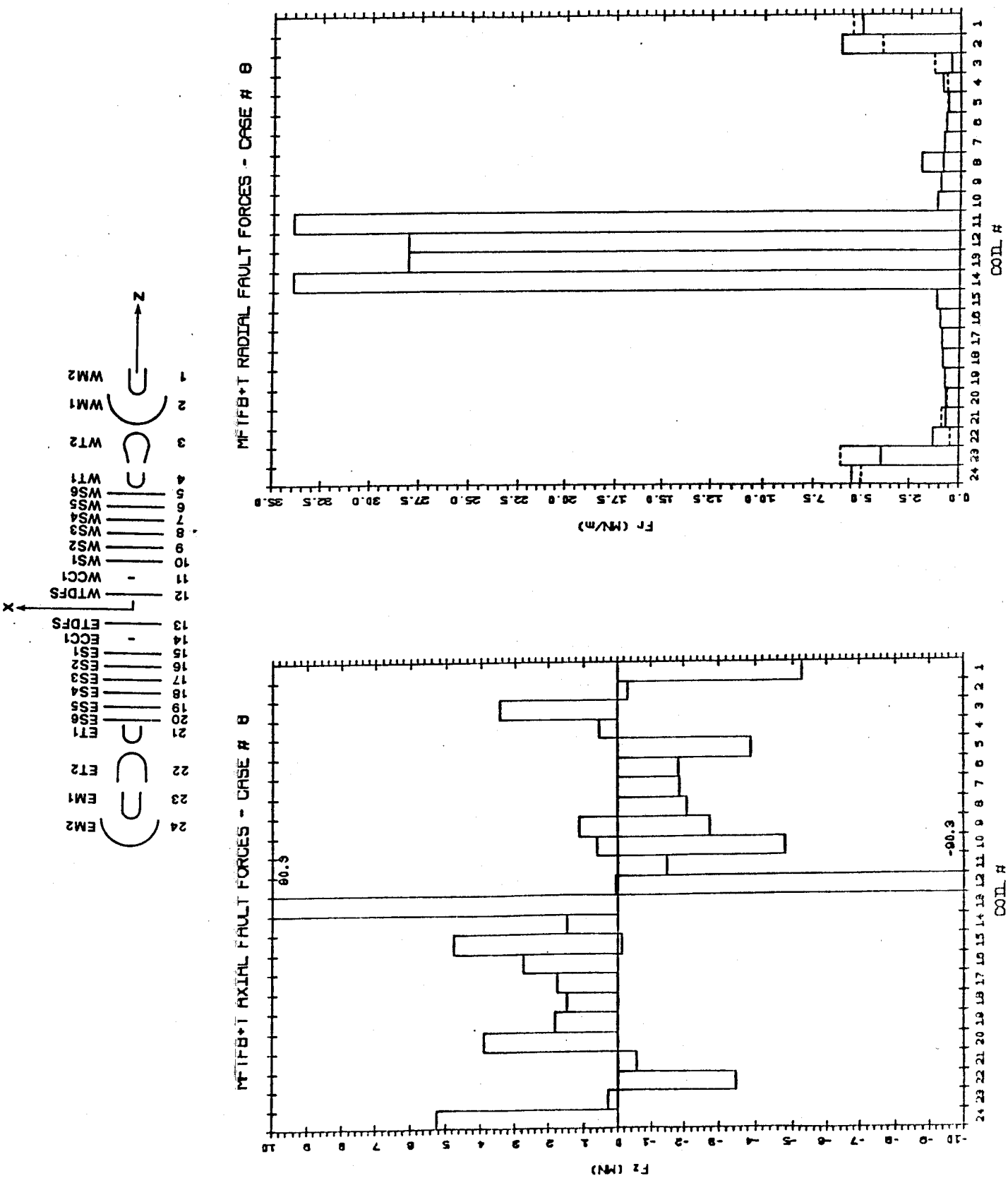

Figure 4.17- Coil #8 shorted

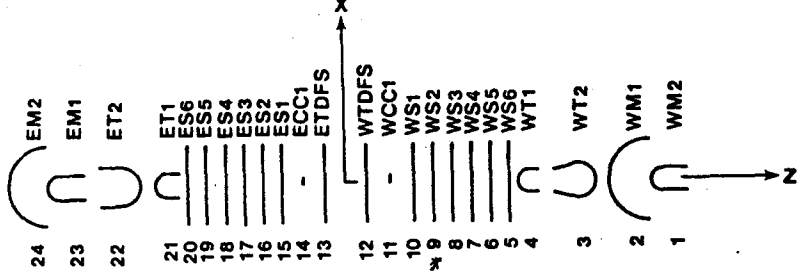

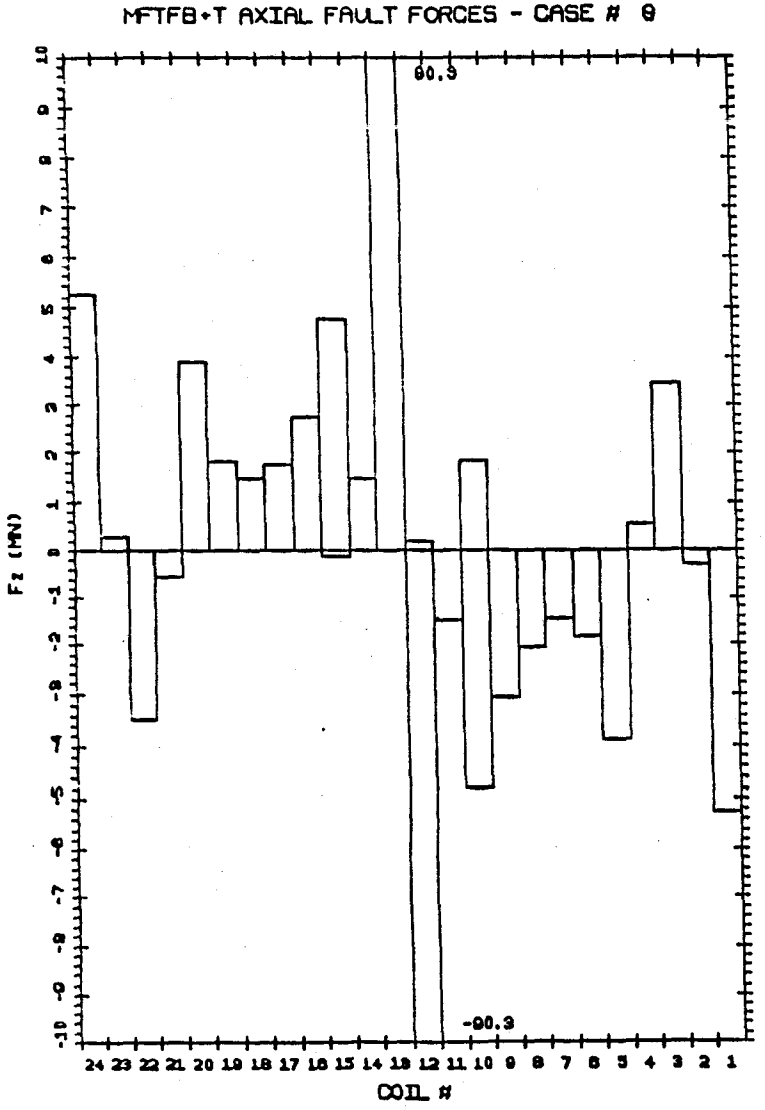

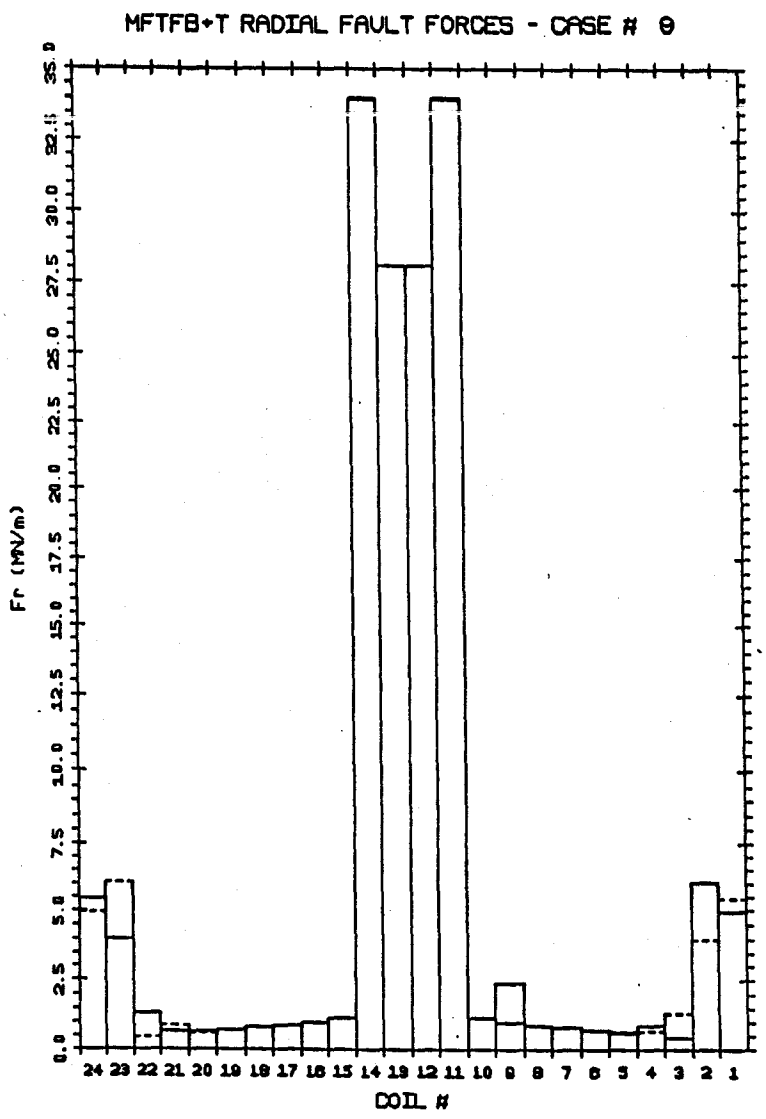

Figure 4.18 - Coil #9 shorted

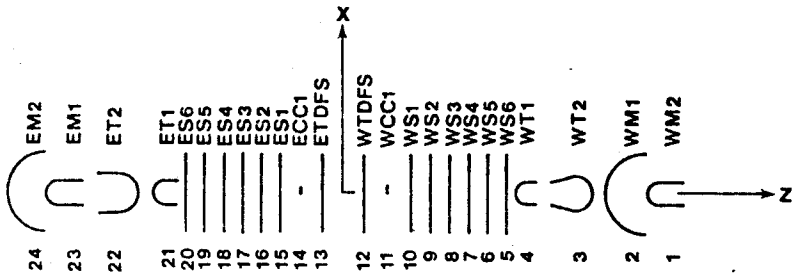

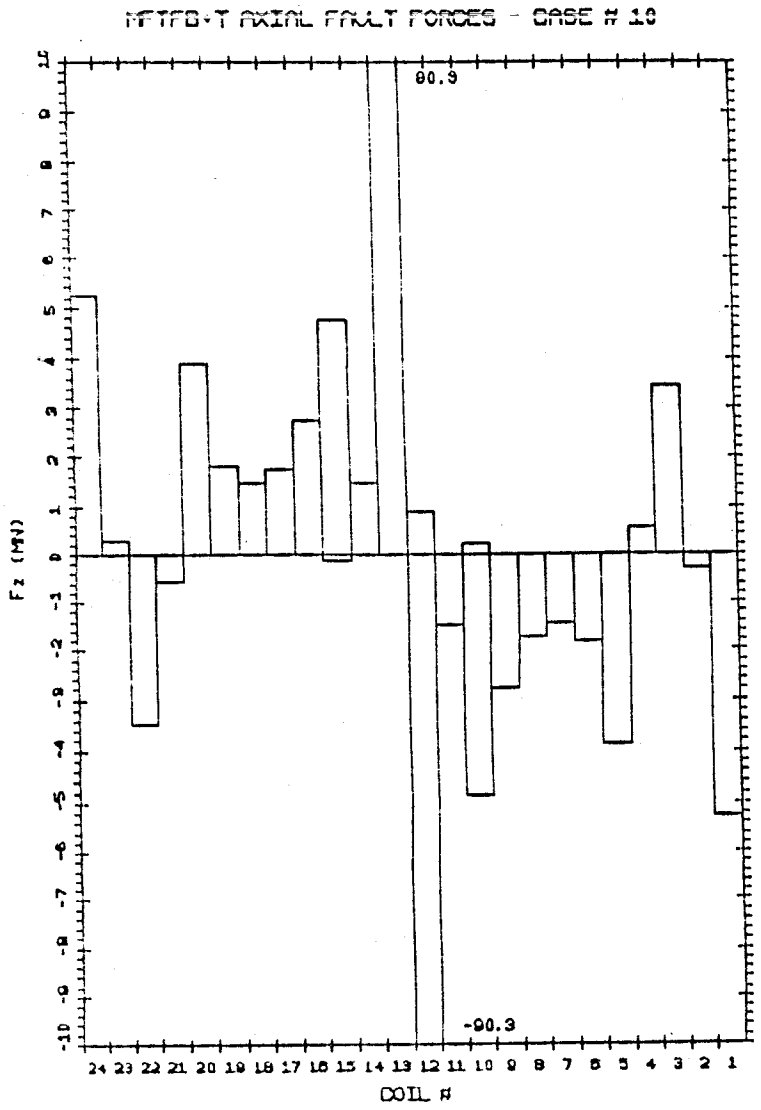

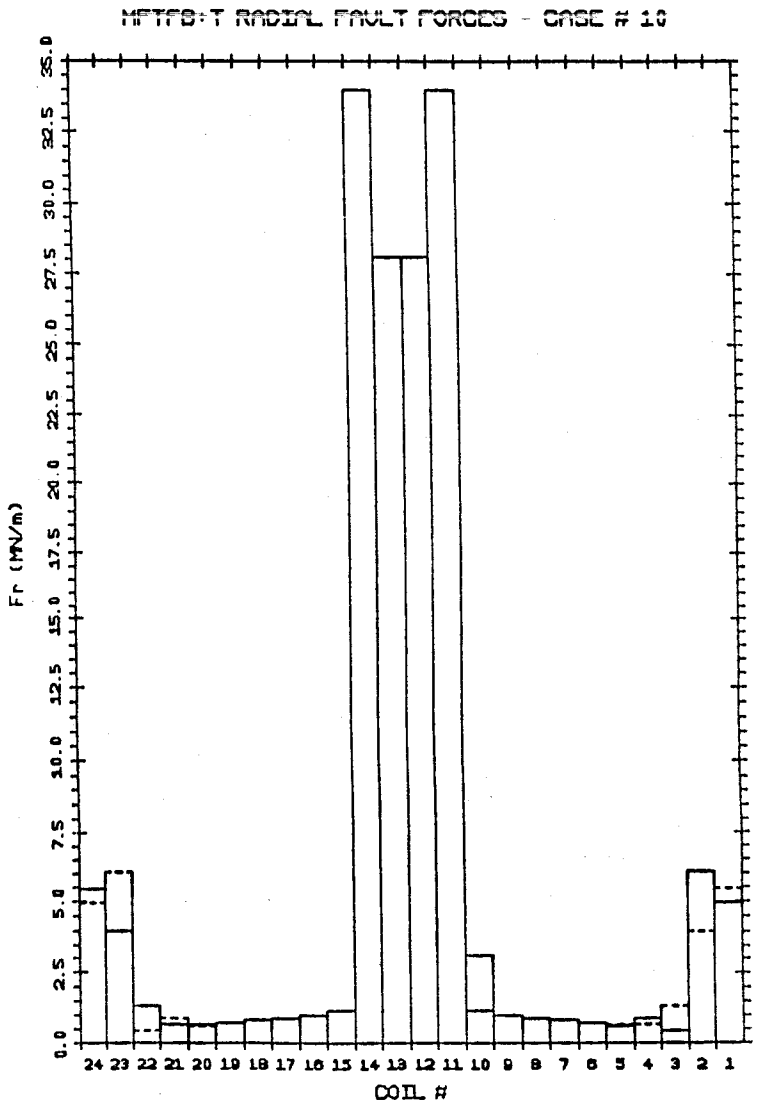

Figure 4.19 - Coil #10 shorted

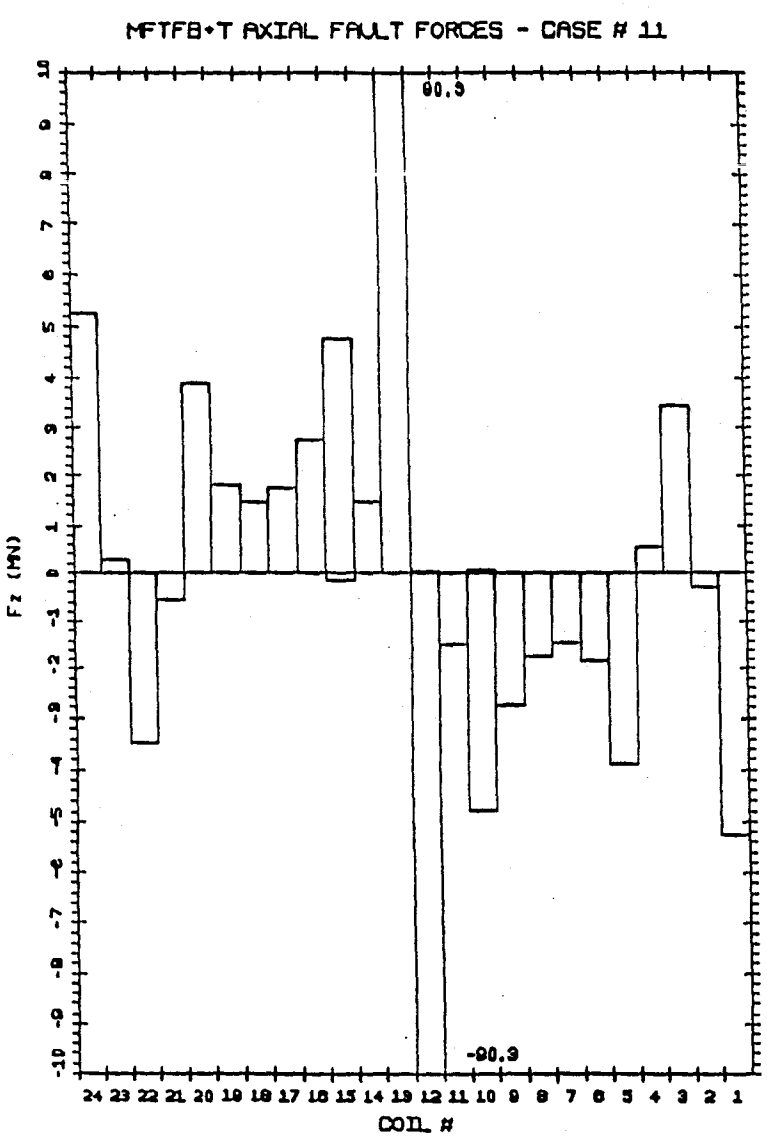

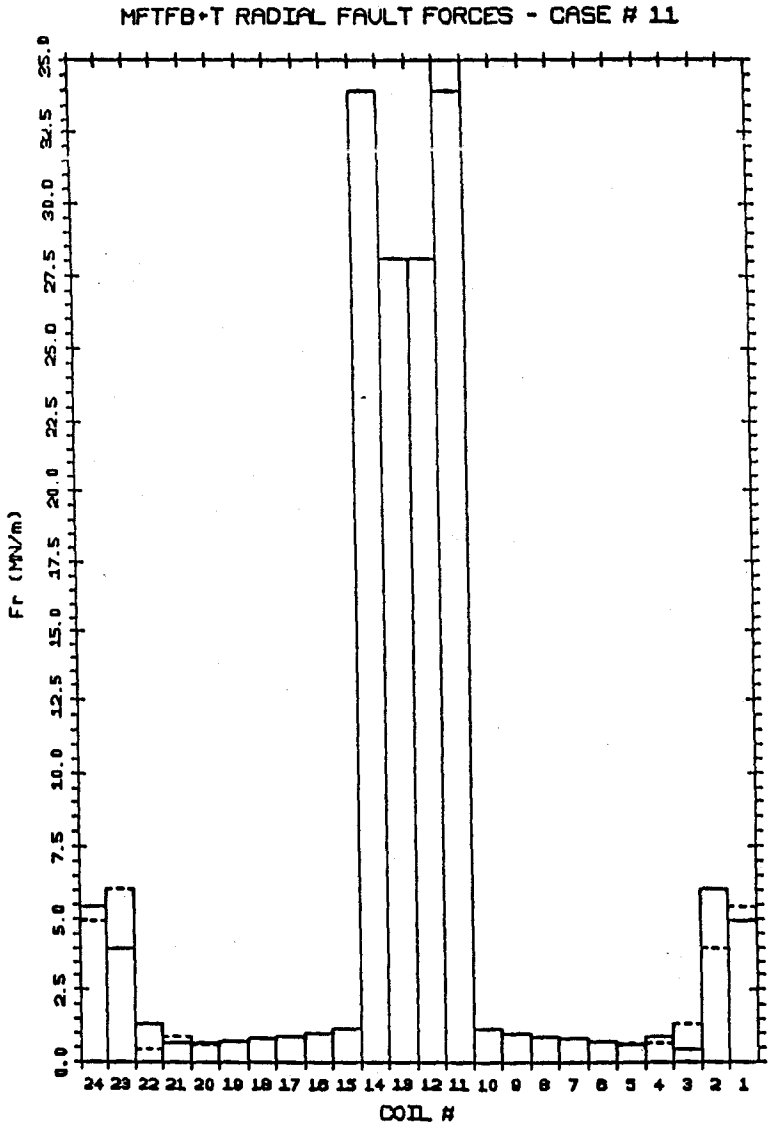

Figure 4.20 - Coil #11 shorted

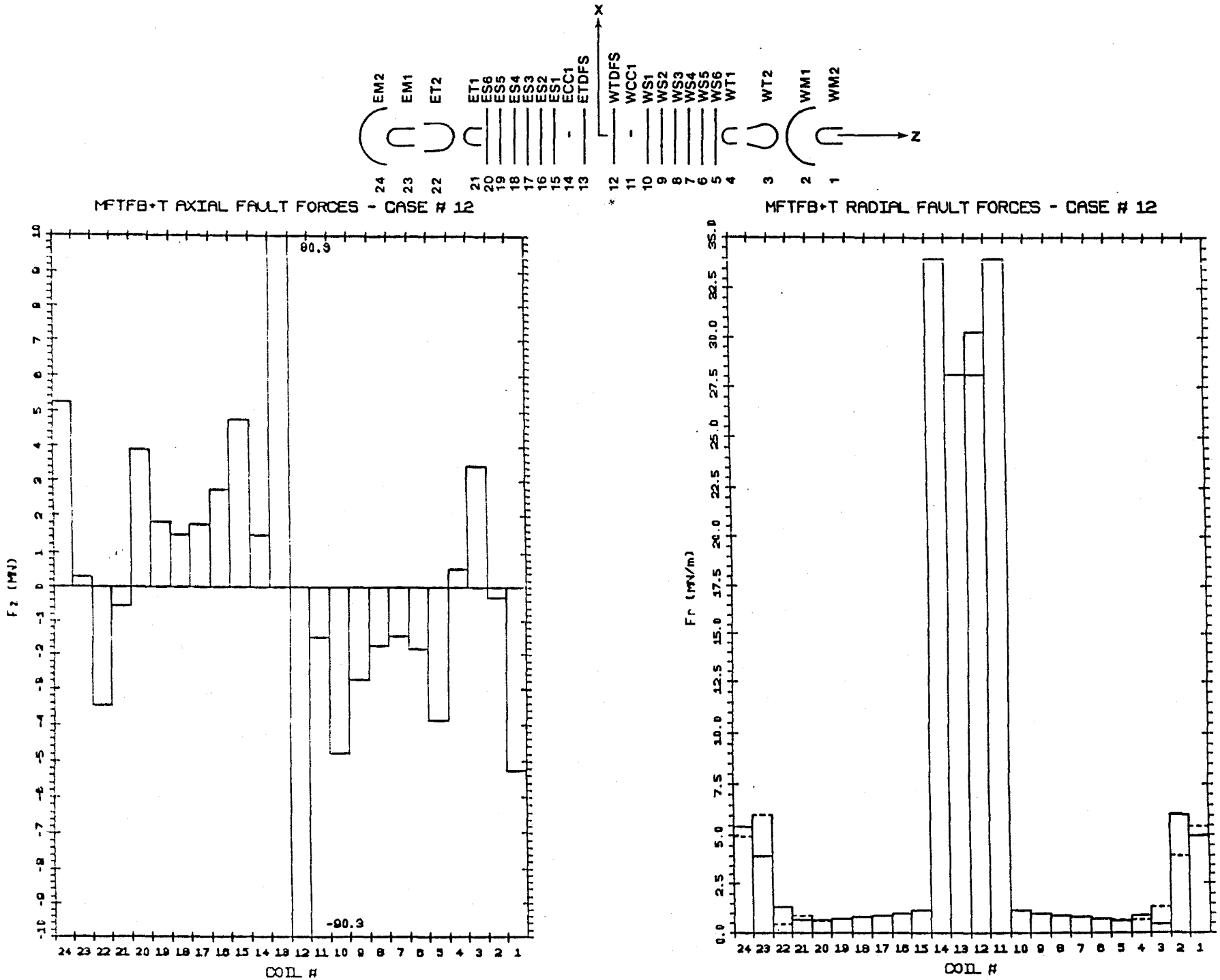

Figure 4.21 - Coil #12 shorted

5.0 CONCLUSIONS

A large number of possible normal operating and fault conditions for the MFTFB+T mirror machine have been investigated to estimate the worst case coil loadings. The results from these analyses are summarized in section 1.0. More detailed results are presented in sections 2.0 through 4.0.

In general, the four C-shaped magnets at each machine end (WM2, WM1, WT2,and WT1) experience the worst case loading under static current conditions. The central cell solenoids (WS6, WS5, WS4, and WS3) experience peak loads during discharge transients with a neighboring coil short-circuited. The coils at the machine center (WS2, WS1, WCC1, WTDFS2, etc.) have peak axial loads that occur primarily in the static condition. However, the peak radial loads occur during the discharge transients.

The axial loading investigated was the net force on a coil and tells nothing of the distribution of the load. The radial loading was considered at two points within the coils as an indicator of when the worst case load probably occurs. The load conditions are predicated on a certain coil/circuit configuration. If this configuration changes or if a coil operating current is altered, the new static and transient load scenarios should be reconsidered.

The current scenarios chosen for the analyses were by no means exhaustive from a fault condition standpoint. An entire class of faults which requires consideration involves system behavior during discharge execution with a section of one of the superconducting coils in the resistive state. Even though the coils are designed to be stable under usual conditions, that is complete LHe coolant immersion, a resistive region is possible in the event of a fault in the form of a low helium level. The temperature rise in a resistive region which is not immersed is strongly dependent on the coupled discharge character of the circuits and the level of operating current and dump voltage selected.

PFC BASE MAILING LIST

Argonne National Laboratory, TIS, Reports Section
Associazione EURATOM - CNEN Fusione, Italy, The Librarian
CRPP, Switzerland, Troyon, Prof. F.
Central Research Institute for Physics, Hungary, Preprint Library
Chinese Academy of Sciences, China, The Library
Eindhoven University of Technology, Netherlands, Schram, Prof. D. C.
The Flinders University of S.A., Australia, Jones, Prof. I.R.
General Atomic Co., Overskei, Dr. D.
International Atomic Energy Agency, Austria,
Israel Atomic Energy Commission, Soreq Nucl. Res. Ctr., Israel
JET, England, Gondhalekar, Dr. A.
Kernforschungsanlage Julich, FRG, Zentralbibliothek
Kyushu University, Japan, Library
Max-Planck-Institut fur Plasma Physik, FRG, Main Library
Nagoya University, Institute of Plasma Physics, Japan
Physical Research Laboratory, India, Sen, Dr. Abhijit
Rensselaer Polytechnic Institute, Plasma Dynamics Lab.
South African Atomic Energy Board, S. Africa, Hayzen, Dr. A.
UKAEA, Culham Laboratory, United Kingdom, Librarian
Universite de Montreal, Lab. de Physique des Plasmas, Canada
University of Innsbruck, Inst. of Theoretical Physics, Austria
University of Saskatchewan, Plasma Physics Lab., Canada
University of Sydney, Wills Plasma Physics Dept., Australia

INTERNAL MAILINGS

MIT Libraries
Industrial Liaison Office
G. Bekefi, A. Bers, D. Cohn, B. Coppi, R.C. Davidson,
T. Dupree, S. Foner, J. Freidberg, M.O. Hoenig, M. Kazimi,
L. Lidsky, E. Marmar, J. McCune, J. Meyer, D.B. Montgomery,
J. Moses, D. Pappas, R.R. Parker, N.T. Pierce, P. Politzer,
M. Porkolab, R. Post, H. Praddaude, D. Rose, J.C. Rose,
R.M. Rose, B.B. Schwartz, R. Temkin, P. Wolff,
T-F. Yang